-Dynamic Properties of Clean Sand and Expansive Clay from Resonant Column Studies-

-Troyee Tanu Dutta-

A Dissertation Submitted to
Indian Institute of Technology Hyderabad
In Partial Fulfillment of the Requirements for
The Degree of Master of Technology

भारतीय प्रौद्योगिकी संस्थान हैदराबाद
Indian Institute of Technology Hyderabad

Department of Civil Engineering

December, 2015

Declaration

I declare that this written submission represents my ideas in my own words, and where others' ideas or words have been included, I have adequately cited and referenced the original sources. I also declare that I have adhered to all principles of academic honesty and integrity and have not misrepresented or fabricated or falsified any idea/data/fact/source in my submission. I understand that any violation of the above will be a cause for disciplinary action by the Institute and can also evoke penal action from the sources that have thus not been properly cited, or from whom proper permission has not been taken when needed.
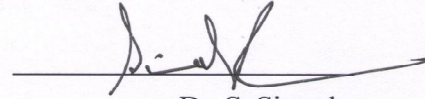
_____

(Signature)

Troyee Tanu Dutta

CE13M0003

Approval Sheet

This thesis entitled 'Dynamic Properties of Clean Sand and Fly Ash Stabilized Expansive Clay from Resonant Column Studies' is approved for the degree of Master of Technology from IIT Hyderabad.
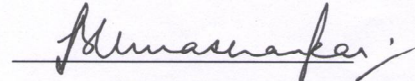
-Dr. S. Sireesh-

Associate Professor

Department of Civil Engineering

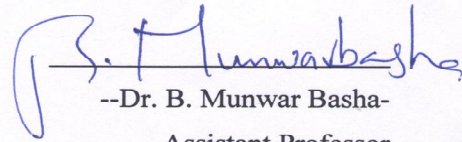Indian Institute of Technology Hyderabad

-Dr. B. Umashankar-

Assistant Professor

Department of Civil Engineering
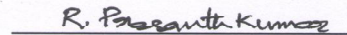
Indian Institute of Technology Hyderabad

--Dr. B. Munwar Basha-

Assistant Professor

Department of Civil Engineering

Indian Institute of Technology Hyderabad

-Dr. R. Prasanth Kumar-

Associate Professor

Department of Mechanical and Aerospace Engineering

Indian Institute of Technology Hyderabad

Acknowledgements

Dedicated to

Parents

Abstract

Design of structures subjected to different dynamic loads requires the dynamic properties of soil. The dynamic load may come from earthquakes, pile driving operations, vibrations from machines, ocean waves, blasting operations etc. In the present study, a fixed free type of resonant column had been used to determine the dynamic properties of clean sand and moderately expansive soil. The dynamic properties which are mostly discussed in the available literatures are shear modulus and damping ratio of soil. Another important dynamic property which is not given due consideration is the Poisson's ratio of soil. Proper estimation of the Poisson's ratio is required as it signifies the stress and deformation characteristics of the soil. By performing resonant column tests in both torsional mode and flexural mode of excitation, it is possible to determine the Poisson's ratio of soil. In the first part of the study, resonant column tests were performed on poorly graded clean sand. The influence of shear strain, confining pressure, and relative density on the dynamic properties of clean sand was discussed. Tests were performed on both dry sand and fully saturated sand to study the influence of saturation on the dynamic properties of sands. After that resonant column tests were performed on expansive clay to understand the dynamic behavior of expansive soil. First series of tests were performed on expansive clay prepared at optimum moisture content. After that tests were performed on fully saturated soil. It was observed that suction of the soil significantly influences the dynamic properties of soil. The suction measurement was done by performing filter paper tests. The influence of shear strain and confining pressure on the dynamic properties of expansive clay were also discussed. Resonant column tests were then performed on fly ash treated expansive soil. Class C fly ash obtained from Neyvelli Lignite Corporation Limited was used in the present study. It was observed that there has been a considerable improvement in the dynamic properties of expansive soil when treated with fly ash. A series of unconfined compressive strength tests were also performed on both untreated and treated expansive soil to determine the strength characteristics of soil. Filter paper tests were performed on stabilized expansive soil to understand the influence of

suction on the dynamic properties of stabilized soils. X-ray powder diffraction study was performed on both untreated and fly ash treated expansive clay to qualitatively identify the minerals formed due to stabilization. Finally, design of a machine foundation, resting on expansive soil, subjected to vertical vibrations is demonstrated to control the resonance of the stabilized soil-foundation system.

Nomenclature

G - Shear modulus, MPa

D - Damping ratio, %

v - Poisson's ratio

G_{max}- Small strain shear modulus, MPa

D_{min}- Small stain damping ratio

v_{min} – Small strain Poisson's ratio

V_s- Shear wave velocity, m/s

f - Frequency of excitation, Hz

L - Length of the specimen, m

I - Mass polar moment of inertia of the soil specimen, kg m^2

I_o- Mass polar moment of inertia of the electromagnetic drive system, kg m^2

Z_o- Vibration amplitude after excitation power is switched off

Z_n - Vibration amplitude after nth cycle

n - Number of cycles

ω_f - Circular resonant frequency in flexural mode, rad/s

E - Young's modulus of the soil specimen, MPa

I_b - Area moment of inertia of the specimen, m^4

h_{0i}, h_{1i} - Heights at the bottom and top respectively of the added mass m_i, m

m_T - Mass of the soil specimen, kg

m_{am} - mass of the top plate of the calibration bar, kg

m_b - mass of the top cap, kg

m_x - mass of the mass of drive system, kg

m_{am} - mass of the added calibration mass, kg

I_y - Area moment of inertia, m^4

I_{yi} - Area moment of inertia of mass m_i, m^4

V_{LF} - Longitudinal wave velocity, m/s

ρ - Density of the soil specimen, kg/m^3

G/G_{max} - Normalized shear modulus

σ_3 - Total confining pressure, kPa

$\sigma_3^{'}$ - Effective confining pressure, kPa

k - Stiffness of the soil

I_{am} - Mass polar moment of inertia of the added mass

LL - Liquid limit

PL - Plastic limit

PI - Plasticity index

AASHTO - American Association of State Highway and Transportation Officials

USCS - Unified Soil Classification System

G_s - Specific gravity

C_c - Coefficient of compression

C_r - Coefficient of recompression

P_r - Pre-consolidation pressure

γ_{dmax} - Maximum dry density, kN/m^3

γ_{dmin} - Minimum dry density, kN/m^3

e_{max} - Maximum void ratio

e_{min} - Minimum void ratio

C_u - Coefficient of uniformity

C_c - Coefficient of curvature

XRF- X-Ray Florescence

UCS – Unconfined compressive strength

FA - Fly ash

LVDT - Linear variable displacement transducer

R_D - Relative density

S - Suction, kPa

S_r – Degree of saturation

XRPD - X-Ray powder diffraction

V_d - volume of soil specimen recorded from the graduated cylinder having distilled water

V_k - volume of soil specimen recorded from the graduated cylinder having kerosene

CSH- Calcium silicate hydrate

CAH- Calcium aluminum hydrate

r_o- Equivalent radius

L- Length of the foundation,

B - Width of the foundation

B_z - Mass ratio,

W - Weight of the machine and the foundation

Contents

Chapter 1

Introduction

1.1   Problem statement

Design of structures subjected to various dynamic loads such as earthquakes, pile driving operations, vibrations from machines, ocean waves, blasting operations etc. require proper estimation of dynamic properties of soil. Various techniques are adopted by several researchers [1-4] to measure the dynamic properties of soil. It includes the use of both field and laboratory techniques. Field tests include the seismic down-hole test, up-hole test, seismic cross-hole test, seismic reflection, seismic refraction, suspension logging, spectral analysis of surface wave, tomography, cone penetration test, dilatometer test. The commonly used laboratory tests are resonant column test, ultrasonic pulse test, cyclic triaxial test, cyclic direct simple shear test and cyclic torsional shear test. The advantages of using laboratory tests over the field tests are the availability of efficiently controlled boundary conditions and provision for applying higher values of strain in the laboratory which helps in the accurate estimation of the damping ratio.

The test which is commonly performed for the accurate determination of dynamic properties of soil in a laboratory is the resonant column test. The main advantage of using resonant column test is a provision to perform the test at small value of shear strain. The testing procedure and data interpretation had been dealt extensively in the literature [5, 6]. The dynamic properties which are given prime focus are the shear modulus (G) and damping ratio (D). Considerable research had been undertaken to find the effect of various factors on the shear modulus and damping ratio of soil using both field and laboratory technique [3, 4, 7-16]. Another important dynamic soil property which has not been discussed much in the available literature is Poisson's ratio of soil. Poisson's ratio is often considered as an elastic

constant and while the values of Poisson's ratio do not vary much for a particular soil type under static loads, it is commonly taken as a constant. Proper estimation of the Poisson's ratio is of paramount importance as it signifies the stress and deformation characteristics of the soil. A limited research has been undertaken to study the influence of different parameters on the Poisson's ratio of soil [17-20]. The present thesis work is partially motivated by this research need.

Expansive soil contains minerals such as montmorillonite which can absorb water and cause increase in volume of the soil. Due to fluctuation in moisture content expansive soils exhibits excessive heaving which causes damage to light weight structures resting on it. The problems associated with expansive soil are prevalent worldwide. In India the expansive soil is called as black cotton soil since it is black in color and it facilitated the growth of cotton plant. Almost 20 % of the entire Indian landmass is covered with black cotton soil and it includes nearly all the Deccan Plateau, Madhya Pradesh, Maharashtra, Andhra Pradesh, Uttar Pradesh, Karnataka, and parts of Gujarat.

Treatment of expansive soil is done by means of stabilizers. Generally lime or cement is used as stabilizer to treat expansive soil. In addition, low calcium based admixtures such as fly ash, ground granulated blast furnace slag etc. have been promoted to treat expansive soils. The ever increasing demand for energy has resulted in the installation of several thermal power plants across India. Fly ash is a material which is obtained from flue gas of a furnace which is fueled with coal. There is tremendous production of fly ash from those power plants. By the end of the financial year 2017, it is estimated that there will be a production of nearly 300-400 million tons of fly ash per year in India. It leads to severe problem of safe disposal and beneficial utilization of these excessive quantities of fly ash that is generated. In the present study class C fly ash has been used to stabilize a moderately expansive soil. It is observed that limited study has been performed to determine the dynamic properties of stabilized expansive soil [21-24]. Therefore, there is great need to understand the dynamic behavior of stabilized expansive soil. The present thesis work is further motivated by this research need.

1.2   Objective and scope

The focus of the study can be broadly classified into two parts. In the first part of the study, dynamic properties of clean sand is determined with a special emphasis given to Poisson's ratio. In second part of study, stabilization of expansive soil by means of fly ash is performed and the effect of fly ash stabilization on the dynamic properties of expansive soil is elaborately discussed.

The scope of the present research work includes:

1. To review the available literature on the dynamic properties of clean sands, untreated and treated expansive soil and stabilization of expansive soil by using additives.
2. To calibrate the resonant column device to perform tests in both torsional and flexural mode of excitation.
3. To determine the dynamic properties of clean sand using resonant column tests.
4. To study the influence of saturation on the dynamic properties of clean sands.
5. To evaluate the dynamic properties of expansive soil and to understand the influence of saturation on the dynamic properties of expansive soil.
6. To stabilize the expansive soil using class C fly ash.
7. To perform resonant column tests on fly ash stabilized expansive soil.
8. To perform unconfined compression strength test to determine the improvement in compressive strength with stabilization.
9. To perform X-Ray powder diffraction study to qualitatively identify the compounds present in untreated and treated soil.
10. To show a design problem of machine foundation and to evaluate the improvement in the factor of safety with treatment.

1.3   Thesis outline

Chapter 2 includes the review of literature available on dynamic properties of soil and stabilization of expansive soil using additive.

Chapter 3 describes the test procedure and calibration exercise for performing both torsional and flexural tests using resonant column apparatus.

Chapter 4 includes the properties of different materials used and the sample preparation techniques that were adopted in the study.

Chapter 5 gives the dynamic properties of sand and effect of different parameters on dynamic properties.

Chapter 6 is devoted to the dynamic properties of expansive soil and influence of various parameters on dynamic properties.

Chapter 7 presents the stabilization of expansive soil using fly ash and the effect of stabilization on the dynamic properties.

Chapter 8 includes the conclusion and summary of the present research work and also provides some recommendations for future work.

Chapter 2

Literature Review

2.1   Dynamic properties of soil

The determination of dynamic properties of soil started way back in 1930's when Ishimoto and Iida developed the first resonant column apparatus. Ishimoto and Iida (1936) designed a device to compute longitudinal wave velocity and Young's modulus of soil. They performed resonant column tests in longitudinal mode of excitation on silty clay, silts, clay and loam. Figures 2.1 and 2.2 give the variation of longitudinal wave velocity and Young's modulus of soil respectively with the increase in moisture content. It was observed that both longitudinal wave velocity and Young's modulus decrease with the increase in moisture content.

Ishimoto and Iida (1937) also developed a device to determine transverse wave velocity, modulus of rigidity and Poisson's ratio of soil. Figures 2.3, 2.4 and 2.5 give the variation of transverse wave velocity, modulus of rigidity and Poisson's ratio with the increase in moisture content. It was observed that both transverse wave velocity and modulus of rigidity decrease with the increase in moisture content whereas Poisson's ratio increases with increase in moisture content.
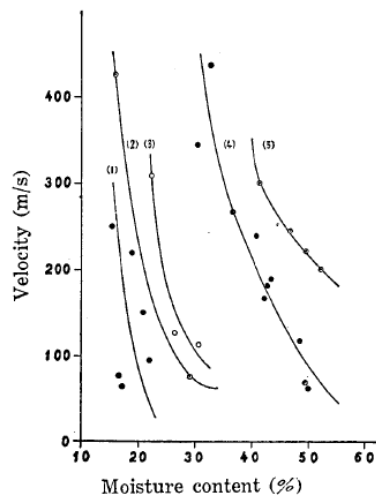
(1) Loam of No. 1. (2) Silt of Komatu-
gawa. (3) Clay of No. 2. (4) Silty-clay
of Maru-no-uti. (5) Loam of Hongô.

Figure 2.1: Variation of longitudinal wave velocity with moisture content (Ishimoto and Iida 1936)
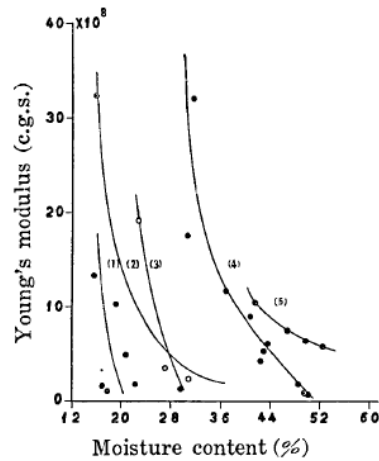
(1) Loam of No. 1. (2) Silt of Komatu-
gawa. (3) Clay of No. 2. (4) Silty-clay
of Maru-no-uti. (5) Loam of Hongô.

Figure 2.2: Variation of Young's modulus with moisture content (Ishimoto and Iida 1936)

6
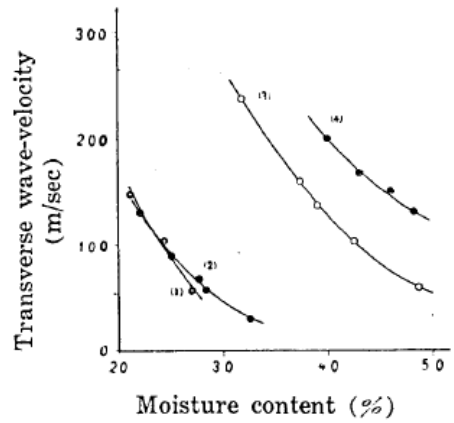
(1) Silt of Komatugawa. (2) A kind of clay. (3) Silty-clay of Maru-no-uti. (4) Loam of Hongô.

Figure 2.3: Variation of transverse wave velocity with moisture content (Ishimoto and Iida 1937)
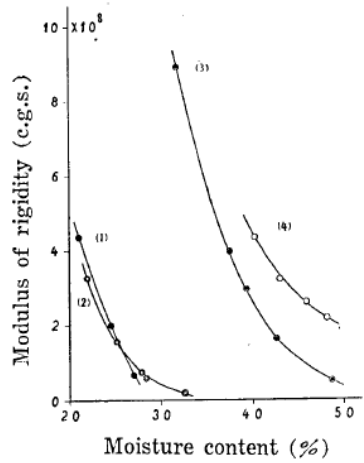
(1) Silt of Komatugawa. (2) A kind of clay. (3) Silty-clay of Maru-no-uti. (4) Loam of Hongô.

Figure 2.4: Variation of modulus of rigidity with moisture content (Ishimoto and Iida 1937)
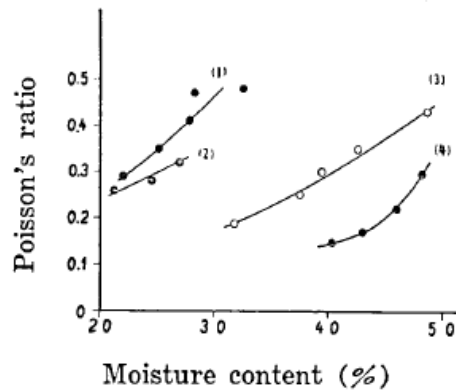
Figure 2.5: Variation of Poisson's ratio with moisture content (Ishimoto and Iida 1937)

Iida (1938) by performing resonant column tests on sand observed that torsional wave velocity and longitudinal wave velocity decrease with increase in moisture content. Figure 2.6 give the variation of torsional and longitudinal wave velocity with porosity. It depicts that wave velocity decreases with the increase in porosity of the soil and proves that closeness of the particle significantly influence the elastic properties
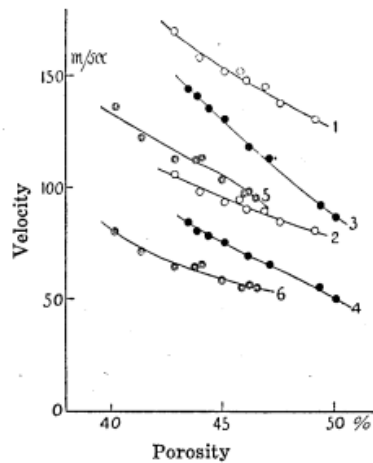
Figure 2.6: Variation of velocity with porosity (Iida 1938)

8

Hall and Richart (1963) by performing resonant column tests on Ottawa sand and glass beads observed that logarithmic decrement increases with the increase in wave amplitude but it decreases with the increase in confining pressure. It is also observed that the effect of density on logarithmic decrement is small.

By performing resonant column tests on Ottawa sand, Hardin and Richart (1963) stated that shear wave velocity decreases linearly with void ratio and is independent of grain size and gradation. Hardin and Richart (1963) also gave an empirical equation which relates the shear wave velocity to the confining pressure and void ratio for angular sands. The shear wave velocity can be obtained from equation (2.1).

$$V_s = (18.42 - 6.1986e)\sigma_3^{1/2} \tag{2.1}$$

where, V_s =shear wave velocity (m/s); e =void ratio; σ_3 =confining pressure (N/ m^2).

Hardin (1965) concluded that initial tangent modulus of dry sand is independent of the rate of loading. Hardin and Music (1965) designed and built a new apparatus that will fit into an ordinary triaxial test chamber. The apparatus can be used to measure shear modulus and damping ratio of the soil specimen in a triaxial apparatus.

Lawrence (1965) performed ultrasonic pulse test in Ottawa sand and Boston blue clay. In this test, ferreoelectric ceramics are used to produce and receive a torsional shear wave in cylindrical soil specimen. From Figure 2.7, it was observed that shear wave velocity increases with increase in hydrostatic stress. It was also observed that shear wave velocity decreases with the increase in void ratio which can be seen from Figure 2.8.

Hardin and Black (1966) by performing resonant column tests on sand observed that shear modulus is independent of the deviatoric component of the initial state of stress. It was also stated that small strain stiffness is independent of the rate of loading. By performing resonant column tests on normally consolidated clay, Hardin and Black (1968) observed that shear modulus is independent of the deviatoric component of the ambient octahedral shear stress and also stated that there is a secondary influence of shear modulus with time which cannot be accounted for by the changes in void ratio.

Humphries and Wahls (1968) by performing resonant column test on remolded kaolinite and bentonite observed that shear modulus increases with increasing confining pressure and decreasing void ratio. It is also observed that shear modulus decreases with increasing amplitudes of vibration and there is a significant influence of stress history on shear modulus.
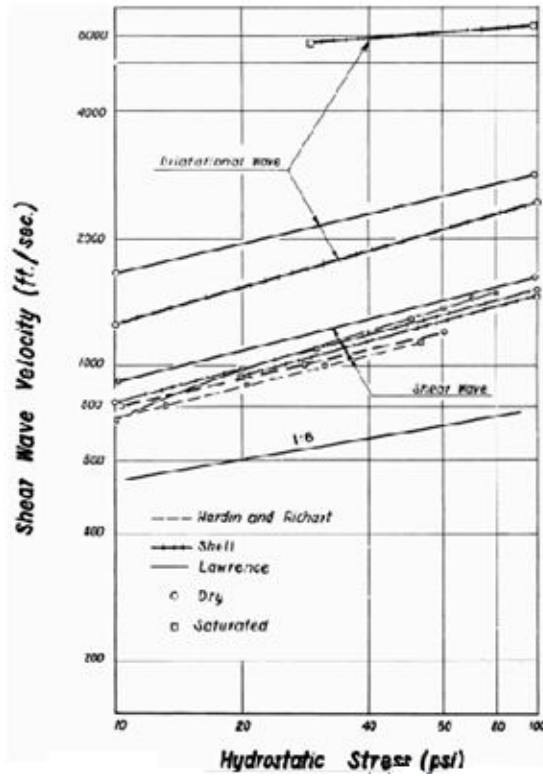
Figure 2.7: Variation of shear wave velocity with hydrostatic stress in Ottawa sand (Lawrence 1965)
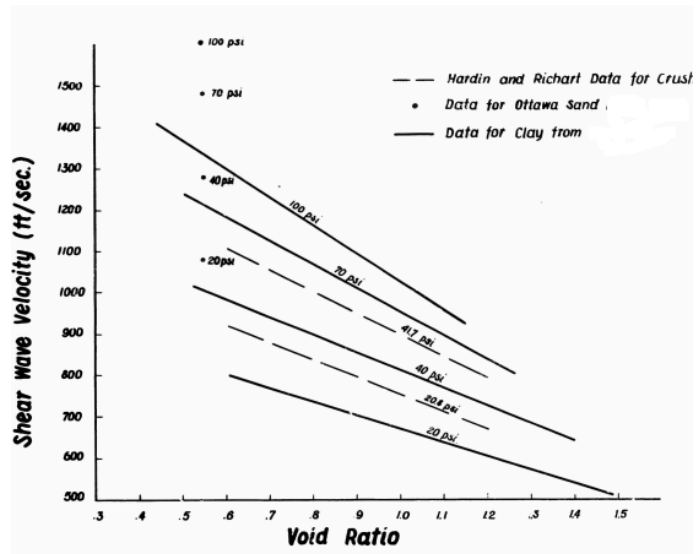
Figure 2.8: Variation of shear wave velocity with void ratio (Lawrence 1965)

10

Seed and Idriss (1970) summarized all the available data on sands and clays and gave empirical equations based on previous results. Seed and Idriss (1970) also proposed the upper and lower bound of modulus reduction (G/G_{max}) of sands (Figure 2.9). It was also observed that modulus reduction (G/G_{max}) increases with the increase in confining pressure. They also observed that shear modulus values of saturated clays obtained from the laboratory tests are lower than those obtained from in situ tests. They concluded that this difference in shear modulus of saturated clay obtained from laboratory tests and in situ tests is due to sample disturbance caused in laboratory tests. Table 2.1 gives the different test procedures for measuring dynamic properties of soil as given by Seed and Idriss (1970).
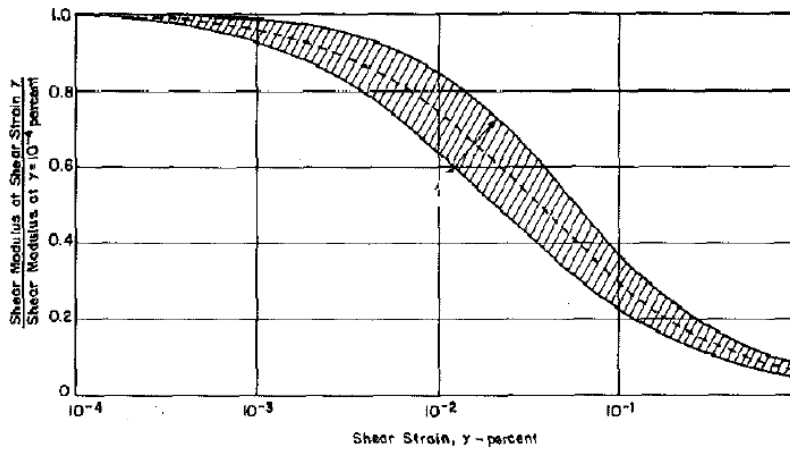
Figure 2.9: Variation of normalized shear modulus (G/G$_{max}$) with shear strain (Seed and Idriss 1970)

11

Table 2.1: Test procedures for measuring dynamic properties of soil (Seed and Idriss 1970)

General Procedure	Test Procedure	Approximate strain range	Properties determined
Determination of hysteresis stress strain relationships	Triaxial Compression	10^{-2} % to 5 %	Modulus; Damping
	Simple shear	10^{-2} % to 5 %	Modulus; Damping
	Torsional shear	10^{-2} % to 5 %	Modulus; Damping
Forced vibration	Longitudinal vibrations	10^{-4} % to 10^{-2} %	Modulus; Damping
	Torsional vibrations	10^{-4} % to 10^{-2} %	Modulus; Damping
	Shear vibrations-lab	10^{-4} % to 10^{-2} %	Modulus; Damping
	Shear vibrations-field	10^{-4} % to 10^{-2} %	Modulus
Forced vibration	Longitudinal vibrations	10^{-3} % to 1 %	Modulus; Damping
	Torsional vibrations	10^{-3} % to 1 %	Modulus; Damping
	Shear vibrations-lab	10^{-3} % to 1 %	Modulus; Damping
	Shear vibrations-field	10^{-3} % to 1 %	Modulus
	Compression waves	$\simeq 5 \times 10^{-4}$ %	Modulus
	Shear waves	$\simeq 5 \times 10^{-4}$ %	Modulus
	Rayleigh waves	$\simeq 5 \times 10^{-4}$ %	Modulus
Field Seismic Response	Measurement of motions at different levels in deposits		Modulus; Damping

Hardin & Drnevich (1972a) also proposed an empirical equation which gives the value of small strain shear modulus using the void ratio and confining pressure for angular sands. The correlation is given by equation (2.2):

$$G_{max} = 102150.95 \frac{(2.973 - e)^2}{(1 + e)} \sigma_3^{1/2} \qquad (2.2)$$

Where, G_{max} =small strain shear modulus (N/ m^2); e =void ratio; σ_3 =confining pressure (N/ m^2).

Hardin and Drnevich (1972b) by performing resonant column tests and cyclic simple shear tests on sands and clays discussed the influences of different parameters on shear modulus and damping ratio of soil. They observed that for sands most important parameters which influence the dynamic properties of sands are strain amplitude, confining pressure and void ratio and for clays are strain amplitude, confining pressure, void ratio and degree of saturation.

Affifi and Richart (1973) studied the effect of time of confinement and stress history by performing resonant column tests on Ottawa sands and Kaolinite clays. The effect of overconsolidation is found to be insignificant for sands whereas for fine grained soils such as silts and clays the influence of overconsolidation can be exhibited by reduction of void ratio. It was observed that with the increase in over-consolidation ratio the shear modulus of the clay increases. Affifi and Richart (1973) also observed that the time dependent increase in shear modulus is relatively unimportant for soils having $D_{50} > 0.04$. However for soils having $D_{50} \leq 0.04$, the increase of shear modulus with time is significant.

Ohsaki and Iwasaki (1973) provided empirical correlation for the determination of small strain shear modulus from standard penetration tests N value obtained from different sites. The empirical equation is given below:

$$G_{max} = 1200 \times N^{0.8} \tag{2.3}$$

Where G_{max} = small strain shear modulus (tons/sq. m), N= number of blows per foot in standard penetration test.

It was also mentioned that dynamic Poisson's ratio decreases with increase in shear modulus of the soil (Figure 2.10).

Iwasaki and Tatsuoka (1977) by performing resonant column tests on sands observed that shear modulus decreases with the increase in uniformity coefficient and fines content. Iwasaki et al. (1978) by performing resonant column tests and torsional shear tests on sands gave empirical equation to obtain shear modulus with increase in shear strain.
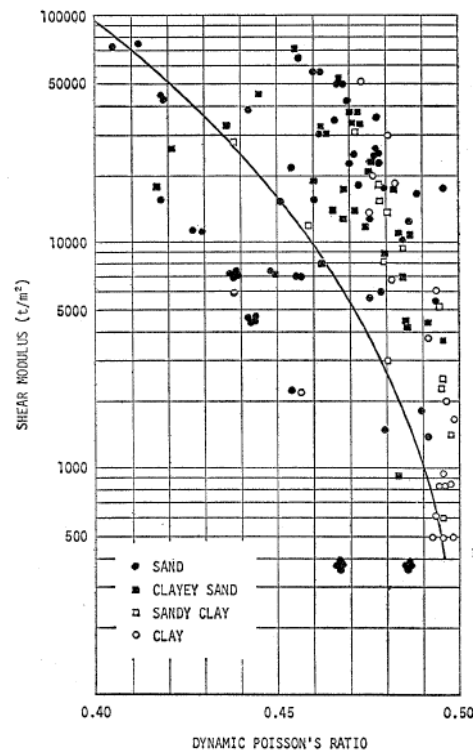
Figure 2.10: Dynamic Poisson's ratio and shear moduli (Ohsaki and Iwasaki 1973)

By performing modified cyclic triaxial tests on Toyoura sand, Kokusho (1980) proposed empirical correlation for determination of shear modulus of sand. It was also inferred that Poisson's ratio decreases with increase in confining pressure and increases with increase in void ratio as shown in Figure 2.11. Kokusho (1980) also observed that damping ratio values obtained from modified cyclic tiaxial tests were lower than those obtained from previous literatures. It was mentioned that this reduced value of damping ratio is due to the fact that modified triaxial apparatus is free from mechanical friction.

Kokusho et al. (1982) observed that time dependent increase in shear modulus depends greatly on the plasticity index of the soil. A time dependent decrease in damping ratio is also observed. It was also stated that G/G_o curve shifts to the right with the increase in plasticity index. Figure 2.12 gives the variation of   damping ratio with plasticity index. It was observed that at low values of shear strain, damping ratio of low plasticity soil and high plasticity soil is comparable. However, at higher values of shear strain, damping ratio of high plasticity soil is smaller than low plasticity soil. It was also mentioned that in comparison to sand, there is high variability in the shear modulus and damping ratio of

14

cohesive soils and it is prudent to do in-situ test or lab test before using these values for designs.
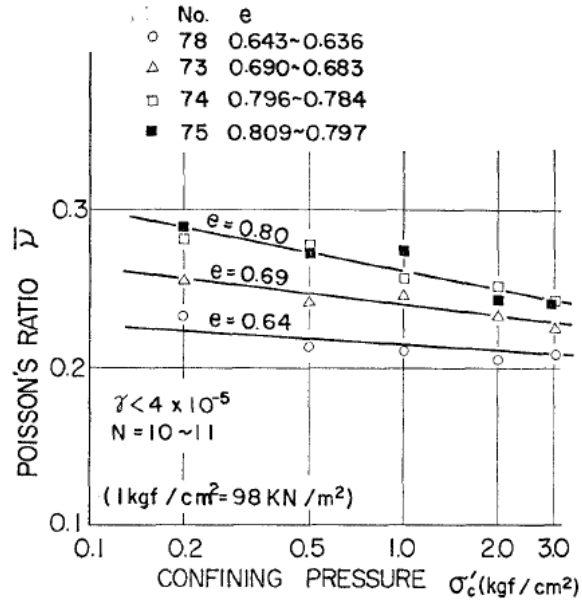
Figure 2.11: Variation of Poisson's ratio with confining pressure (Kokusho 1980)
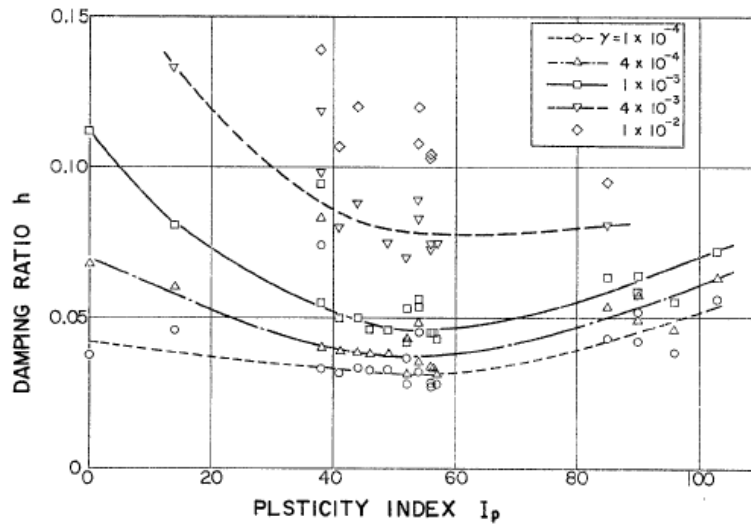
Figure 2.12: Variation of damping ratio with plasticity index (Kokusho et al. 1982)

15

Wu et al. (1985) performed an extensive study using resonant column apparatus on different sands and silts to understand the influence of saturation on the small strain shear modulus of the soil. Figure 2.13 gives variation of small strain shear modulus with degree of saturation for glacier way silt. It can be observed that with the increase in saturation from perfectly dry state to an optimum value, small strain shear modulus increases but with further increase in degree of saturation there is reduction in the small strain shear modulus of soil. It was attributed to the capillary induced suction present in partially saturated soil. It was also noted that this increase in small strain shear modulus is higher for smaller effective grain diameter and lower values of effective confining pressure (Figure 2.14).
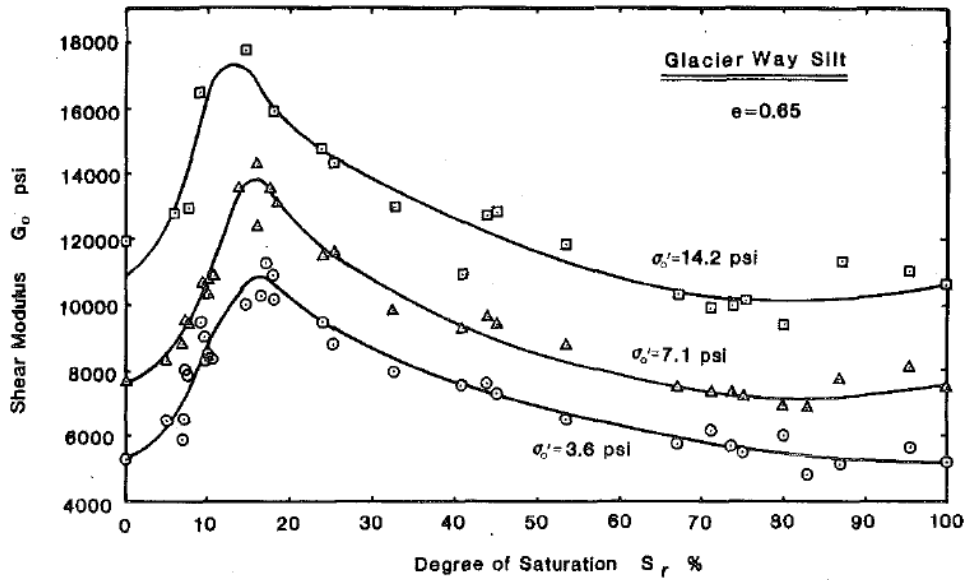
Figure 2.13: Variation of small strain shear modulus with degree of saturation (Wu et al. 1984)

16
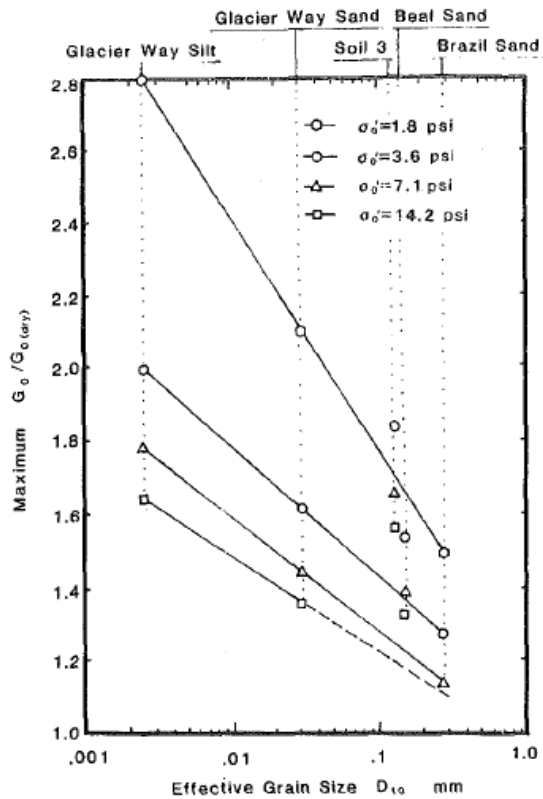
Figure 2.14: Variation of G_o/G_o (dry) with effective grain size (Wu et al. 1984)

Ray and Woods (1988) by performing resonant column test and torsional shear test on sands and silts concluded that shear modulus of sand increases with increase in number of cycles. However, the shear modulus of silt decreases with increase in number of cycles for silt. It is also observed that damping ratio decreases with the increase in number of cycles for all soils. Damping ratios can decrease to as low as 50 % at the end of 200 cycles. Saxena and Reddy (1989) performed resonant column tests on Montery No. 8 sand and proposed equations for the calculation of small strain shear modulus and small strain Young's modulus. Empirical equations were also proposed to calculate Poisson's ratio from small strain shear modulus of sand.

Dobry and Vucetic (1987) conducted an extensive review on the dynamic properties and seismic response of clays and discussed the influence of different parameters on the small strain shear modulus (G_{max}), modulus reduction (G/G_{max}) and damping ratio (D) for normally consolidated and moderately over-consolidated clays. Table 2.2 gives effect of increase of different parameters on dynamic properties of clays.

17

Table 2.2: Test procedures for measuring dynamic properties of soil (Seed and Idriss 1970)

Increasing factor	Small strain shear modulus (G_{max})	Normalized shear modulus (G/G_{max})	Damping ratio (D)
Confining pressure	Increases	Stays constant or increases	Stays constant or decreases
Void ratio	Decreases	Increases	Decreases
Geological age	Increases	May increase	Decreases
Overconsolidation ratio (OCR)	Increase	Not affected	Not affected
Plasticity Index	Increases if OCR>1 Stays constant if OCR=1	Increases	Decreases
Cyclic strain	-	Decreases	Increases
Frequency of cyclic loading	Increases	Probably not affected if G and G_{max} are measured at same frequency	Stay constant or may increase
Number of loading cycles (N)	Decreases after N cycles of large cyclic strain but recovers later with time	Decreases after N cycles of large cyclic strain (G_{max} measured before N cycles)	Not significant for moderate cyclic strain and number of loading cycles

To understand the influence of degree of saturation on the small strain shear modulus, Qian et al. (1993) performed resonant column tests on different types of natural sands. Figure 2.15 gives the variation of G/G_{dry} with degree of saturation for different confining pressures. It is observed that small strain shear modulus of sand shows a peak value at an optimum degree of saturation (about 3 %). This is due to the presence of capillary suction in partially saturated soil. This increase in shear modulus is more pronounced at lower values of confining pressure. It can also be seen that there is no influence of confining pressure on optimum degree of saturation.

18
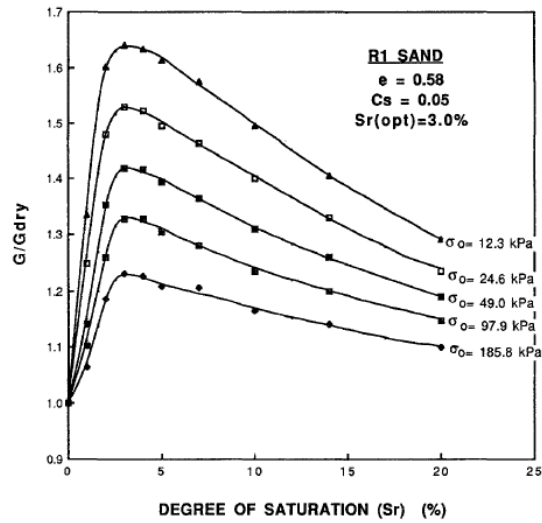
Figure 2.15: Variation of G_o/G_{dry} with degree of saturation for different confining pressures (Qian et al. 1993)

Figure 2.16 gives the variation of G/G_{dry} with degree of saturation for different void ratios. It can be observed that the increase in shear modulus with saturation is more significant for soil sample having lower void ratios. The optimum degree of saturation increases with the increase in void ratio.
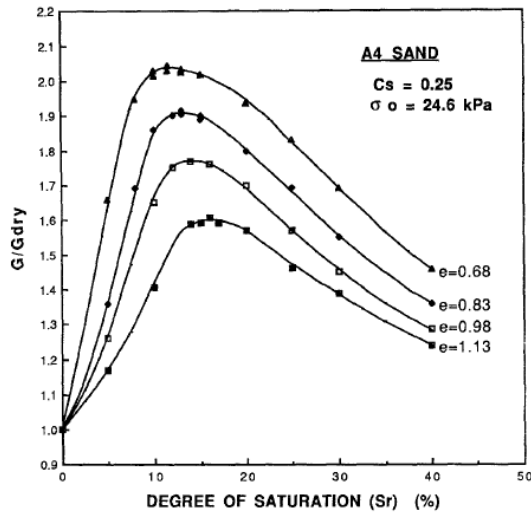
Figure 2.16: Variation of G_o/G_{dry} with degree of saturation for different void ratios (Qian et al. 1993)

19

Souto et al. (1994) by compared results obtained from resonant column tests and bender elements tests on sands, gravels, tills and rocks and stated that bender element gives higher value of test results compared to resonant column tests for confining pressure of 100 kPa and above and grain size of greater than 8 mm. Lo Presti et al. (1997) performed resonant column tests on sand and observed that shear modulus increases and damping ratio decreases with the increase in number of loading cycles. It is also stated that shear modulus and damping ratio are almost insensitive to loading frequency. Cascante et al. (1998) discussed the procedure and data reduction for performing flexural tests using resonant column apparatus. It was observed that longitudinal and shear waves are affected by state of stress and are influenced by stress history to a lesser extent.

Kumar and Madhusudhan (2010) performed bender and extender element tests on sands of three different particle sizes. Figures 2.17, 2.18 and 2.19 give the variation of Poisson's ratio with relative density for fine grained sand, medium grained sand and coarse grained sand respectively. It can be concluded that Poisson's ratio decreases with increase in confining pressure and relative density. It can also be observed that the influence of confining pressure on Poisson's ratio is significant for fine grained sand and less for medium and coarse sand.
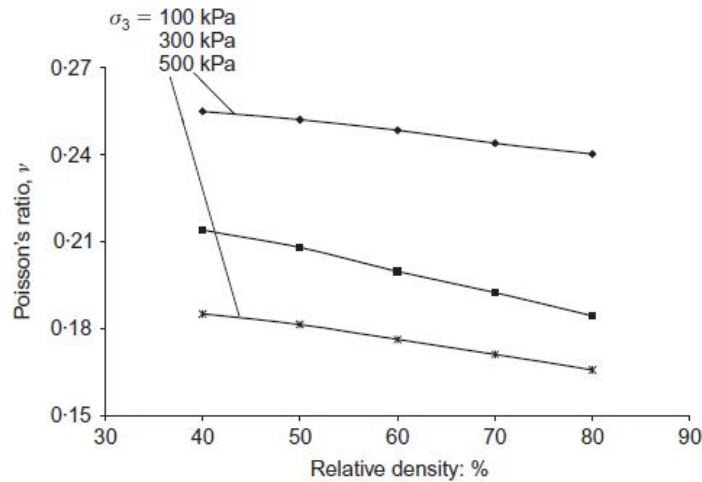
Figure 2.17: Variation of Poisson's ratio with relative density for fine grained sand (Kumar and Madhusudhan 2010)

20
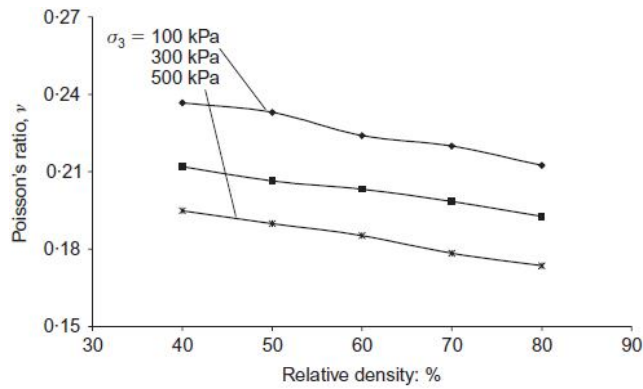
Figure 2.18: Variation of Poisson's ratio with relative density for medium grained sand (Kumar and Madhusudhan 2010)
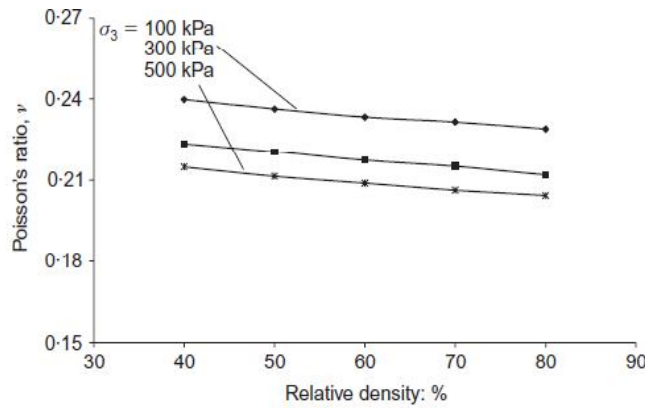
Figure 2.19: Variation of Poisson's ratio with relative density for coarse grained sand (Kumar and Madhusudhan 2010)

Figures 2.20, 2.21 and 2.22 give the variation of Poisson's ratio with small strain shear modulus (G_{max}) for fine grained sand, medium grained sand and coarse grained sand respectively. It can be seen that strain shear modulus (G_{max}) decreases almost linearly with the increase in Poisson's ratio of soil.
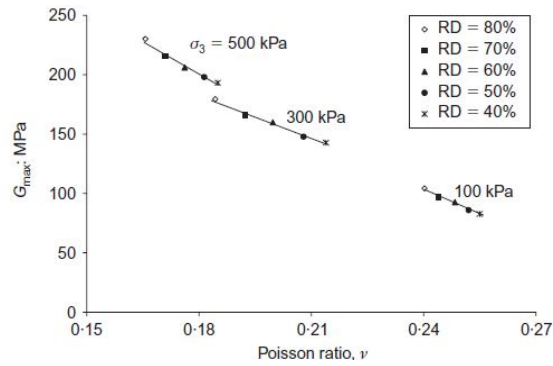
Figure 2.20: Variation of small strain shear modulus (G$_{max}$) with Poisson's ratio for fine grained sand (Kumar and Madhusudhan 2010)
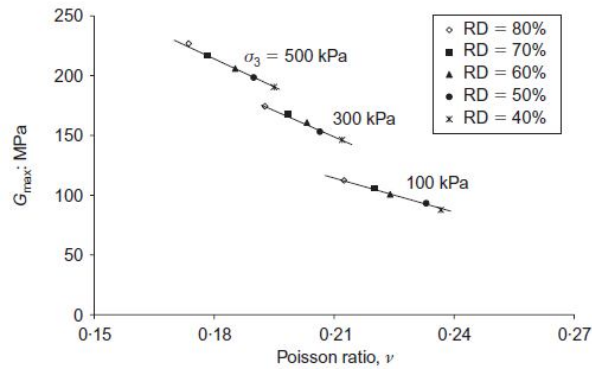
Figure 2.21: Variation of small strain shear modulus (G$_{max}$) with Poisson's ratio for medium grained sand (Kumar and Madhusudhan 2010)
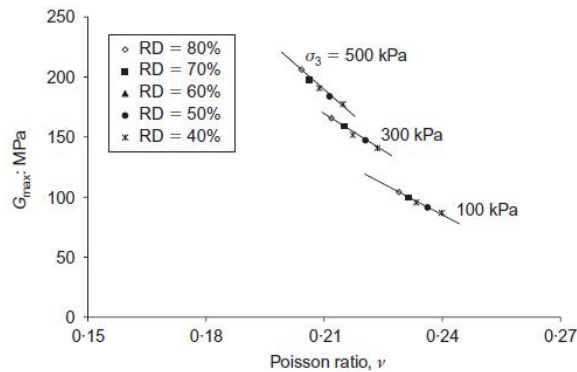
Figure 2.22: Variation of small strain shear modulus (G$_{max}$) with Poisson's ratio for coarse grained sand (Kumar and Madhusudhan 2010)

2.2   Background on Soil Stabilization

Stabilization of soil by means of addition of lime had been performed from time immemorial. Ancient Greek civilization and Mesopotamian Civilization used to stabilize earth roads and Romans and Greeks used soil lime mixtures to improve soil quality (McDowell 1959). In the United States the damage coming from expansive soil is far more than floods, hurricanes, tornadoes and earthquakes combined together (Jones and Holtz, 1973). In the United States, stabilization of soil by means of hydrated lime was first reported by McCaustland way back in 1925. National Lime Association of America (1954), Jones (1958) and Lund and Ramsey (1959) suggested the stabilization of expansive soils using hydrated lime and Portland cement to improve plasticity index of expansive soils. McDowell (1959) described the stabilization of Texas soil using lime and lime fly ash stabilization. Eades and Grim (1966) described a quick test to obtain the optimum lime content required to fulfill initial reactions and provide adequate lime for long term strength gain. This test requires sufficient lime to be added to the soil to satisfy all immediate reactions and still provide sufficient residual lime to maintain pozzolanic reactions. The addition of lime creates a high pH environment to dissolve the silica and alumina. It also provides sufficient free calcium for long term strength gain by pozzolanic reactions. Eades et al. (1963) observed that stabilization of soils of different morphology requires different quantity of limes. Thompson (1966) stated that stabilization of soil using lime occurs through four mechanisms: 1) cation exchange 2) flocculation 3) carbonation reactions 4) pozzolanic reactions. The first two mechanisms result in improvement in workability and occur as a result of change in charges of the clay. Saride et al. (2013) observed that lime is more effective than cement in reducing the plasticity index of expansive organic clay. The authors observed an increase in the UCS of both lime and cement treated organic expansive soils are reduced after 28 days of curing period due to organics.

There are several research studies indicating the utilization of low calcium based stabilizers such as ground granulated blast furnace slag (GGBFS), fly ash, bottom ash, pond ash etc. to treat the expansive soils [54-57]. However, fly ash is a high potential stabilizer as it generally contains sufficient amount of calcium oxide (CaO), silicon dioxide (SiO_2) and aluminum oxide (Al_2O_3) along with other required basic mineral oxides necessary for forming pozzolanic compounds. Fly ash is classified as either class C or F based on the available CaO content in it. According to American Society for Material and Testing (ASTM C618-12a) a fly ash can be classified as class C if the CaO content is more than 10% and class F is the CaO is less than 10%. Ferguson (1993) used fly ash produced from sub-bituminous soil to reduce the swell potential of expansive soil and to improve the

capacity of the subgrade to carry traffic loads. Nicholson and Kashyap (1993) by using high quality fly ash admixtures to treat poor to marginal type of soil reported an improvement in the UCS, increase in California bearing ratio (CBR) of more than 10 times, reduction in plasticity, reduction in swell and increased workability of the treated soils. Mishra (1998) used Class C fly ash to treat four different types of clays and observed that there was an improvement in UCS with the addition of fly ash, however, compaction delays causes significant reduction in UCS of the treated soils. Cokca (2001) by treating expansive soil with both high calcium and low calcium observed that there is a reduction in plasticity index, swell potential and activity of the soil with increase in the percentage of stabilizer and curing periods. Pandian and Krishna (2003) observed a significant improvement in CBR values of black cotton soils when treated with class C fly ash. Edil et al. (2006) by treating soft fine grain soil with class C and class F fly ash, observed a significant improvement in CBR and resilient modulus (M_r) of the soil.

2.3   Dynamic Properties of Stabilized Soils

Limited studies are performed to determine the dynamic properties of untreated and treated expansive soils (Chae and Chiang 1978, Au and Chae 1980, Fahoum et al. 1996, Hoyos et al. 2004).Chae and Chiang (1978) made the first study to determine the dynamic properties of treated and untreated soils. Resonant column (RC) tests were performed on uniform sand and silty clay with cement, lime and lime-fly ash mixes. It was observed that dynamic properties can be improved by treatment. Similar observation was made by Au and Chae (1980) by performing resonant column tests on expansive soil treated with salts, lime, and lime-salt mixtures.

Fahoum et al. (1996) performed a series of cyclic triaxial tests on lime treated sodium montmorillonite clay and calcium montmorillonite clay. Figures 2.23 and 2.24 give the variation of G(treated)/G(untreated) with percentages of lime for sodium and calcium montmorillonite clays respectively. It was observed that G(treated)/G(untreated) ratio increases with the increase in lime dosage. This is due to higher rigidity of treated soils.
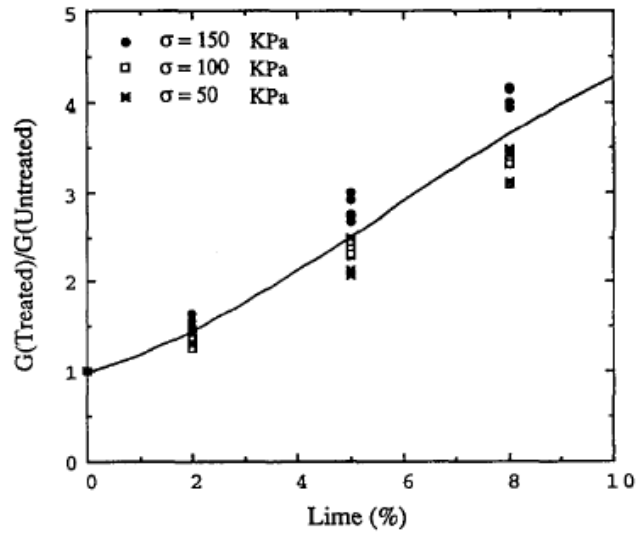
Figure 2.23: Variation of G(treated)/G(untreated) with percentages of lime for sodium montmorillonite clay (Fahoum et al. 1996)
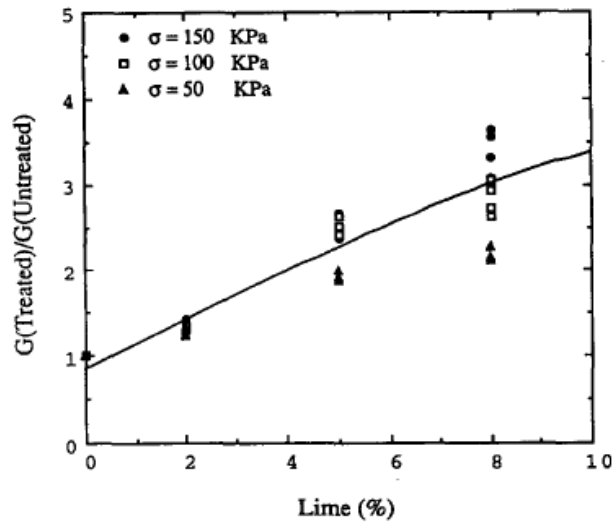
Figure 2.24: Variation of G(treated)/G(untreated) with percentages of lime for calcium montmorillonite clay (Fahoum et al. 1996)

25

Figures 2.25 and 2.26 give the variation of D(treated)/D(untreated) with percentages of lime for sodium and calcium montmorillonite clays respectively. It was observed that D(treated)/D(untreated) ratio decreases with the increase in lime dosage.
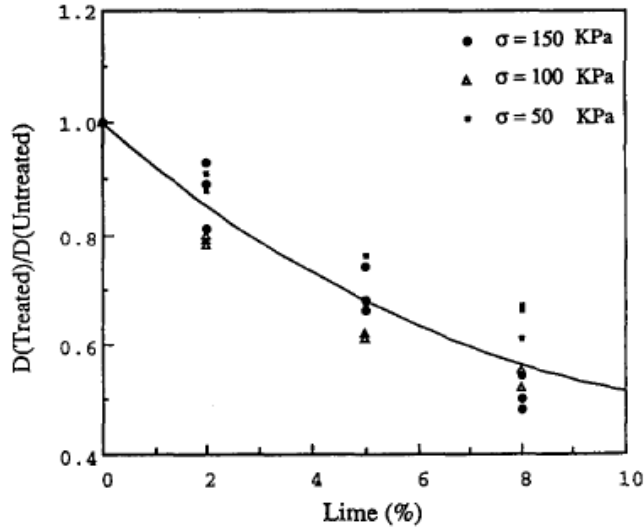
Figure 2.25: Variation of D(treated)/D(untreated) with percentages of lime for calcium montmorillonite clay (Fahoum et al. 1996)
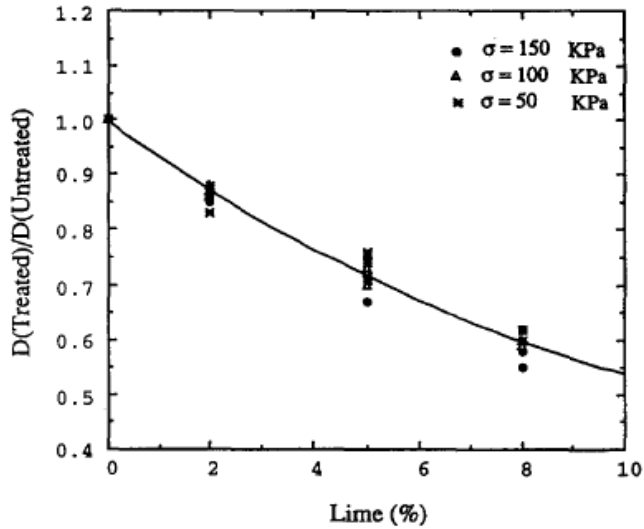
Figure 2.26: Variation of D(treated)/D(untreated) with percentages of lime for sodium montmorillonite clay (Fahoum et al. 1996)

Hoyos et al. (2004) performed resonant column tests on chemically treated sulfate rich clays to understand the influence of compaction moisture content on dynamic properties of soil. Figure 2.27 gives the variation of small strain shear modulus (G_{max}) with confinement duration for different compaction moisture contents for Class F fly ash treated clay. It was observed that for class F fly ash stabilized clays, maximum shear modulus is observed when the soil-fly ash mixture is compacted at its optimum moisture content. Figure 2.28 presents the variation of small strain damping ratio (D_{min}) with isotropic confinement for different compaction moisture contents for Class F fly ash treated clay. It was observed that specimens prepared at 95 % wet of optimum give higher values of small strain damping ratio (D_{min}).
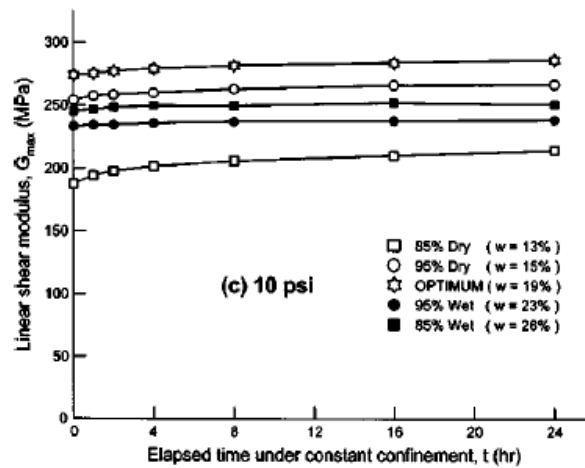
Figure 2.27: Variation of small strain shear modulus (G_{max}) with confinement duration for different compaction moisture contents for Class F fly ash treated clay (Hoyos et al. 2004)
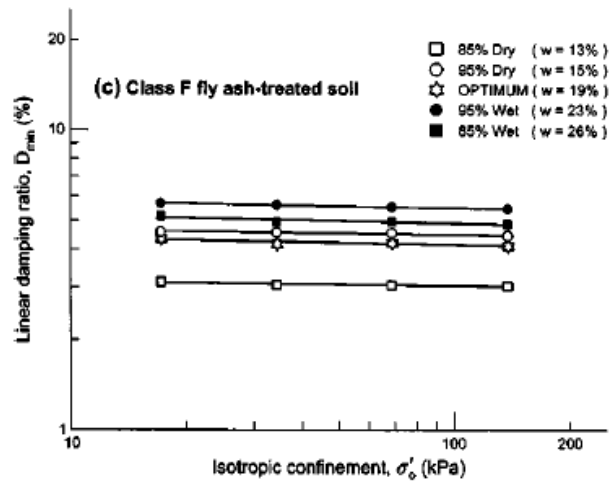
Figure 2.28: Variation of small strain damping ratio (D$_{min}$) with isotropic confinement for different compaction moisture contents for Class F fly ash treated clay (Hoyos et al. 2004)

28

Chapter 3

Resonant Column Test and Calibration

3.1 Overview

The resonant column test has been widely used to determine the dynamic properties of soil way back from 1930's, when it was developed by two Japanese engineers [25-26]. In United States, the earliest resonant column device was used to determine the shear velocities of rock specimens [62]. In 1960's, the resonant column apparatus has been used to determine the dynamic properties of soil by several researchers [1, 64, 65]. It has been subsequently modified to apply anisotropic stress [31], testing hollow specimen [65], and application of high value of shear strain [66]. During the 1970's, Professor Stokoe and his students from University of Texas at Austin have developed a new version of fixed free resonant column apparatus which has been used subsequently for four decades now. American Society of Testing Materials [6] has standardized the Stokoe version of Resonant Column Apparatus. Kim and Stokoe (1994) further modified the resonant column apparatus to perform torsional shear test in resonant column apparatus. Cascante et al. (1998) gave the testing procedure and data reduction to perform flexural tests in resonant column apparatus. Further improvements were made by researchers to perform suction controlled resonant column tests [68-69] to understand the dynamic behavior of unsaturated soils. At present, resonant column test is considered as the most reliable test for the determination of dynamic properties of soils.

3.2 Fundamentals of resonant column tests

3.2.1 Introduction

In this test, a cylindrical soil specimen is subjected to a torsional or flexural excitation by using an electromagnetic drive system and then looking for the resonant frequency. Figure 3.1 gives the electromagnetic drive system used in the present study. The drive system consists of four electromagnets.

For performing the test in both torsional as well as flexural mode, four electromagnets were used in two different directions. Figure 3.2 gives the arrangement of magnets for performing both torsional test and flexural test. During the torsional mode, the two pairs of magnets work in series which apply a net torque to the soil specimen. For applying the flexural excitation, only one pair of magnetic coils work to apply a net horizontal force at the top of the specimen. Initially a low value of frequency is applied. After that the frequency is gradually increased. The frequency at which it shows a peak value of amplitude gives the resonant frequency of the specimen.
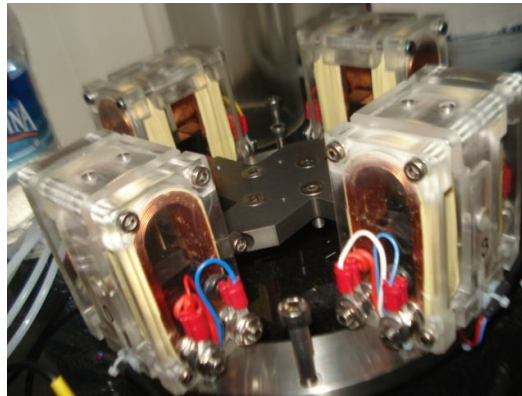
Figure 3.1: Electromagnetic drive system
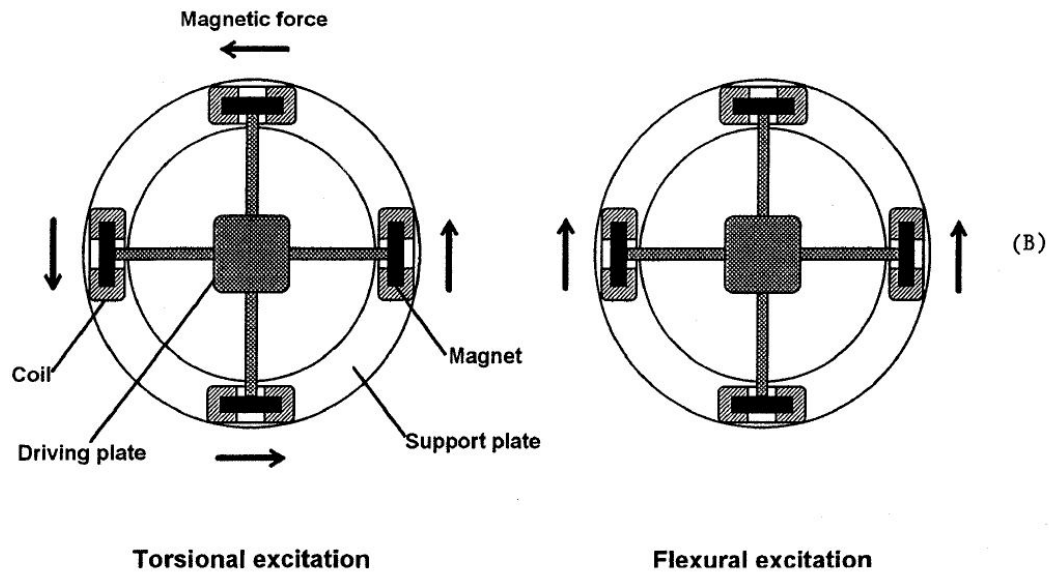
Figure 3.2: Torsional and flexural excitation (Cascante et al. 1998)

3.2.2   Types of resonant column

There are a variety of resonant column apparatus that had been developed throughout the course of time. The three most commonly used resonant column apparatus based on boundary conditions are free-free, fixed-free and fixed-fixed type. The fixed-free type of resonant column test is the most widely used to determine dynamic properties of soils. In this apparatus, the bottom of the specimen is fixed to the pedestal while the top surface is left free to vibrate.

3.3   Testing procedure

The resonant column apparatus used in the present study is developed by GDS Instruments Limited. It is a Stokoe type fixed free resonant column apparatus. Figure 3.3 gives the resonant column used in the present study. Figure 3.4 gives the arrangement of resonant column apparatus. When resonant column test is started, the computer sends an instruction to the resonant column controller to generate a sine wave signal of desired amplitude. The signal is then forwarded to the power amplifier to magnify and then sent back to the resonant column controller. The amplified signal is then split into four equal parts sent to four coils in the R. C. unit. The specimen is vibrated by means of torque generated by the electromagnetic drive system. The charge signal recorded by the accelerometer at the time of vibration is sent to the charge amplifier and then further transferred to the computer by means of resonant column controller. The computer displays the amplitude vs. frequency

31

plot and the frequency at which it gives the peak value of amplitude signifies the resonant frequency of the specimen.
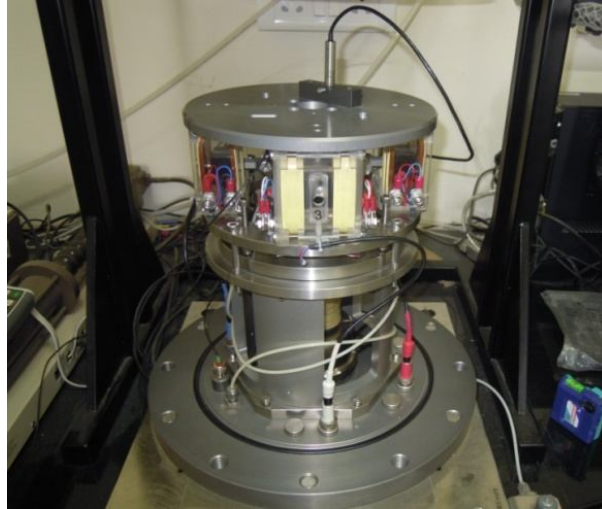
Figure 3.3: Fixed-Free resonant column used in the study
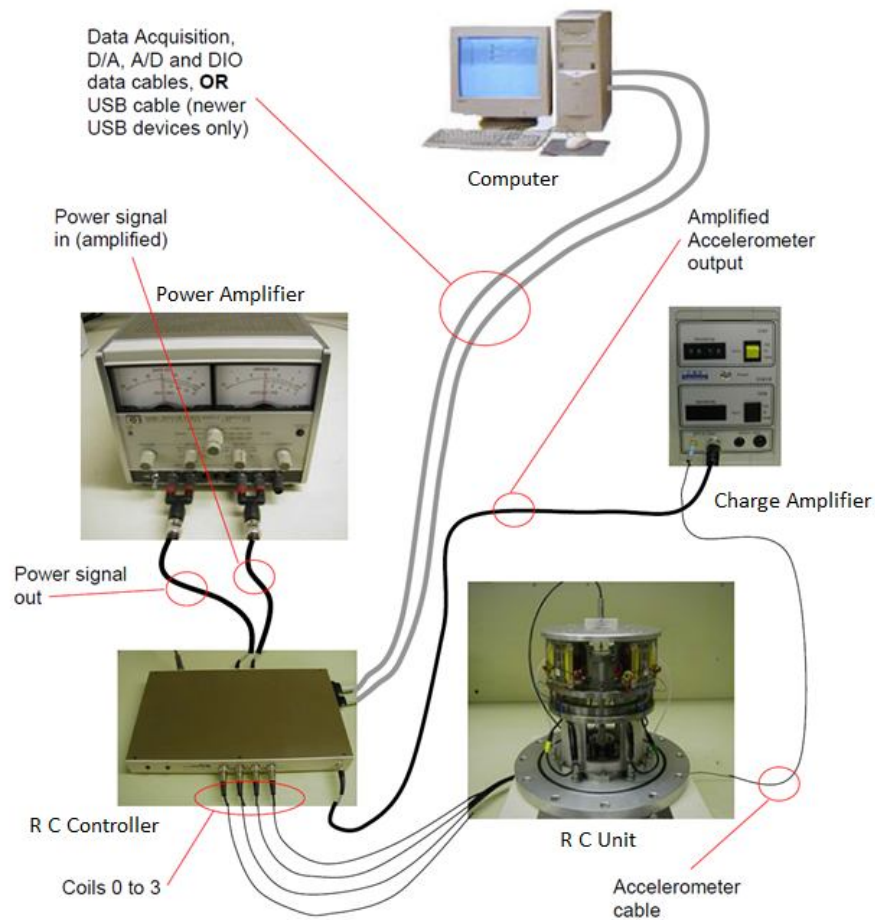
Figure 3.4: Arrangement of resonant column apparatus (GDS Handbook, 2008)

3.3.1 Determination of shear modulus

The shear modulus, G is determined from the resonant frequency and specific characteristics of the device.

$$G = \rho \cdot V_s^2 \tag{3.1}$$

where, G =shear modulus of the soil sample; V_s = shear wave velocity can be obtained from equation (3.2).

Shear wave velocity can be obtained from the resonant frequency.

$$V_s = \frac{2\pi f L}{\beta} \tag{3.2}$$

where, f = resonant frequency (Hz); L = length of the specimen; β = a factor that can be obtained from equation (3.3).

$$\frac{I}{I_o} = \beta.\tan(\beta) \tag{3.3}$$

where, I = mass polar moment of inertia of the soil specimen; and I_o = mass polar moment of inertia of the electromagnetic drive system.

The mass polar moment of inertia of the electromagnetic drive system can be determined experimentally which is discussed in section 3.4.

3.3.2   Determination of damping ratio

After the resonant frequency was determined, the excitation power is switched off and the specimen was allowed to freely vibrate. The damping is determined by logarithmic decrement method from the free vibration curve.

$$D(\%) = \frac{1}{2\pi n}\ln\left(\frac{Z_o}{Z_n}\right) \tag{3.4}$$

where, D =damping ratio; Z_o =vibration amplitude after excitation power is switched off; Z_n =vibration amplitude after n[th] cycle; n =number of cycles.

3.3.3   Determination of Poisson's ratio

Resonant column tests have to be performed in both torsional and flexural modes of excitation for determining the Poisson's ratio of the soil sample. Cascante et al. (1998) gave the circular resonant frequency for a soil specimen of length L by using Rayleigh's method and considering N distributed mass m_i as:

$$\omega_f^2 = \frac{3EI_b}{L^3\left[\frac{33}{140}m_T + \sum_{i=1}^{n}m_i h(h0_i,h1_i)\right]} \tag{3.5}$$

$$h(h0i,h1i) = mi\left[1 + 3\frac{(h1i + h0i)}{2L} + \frac{3}{4}\left(\frac{h1_i^2 + h1ih0i + h0_i^2}{L}\right)^2\right] \tag{3.6}$$

where, $h0_i$ and $h1_i$ are the heights at the bottom and top respectively, of mass i, measured from the top of the soil specimen; ω_f = circular resonant frequency in flexural mode; E = Young's modulus of the soil specimen; I = area moment of inertia; m_T = mass of the soil specimen.

Equation (3.6) can also be expressed in terms of centre of gravity, y_{ci} and area moment of inertia, with respect to centre of gravity, I_{yi} of each mass, m_i.

$$h(y_{ci}, I_{yi}) = 1 + \frac{3y_{ci}}{L} + \frac{9}{4L^2}\left[\frac{I_{yi}}{m_i} + y_{ci}^2\right] \qquad (3.7)$$

Due to complex geometry, area moment of inertia I_y for the drive system is determined by performing calibration exercise. The calibration test for the determination of area moment of inertia I_y for the drive system is discussed in section 3.5.

Now the Poisson's ratio is determined using:

$$\upsilon = \frac{1}{2}\frac{V_{LF}^2}{V_s^2} - 1 \qquad (3.8)$$

where, V_{LF} = longitudinal wave velocity which can be calculated using equation (3.9).

V_s = shear wave velocity calculated using equation (2).

$$V_{LF} = \sqrt{\frac{E}{\rho}} \qquad (3.9)$$

where, E = Young's modulus of the soil specimen determined using equation (3.5); ρ = density of the soil specimen.

3.4   Calibration for performing torsional test

Calibration tests are performed to determine the mass polar moment of inertia I_o of the drive system. The torsional tests were performed by substituting aluminum calibration bars in place of soil specimen of known mechanical properties. Figure 3.5 gives the calibration bars of different sizes and calibration weights used in the present study. Figure 3.6 gives the test setup for performing calibration tests on aluminum calibration bars.

In the resonant column torsion test, the specimen and the drive system can be assumed to be a torsional pendulum with single degree of freedom. The drive system and attached masses are the pendulum mass and the specimen is the torsional spring. For the above system, the equation of motion can be described as:

$$\omega_n = \sqrt{\frac{k}{I}} \tag{3.10}$$

where, ω_n = natural circular frequency of vibration of specimen, k=stiffness of the soil, I=mass polar moment of inertia of all masses at top of specimen.

Figure 3.5: Calibration bars and calibration weights
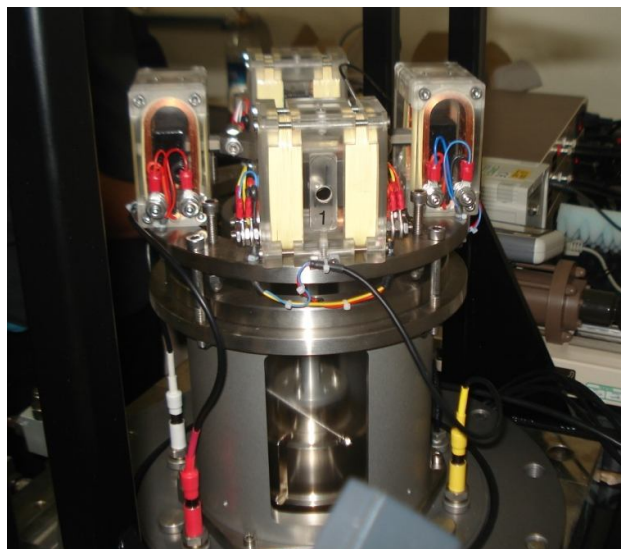
Figure 3.6: Setup for performing calibration tests

A linear expression can be used to express the additional mass in terms of ω_n is given below:

$$I_{am} = \frac{k}{\omega^2} + I_o \qquad (3.11)$$

where, I_{am} = mass polar moment of inertia of the added mass.

By plotting I_{am} against $\left(\dfrac{1}{\omega^2}\right)$, a straight line can be obtained and the slope of the line gives the mass polar moment of inertia of the drive system I_o

Figure 3.7 gives the schematic diagram of the calibration bar with top cap, drive system and added mass attached on top of it. Table 3.1 gives the results obtained from performing calibration tests on aluminium bars of three different bar diameters (d_w) of 10 mm, 12.5 mm, 15 mm.
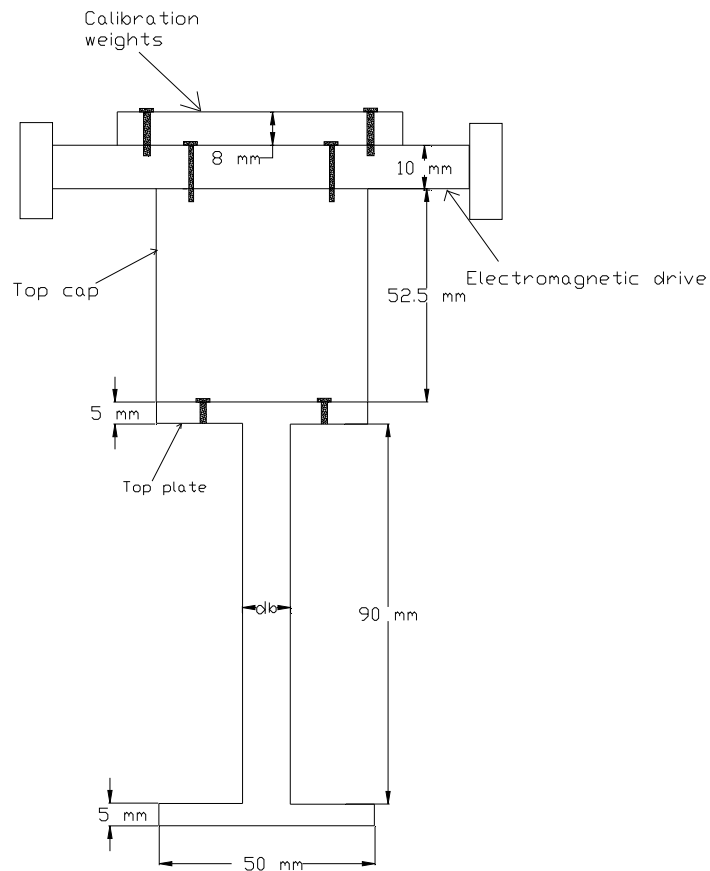
Figure 3.7: Diagram of calibration bar with the different components

3.4.1 Mass polar moment of inertia of top plate

Mass polar moment of inertia of the top plate is determined because calibration weights are only fixed to the top plate.

Diameter of calibration bar=0.05 m.

Height of top plate= 0.005 m.

Volume=9.82×10^{-6} m^3.

Density of aluminium= 2698 kg/m^3.

Mass of the top plate=0.0265 kg

Mass polar moment of inertia of top plate=8.28×10^{-6} kgm^2

3.4.2 Mass polar moment of inertia of calibration weights

Width of calibration weights=0.02 m.

Length of calibration weights = 0.1 m.

Mass of calibration weights =0.132 kg.

Mass polar moment of inertia of calibration weights=1.14×10^{-4} kgm^2.

Table 3.1: Results obtained by performing torisonal calibration tests

Bar diameter, d_b (mm)	Elements	Mass polar moment of inertia of the system (kgm^2)	Total Mass polar moment of inertia of the system, I_{am} (kgm^2)	Resonant frequency (Hz)	Angular velocity, ω (rad/sec)	ω^2	$\dfrac{1}{\omega^2}$
10	Top plate	8.28×10^{-6}	8.28×10^{-6}	41.9	263.27	69308.7	1.44×10^{-5}
	Weight 1	1.14×10^{-4}	1.23×10^{-4}	41.3	259.50	67337.9	1.49×10^{-5}
	Weight 2	1.14×10^{-4}	2.37×10^{-4}	40.7	255.75	65395.6	1.53×10^{-5}
	Weight 3	1.14×10^{-4}	3.51×10^{-4}	40	251.32	63165.47	1.58×10^{-5}
12.5	Top plate	8.28×10^{-6}	8.28×10^{-6}	64.5	405.2655	164240.1	6.09×10^{-5}
	Weight 1	1.14×10^{-4}	1.23×10^{-4}	63.5	398.9823	159186.8	6.28×10^{-5}
	Weight 2	1.14×10^{-4}	2.37×10^{-4}	62.6	393.3274	154706.4	6.46×10^{-5}
	Weight 3	1.14×10^{-4}	3.51×10^{-4}	61.7	387.6725	150290	6.65×10^{-5}
15	Top plate	8.28×10^{-6}	8.28×10^{-6}	91.8	576.7964	332694.1	3.01×10^{-5}
	Weight 1	1.14×10^{-4}	1.23×10^{-4}	90.5	568.6283	323338.1	3.09×10^{-5}
	Weight 2	1.14×10^{-4}	2.37×10^{-4}	89.2	560.4601	314115.6	3.18×10^{-5}
	Weight 3	1.14×10^{-4}	3.51×10^{-4}	87.9	552.292	305026.4	3.28×10^{-5}

Figure 3.8 gives the variation of I_{am} with $\left(\dfrac{1}{\omega^2}\right)$. It is observed that linear plots are obtained when I_{am} is plotted against $\left(\dfrac{1}{\omega^2}\right)$. From the average of the y intercepts of the plots, it is possible to calculate the mass polar moment of inertia of the drive system. The mass polar moment of inertia of the drive system is obtained as *0.0037*.
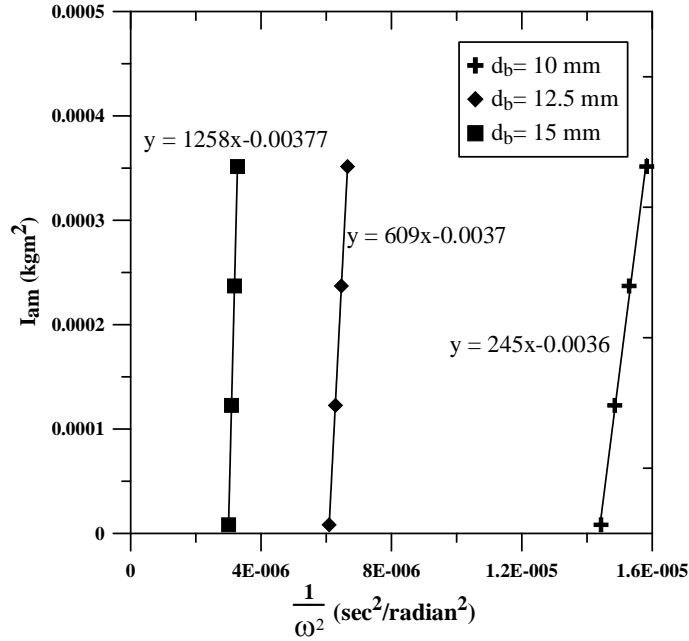
Figure 3.8: Variation of I_{am} with $\left(\dfrac{1}{\omega^2}\right)$

3.5 Calibration for performing flexural test

Due to complex geometry of the electromagnetic drive system, an experimental determination of area moment of inertia (I_y) of the drive system is adopted. In this technique, a single calibration bar and a single calibration weight is used to determine the area moment of inertia (I_y) of the drive system by using equation (3.5).

The process of calibration involves two steps:

a) Determination of resonant frequency in flexural mode of the calibration bar alone.

b) Determination of resonant frequency in flexural mode of the calibration bar with an added calibration weight.

This gives rise to two equations (3.12) and (3.13) as given below:

$$\omega_{f1}^2 = \frac{3EI_b}{L^3\left[\dfrac{33}{140}m_T + m_a h_a + m_b h_b + m_x h_x\right]} \tag{3.12}$$

$$\omega_{f2}^2 = \frac{3EI_b}{L^3\left[\dfrac{33}{140}m_T + m_a h_a + m_b h_b + m_x h_x + m_{am} h_{am}\right]} \tag{3.13}$$

40

where, m_T, m_a, m_b, m_x, m_{am} are the masses of calibration bar excluding the top plate, mass of the top plate of the calibration bar, mass of the top cap, mass of drive system and mass of the added calibration mass respectively and h_a, h_b, h_{am} are the equivalent heights of top plate of the calibration bar, top cap, and added calibration mass and can be determined by using equation (3.6). Due to complex geometry of drive system, the equivalent height of drive system, h_x is the unknown in the equations. Solving these two equations, h_x of the electromagnetic drive system can be determined. Knowing the value of h_x, the area moment of inertia (I_y) of the drive system can then be determined from the equation (3.7). The area moment of inertia (I_y) of the electromagnetic drive system used in the present study is found to be 0.004 m^4.

3.6   Summary

In this chapter, the fundamentals of resonant column tests are discussed. The testing procedure and the data reduction for obtaining shear modulus, damping ratio and Poisson's ratio were mentioned. Moreover, calibration exercises for performing flexural and torsional tests are also elaborately covered. From the calibration tests, the mass polar moment of inertia (I_o) and area moment of inertia (I_y) of the drive system are obtained as 0.0037 and 0.004 respectively.

Chapter 4

Material Used and Sample Preparation

4.1   Introduction

In this chapter, the properties of different materials used and sample preparation techniques adopted in the present study are presented. The material properties of sand, expansive soil and the stabilizer (fly ash) are stated first and then the sample preparation procedures are elaborately discussed.

4.2   Material properties

4.2.1   Sand

The sand used in this study is clean sand free from fines content. The sand is properly washed to remove any fines content passing 75 micron sieve present in the sand. The grain size distribution, maximum and minimum void ratio and specific gravity tests were performed on the sand. The material properties of the sand are given in Table 4.1. The grain size distribution curve of the sand is shown in Figure 4.1. The sand is classified as poorly graded sand with letter symbol SP according to the unified soil classification system (USCS).

4.2.2   Expansive soil

The soil used in this study is dark brownish clay obtained from Indian Institute of Technology Hyderabad campus having a natural moisture content of 5 %. The grain size distribution of the expansive clay is obtained according to ASTM D422-63 and D 1140. Figure 1 gives the grain size distribution curve for the soil used in the present study. The fines content (passing 75µ size) of the soil is 70 % and clay fraction is 40 %. The Atterberg limits including liquid limit (LL), plastic limit (PL) and plasticity index (PI) of the soil are

42

obtained according to ASTM D 4318 and observed to be 58 %, 20 % and 38 % respectively. The soil classification based on American Association of State Highway and Transportation Officials (AASHTO) and Unified Soil Classification System (USCS) is A-7-6 and CH respectively. The soil is having a free swell index of 50 % and can be classified as a moderately expansive soil according to American Society for Testing and Materials standard (ASTM D2487-11); IS 1498-1970; Sridharan and Prakash (2000). In addition, the degree of expansiveness of the soil is *high* based on the LL value (Chen 1975, IS 1498-1970). However, based on the PI of the soil, the degree of expansion of the soil can be considered as *medium* (Chen, 1975, Holtz and Gibbs, 1956, Sridharan and Prakash, 2000). The specific gravity of the soil (G_s) is 2.8. Standard Proctor's compaction test is performed on the soil according to ASTM D698-12e and observed that the OMC of the soil is 22 % and MDD is 1.68 g/cc. Figure 4.3 gives the e-log p plot of the expansive soil used. From the Figure, the swell pressure of the expansive soil is obtained as 0.8 kg/cm^2. The coefficient of compression (C_c), coefficient of recompression (C_r) and pre-consolidation pressure of the soil are 0.26, 0.083 and 0.7 kg/cm^2 respectively.

Table 4.1 Basic Properties of sand

Property	Value
Specific gravity, G_s	2.63
Maximum dry density ($\gamma_{d\ max}$): kN/m³	15.84
Minimum dry density ($\gamma_{d\ min}$): kN/m³	13.98
Maximum void ratio (e_{max})	0.88
Minimum void ratio (e_{min})	0.66
D_{10}: mm	0.47
Coefficient of uniformity, C_u	2.55
Coefficient of curvature, C_c	0.87
Degree of roundness of particle	Angular

4.2.3   Fly ash

The fly ash obtained from Neyveli Lignite Corporation Limited, Tamil Nadu is used in the present study. The specific gravity of the fly ash is 2.16. The gradation of the fly ash is shown in Figure 4.4. The effective particle size, D_{10} of the fly ash used is 0.0195. The fines content in the fly ash is 52 %. The fly ash is non plastic with a liquid limit of 36 %. The classification of fly ash based on USCS is ML. Chemical composition of the fly ash was determined by performing X-Ray Florescence (XRF) test. The chemical compounds which are responsible for pozzolanic reactions are given in Table 4.2. As the amount of calcium oxide (CaO) is 16.5 %, fly ash can be classified as Class C fly ash based on ASTM C618-12a.
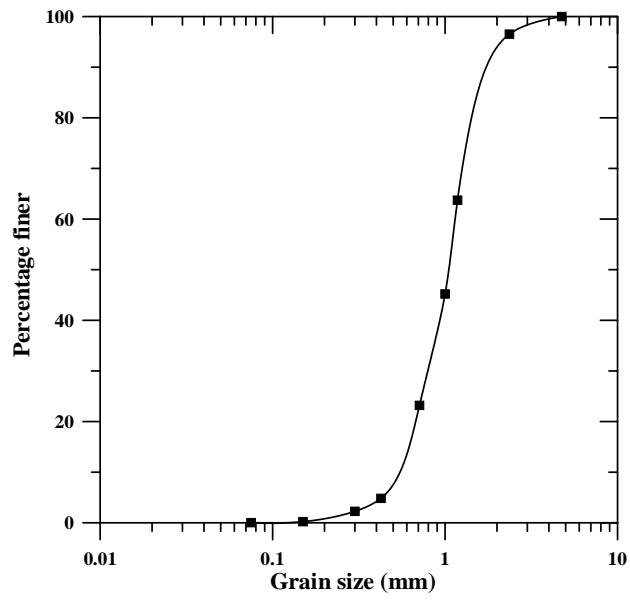
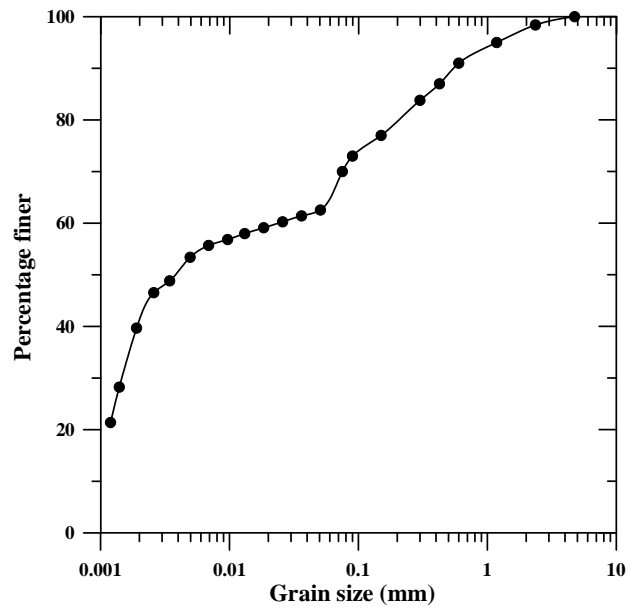**Figure 4.1: Grain size distribution curve for sand**

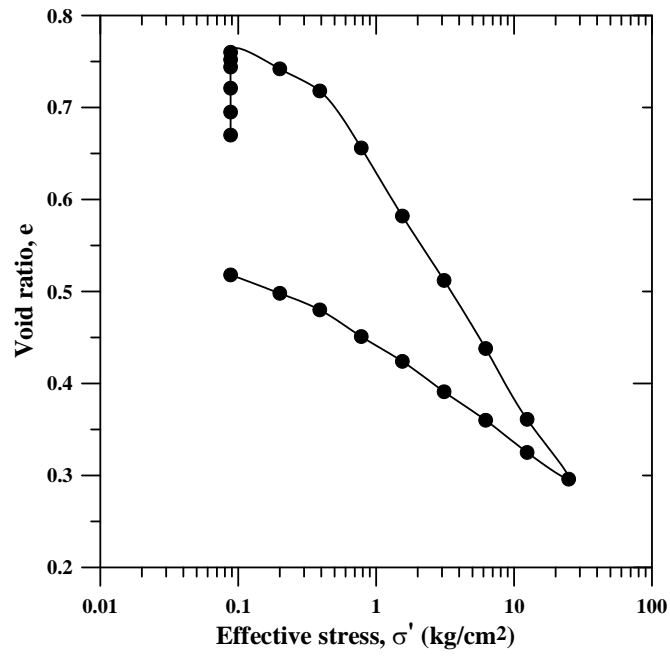**Figure 4.2: Grain size distribution curve of expansive clay**
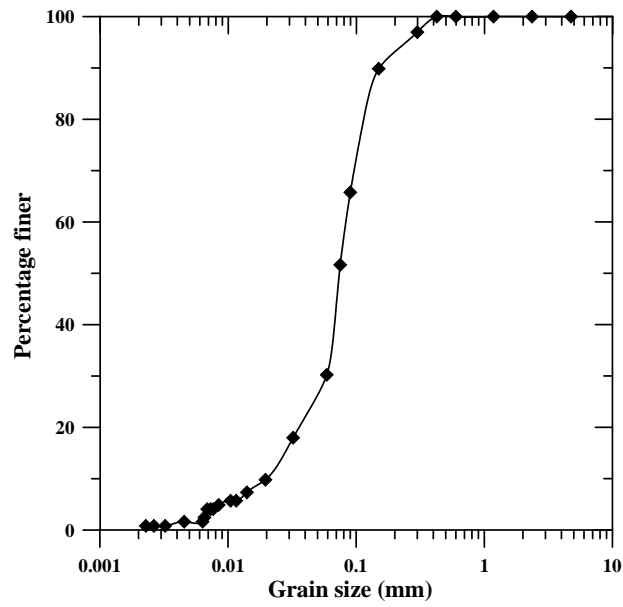
Figure 4.3: e-log p curve of expansive clay

Figure 4.4: Grain size distribution curve of fly ash

46

Table 4.2 Chemical composition of fly ash

Chemical compound	Quantity (%)
Silicon dioxide (SiO_2)	34.52
Calcium oxide (CaO)	16.45
Iron oxide (Fe_2O_3)	4.94
Aluminum oxide (Al_2O_3)	31.87
Magnesium oxide (MgO)	3.04

4.3 Sample Preparation

4.3.1 Preparation of sand sample

The sand specimens are prepared in the resonant column apparatus itself. Figures 4.5 and 4.6 give the steps involved in the preparation of sand sample. Figure 4.5-1 shows measuring the desired quantity of sand which is calculated based on the relative density of the specimen to be prepared. Figure 4.5-2 shows rubber membrane which is connected to the bottom pedestal using O-rings. The split mould is placed outside the rubber membrane. The top part of the rubber membrane is stretched and rolled over the split mould which can be seen from the Figure 4.5-3. A constant vacuum is applied to remove the entrapped air between the split mould and the membrane, so that the membrane sticks (Figure 4.5-4). The sand is gently poured into the split mold by using a funnel (Figure 4.6-1). Then each layer is compacted by means of a tamping rod which weighs 150g (Figure 4.6-2). The sample preparation is done in 5 equal thick layers. By doing few trial sample preparations (calibration exercise), the number of blows required per layer for a desired relative density is determined. The numbers of blows were obtained as 10, 15 and 25 per layer corresponding to 30%, 50% and 75% relative densities of sand respectively. After carefully leveling the top surface of the sand layer, the top cap is placed on top of it (Figure 4.6-3). By opening the drain valve a small back pressure of -20 kPa is applied to the specimen, to keep the specimen intact. The suction which is used to hold the rubber membrane onto the split mould is then stopped and the split mould is gently dismantled and which completes the sand specimen preparation steps (Figure 4.6-4).
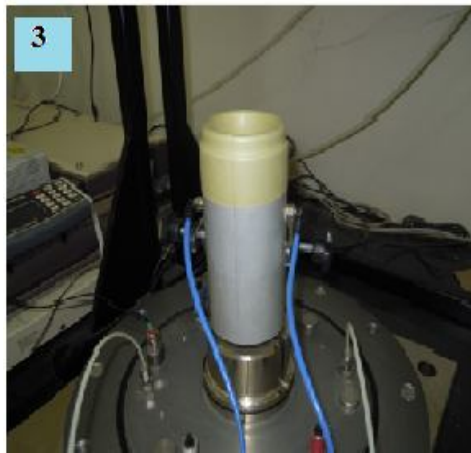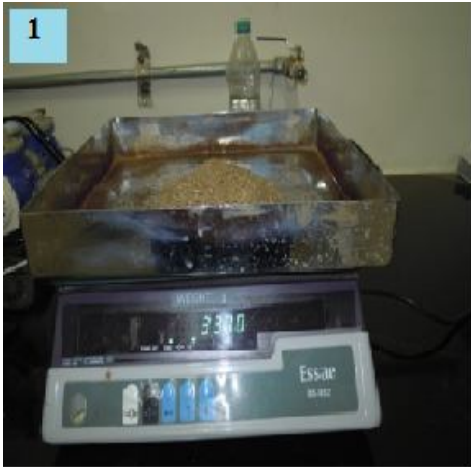
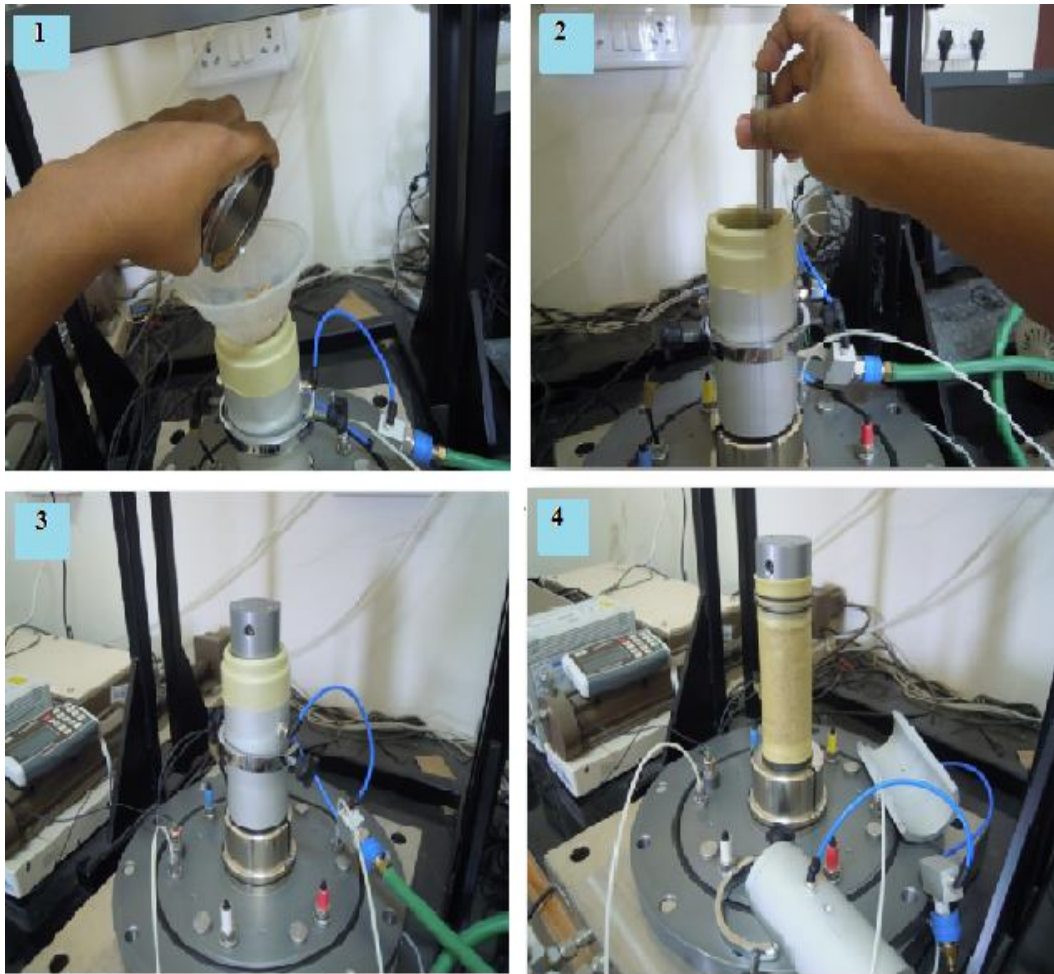**Figure 4.5: Steps involved in sand sample preparation (Part 1)**

Figure 4.6: Steps involved in sand sample preparation (Part 2)

4.3.2 Preparation of untreated and treated expansive soil

Standard Proctor's compaction tests were conducted on untreated and treated samples, prior to the preparation of soil samples for resonant column (RC) studies. For stabilization of expansive soil, fly ash content of 5 to 20% with 5% intervals was added by dry weight of the soil. Figure 4.7 gives the Proctor compaction test results for both untreated and treated soil. It is seen that with the increase in percentage of fly ash, the maximum dry density increases and optimum moisture content decreases. The increase in optimum moisture content is due to the increase of fines (fly ash) which requires higher water content due to increased specific surface area. The presence of fly ash which has a lesser specific gravity causes the reduction in the maximum dry density. The soil specimens were then prepared in a constant volume mould of size 50 mm×100 mm. Figure 4.8 shows the constant volume mould used in the present study. For the preparation of untreated sample, the dry soil was mixed properly with desired quantity of water which is calculated from the optimum moisture content of the soil obtained from standard Proctor compaction test (ASTM D698-12e). For stabilized soil, the required amount of fly ash (5 %, 10 %, 15 %, and 20 %) was first mixed with the dry soil and then water was added based on the amount calculated from the optimum moisture content of the treated soil. For obtaining a uniform mix, the mixing was done for 5 minutes. The samples were then compacted to its maximum dry density in three layers under a static compaction in a triaxial loading frame (Figure 4.9-1). After the specimen was compacted, it was extruded from the top by means of the pedestal (Figure 4.9-2). The prepared specimens are then cured for 1 day, 7 days and 28 days period in a humidity chamber to test for RC and UCS tests at a given curing time. At least two identical specimens are prepared for each combination of soil and fly ash to ensure repeatability of the test results. Triplicate samples are used when error in the measurement exceeds 5%. The cured specimen was gently placed on top of the resonant column pedestal with the help of a mould (Figure 4.9-3). The top cap was then placed on top of the specimen and the rubber membrane was stretched over the top cap and fixed with O rings (Figure 4.9-4). This concludes the sample preparation of untreated and treated expansive soils.
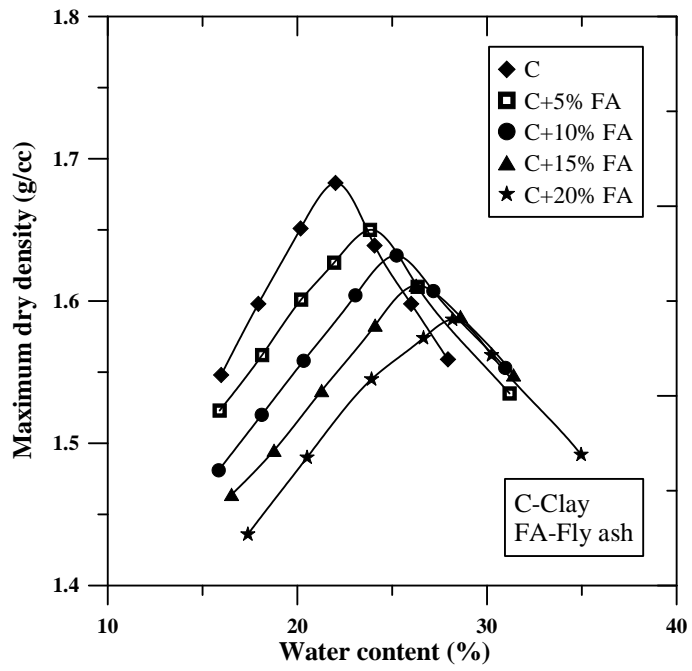
Figure 4.7: Proctor compaction characteristics of treated and untreated clay
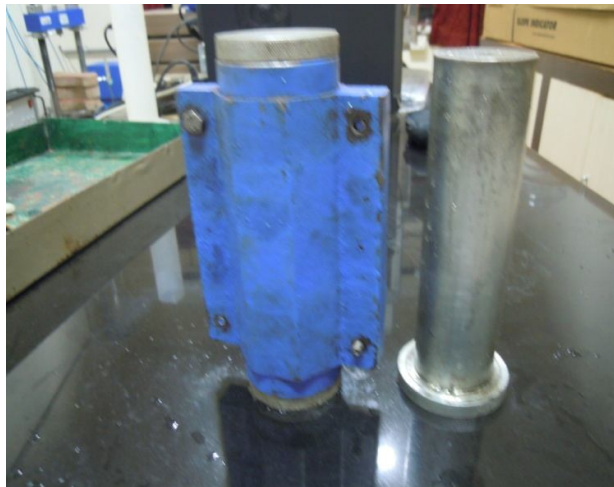
Figure 4.8: Constant volume mould

Figure 4.9: Steps involved in clay sample preparation

4.3.3 Measurement of dimension

After the sample preparation, the next step is to measure the dimension of the specimen. A small error in the measurement of dimensions of the specimen results in significant error in the measurement of the shear modulus and Poisson's ratio of the soil. Figure 4.10 shows the measurement of dimension of the sand specimen. Vernier caliper of precision of 0.01 mm was used to measure the dimension of the specimen. The diameter is measured at five different locations i.e. 10 mm, 30 mm, 50 mm, 70 mm and 90 mm from the top porous stone and average value of diameter is calculated to get an accurate estimation of the diameter of the specimen.

Figure 4.10: Measurement of dimension of specimen

4.4   Installation of testing system

After the preparation of soil sample, the test setup for performing resonant column is done as discussed below:

1. Hollow support cylinder is properly fixed to the base plate with the help of six screws (Figure 4.11-1).
2. Drainage pipes are connected to the top cap of the specimen and are used while saturating the specimen (Figure 4.11-2).
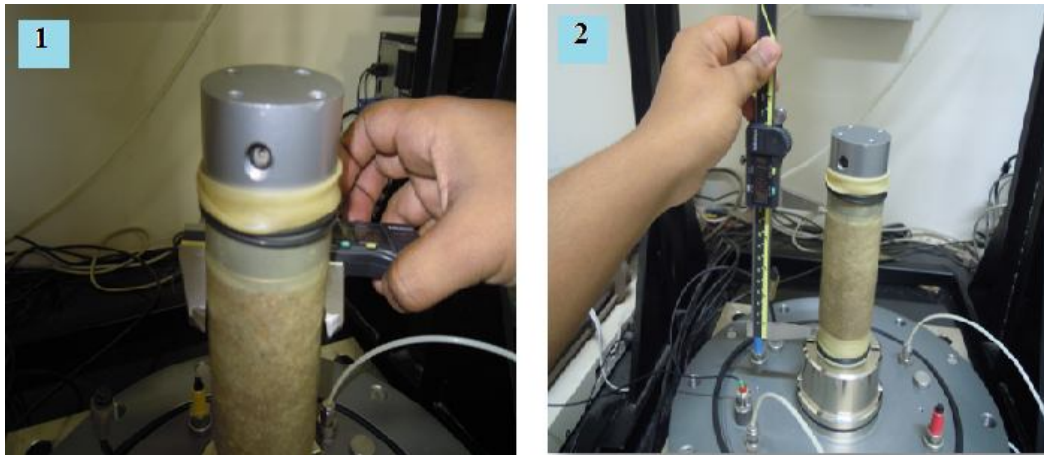3. Electromagnetic drive system is gently placed on top of the specimen. Using the help of four screws the drive system is fixed to the top cap. Spirit level is used to check whether the drive system is exactly horizontal. If the drive system is not properly leveled it will give erroneous results (Figure 4.11-3).
4. The drive system is properly centered so that the magnets remain exactly at the centre of the coil so as to ensure free movement of the magnets inside the coil (Figure 4.9-4).
5. With the help of screws, the electromagnetic drive system is properly connected to the support cylinder (Figure 4.11-4).
6. The accelerometer cable is then connected to the electromagnetic drive system (Figure 4.9-4).
7. LVDT is mounted on top of the drive system to measure the vertical displacement of the sample (Figure 4.11-5).
8. The top plate is fixed to the electromagnetic drive system by means of eight screws. The purpose of the top plate is to provide addition stiffness of the drive system and to house transducers like LVDT (Figure 4.11-5).
9. The confining pressure chamber is then lowered and fixed to the base plate by means of six screws (Figure 4.11-6).

4.5   Summary

In this chapter, the material properties of the sand, expansive clay and fly ash are discussed. The sand used in the present study is poorly graded clean sand which is free from fines content. Moderately expansive clay obtained from Indian Institute of Technology Hyderabad campus has been used in this study. A class C fly ash obtained from Neyveli Lignite Corporation has been used to stabilize the expansive clay. In addition, the sample preparation techniques for sands and clays are also mentioned in this chapter

Figure 4.11: Test setup for performing RC tests

Chapter 5

Dynamic Properties of Clean Sand

5.1   Introduction

This chapter deals with the determination of dynamic properties of clean sand and the influence of different parameters such as confining pressure, shear strain and relative density on the dynamic properties with a special emphasis given to the dynamic properties. The confining pressure variation was made from 50 kPa to 800 kPa to cover a wide range of confining pressure. The shear strain was increased from small strain (10^{-4} %) to medium value of strain (10^{-1} %). Sand samples were prepared at three different relative densities i.e. 30 %, 50 % and 75 % following the technique as specified in Chapter 4.

5.2   Test sequence

In this study two series of tests were performed on clean sand. In the first series, resonant column tests were performed on dry sand. In the second series of tests, the soil specimen was allowed to saturate and the specimens were consolidated at an isotropic effective confining pressure. The full saturation is ensured by performing the B check. A *B-value* close to 0.99 signifies that the specimen is close to 100 percent saturation. While performing the resonant column tests, the drainage valve was closed to conduct the tests under undrained condition to determine the shear modulus, damping ratio and Poisson's ratio of the soil.

5.3 Results and discussions

5.3.1 Effect of Shear Strain on Dynamic Properties

The dynamic properties are significantly influenced by the shear strain. Figures 5.1, 5.2, 5.3 give the variation of shear modulus (G) with shear strain of sand for relative densities of 30 %, 50 % and 75 % respectively. It is clearly seen that the shear modulus (G) decreases with an increase in the shear strain. It is due to loss of stiffness of the specimen with increase in the shear strain. When the shear strain increases, there is a breakage of inter-particle packing between soil grains, which reduces the stiffness and thereby the shear modulus (G) decreases considerably. In addition, higher the relative density, higher is the shear modulus (G) of the specimen at a given confining pressure. However, it can be observed that the shear stiffness is fairly constant between the shear strains from 0.0001 to 0.001% and reduces thereafter. Vucetic (1994) observed similar results and demonstrated that there exists a threshold value of shear strain at which magnitude of shear modulus (G) is 0.99 times the maximum shear modulus (G) at smallest value of shear strain. The threshold values of shear strain for the present samples are calculated as proposed at different relative density with various confining pressures (Table 5.1). It has been observed that the threshold value of strain increases with increase in confining pressure and relative density.
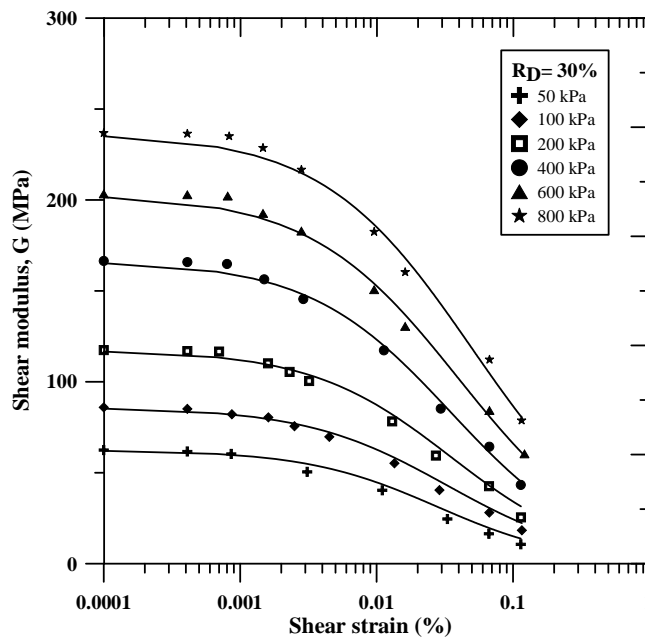

Figure 5.1: Variation of shear modulus (G) with shear strain for relative density of 30 %.
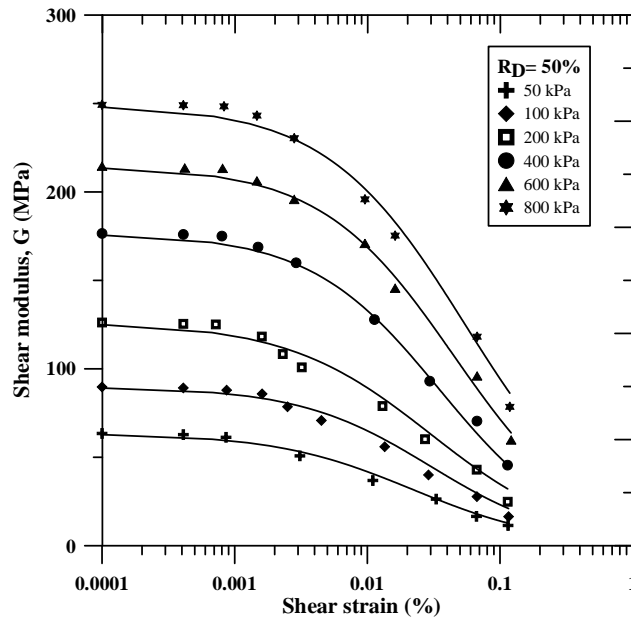
Figure 5.2: Variation of shear modulus with shear strain for relative density of 50 %.
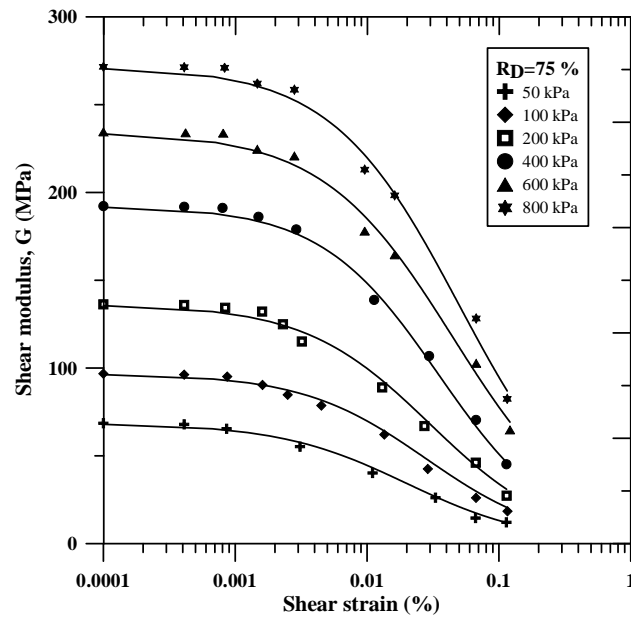
(c)

Figure 5.3: Variation of shear modulus with shear strain for relative density of 75 %.

Table 5.1: Values of threshold shear strain of clean sand

Relative density (%)	Confining Pressure (kPa)	Threshold Shear Strain 10^{-4} (%)
30	50	3.6
	100	4.1
	200	7.2
	400	8.0
	600	8.3
	800	8.5
50	50	3.8
	100	4.3
	200	7.5
	400	8.2
	600	8.6
	800	8.8
75	50	4.1
	100	4.6
	200	7.8
	400	8.5
	600	8.9
	800	9.2

Figures 5.4, 5.5 and 5.6 give the variation of damping ratio (D) with shear strain of sand for relative densities of 30 %, 50 % and 75 % respectively. It is observed that damping ratio (D) increases with increase in shear strain (%). The increase in damping ratio (D) is attributed to the fact that there is a higher loss of energy, which results from higher mobility of sand grains during resonance column test. The damping ratio (D) remains constant at about 1% irrespective of the relative density of the specimen up to a shear strain value of 10^{-2} %. The constant low damping ratio (D) at low shear strain range can be attributed to the higher shear stiffness of the specimens. Thereafter, the damping ratio (D) increases as high as 10% for the relative density of 30%. The damping ratio (D) reduces marginally with increase in the relative density of sand as expected. The damping ratios (D) obtained by various researches on similar sand samples subjected to same confining pressure using resonant column and cyclic triaxial apparatus are also summarized in the Table 5.2 for comparison purposes. It can be seen that the damping ratio (D) obtained from the present study is well within the range of values obtained by various researchers at a given shear strain and confining pressure.

Figure 5.4: Variation of damping ratio with shear strain for relative density of 30 %.
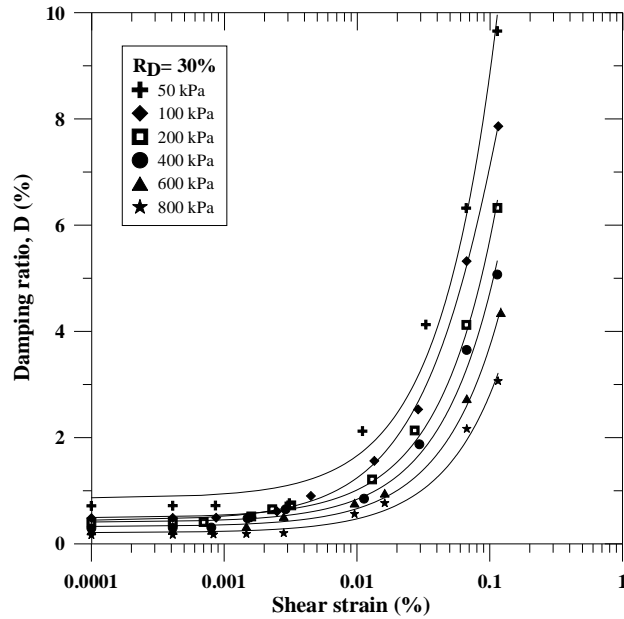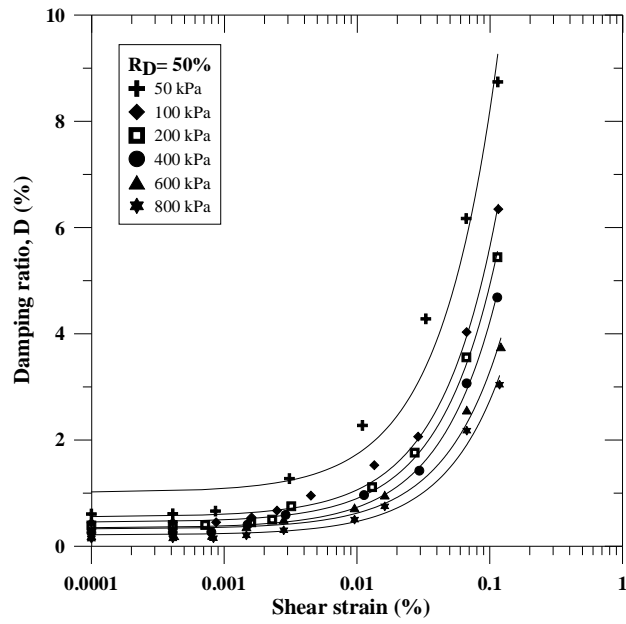
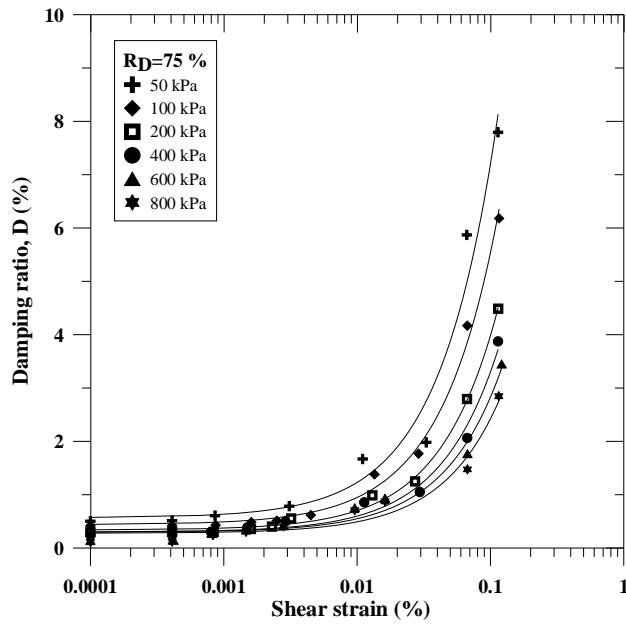**Figure 5.5: Variation of damping ratio with shear strain for relative density of 50 %.**

Figure 5.6: Variation of damping ratio with shear strain for relative density of 75 %.

61

Table 5.2: Comparison of damping ratio with those obtained by various researchers for sandy soils

Reference	Equipment used	Strain level (%)	Confining Pressure (kPa)	Damping Ratio (%)
Seed et al. (1986)	Resonant column test	10^{-4}	100	0.5
Zhang et al. (2005)	Resonant column test	10^{-4}	100	0.5
Present study	Resonant column test	10^{-4}	100	0.5
Kokusho (1980)	Cyclic triaxial	10^{-3}	100	1
Seed et al. (1986)	Resonant column test	10^{-3}	100	0.6
Saxena and Reddy (1989)	Resonant column test	10^{-3}	100	0.5
Zhang et al. (2005)	Resonant column test	10^{-3}	100	0.9
Present study	Resonant column test	10^{-3}	100	0.7
Kokusho (1980)	Cyclic triaxial	10^{-2}	100	2.1
Seed et al. (1986)	Resonant column test	10^{-2}	100	2.5
Saxena and Reddy (1989)	Resonant column test	10^{-2}	100	2
Zhang et al. (2005)	Resonant column test	10^{-2}	100	2.5
Present study	Resonant column test	10^{-2}	100	1.7
Kokusho (1980)	Cyclic triaxial	10^{-1}	100	11
Seed et al. (1986)	Resonant column test	10^{-1}	100	10
Zhang et al. (2005)	Resonant column test	10^{-1}	100	10
Present study	Resonant column test	10^{-1}	100	8

Figures 5.7, 5.8 and 5.9 give the variation of Poisson's ratio (v) with shear strain of sand for relative densities of 30 %, 50 % and 75 % respectively. The Poisson's ratio (v) increases with the increase in the shear strain. It is observed that the Poisson's ratio (v) remains constant at very low strain levels (up to of 5×10^{-4}%) and there has been a gradual increase in Poisson's ratio (v) thereafter. Within this range of shear strain the soil behavior may be considered as elastic. Typical value of Poisson's ratio (v) of sand lies in the range of 0.1 to 0.4 at small strains, and may be more than 0.5 as well at failure (at a high value of shear strain) [72]. In this study at high value of shear strain (10^{-1} %), a very high value of Poisson's ratio of about 0.45 is observed. The Poisson's ratio (v) is high for lower relative density specimens and gradually decreases with increase in the relative density of specimens.
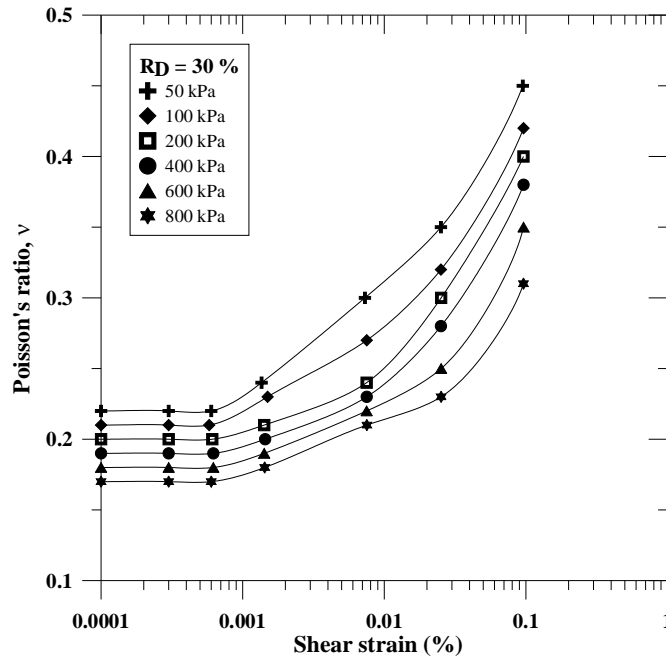

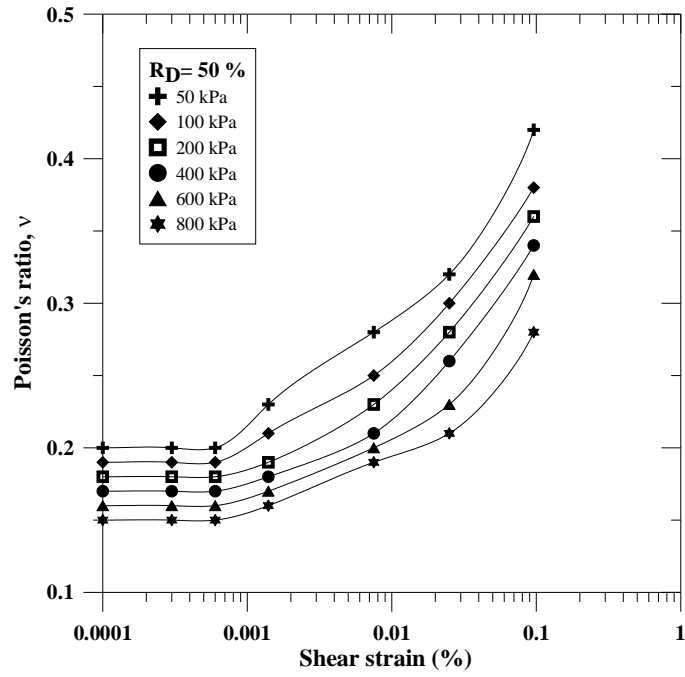**Figure 5.7: Variation of Poisson's ratio with shear strain for relative density of 30 %**

Figure 5.8: Variation of Poisson's ratio with shear strain for relative density of 50 %
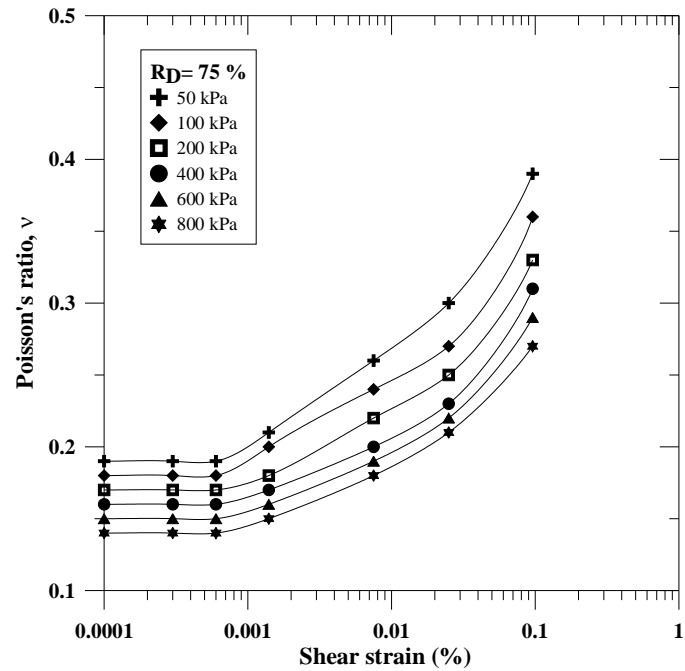

Figure 5.9: Variation of Poisson's ratio with shear strain for relative density of 75 %

Further the data can be analyzed to determine the modulus reduction, which can be defined as a ratio of shear modulus (G) and small strain shear modulus (G_{max}).Generally, granular soils behave linear elastic at a strain range of 10^{-4}% to 10^{-3} % [11]. The value of shear modulus within this range of strain is the small strain shear modulus of the soil (G_{max}). For the determination of small strain shear modulus a strain value of 10^{-4}% is taken in this study. Figures 5.10, 5.11, 5.12 give the modulus reduction (G/G_{max}) curves with shear strain. The modulus reduction curves are compared with the upper and lower bound modulus reduction curves for sands proposed by Seed et al. (1986). Seed et al. (1986) have conducted extensive resonant column studies on sands. The data was analysed while comparing with the then available literature on sands and proposed the upper and lower bound modulus degradation (G/G_{max}) curves. From Figure 5.10, it is observed that at lower relative density (R_D = 30%), all the modulus reduction curves are closer to the lower bound curve proposed by Seed et al. (1986). It can be noticed that the present data plots slightly beyond the lower bound curve for the specimens prepared at various relative densities subjected to lower confining pressures (50kPa) at higher shear strain range (10^{-3} to 10^{-1}%). However, with increase in the relative density the curves are shifting towards the upper bound curve proposed by Seed et al. (1986) which can be seen from Figures 5.11 and 5.12.
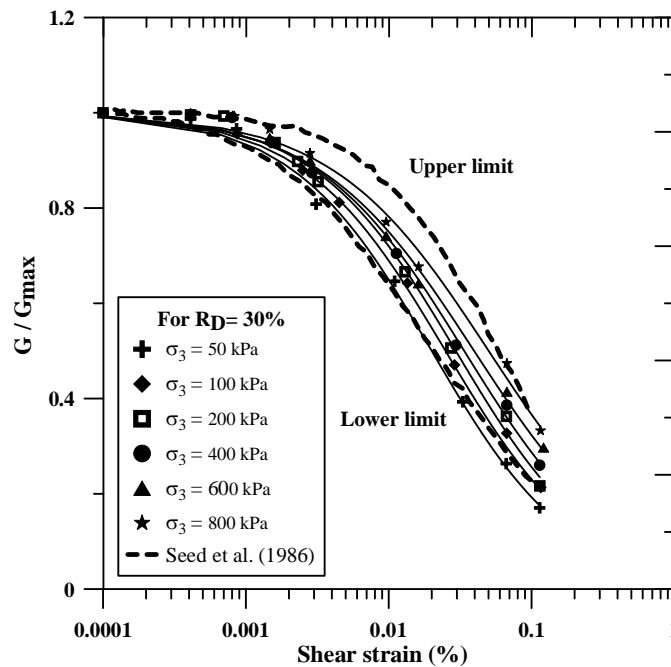

Figure 5.10: Variation of modulus reduction (G/G_{max}) with shear strain for relative density of 30 %
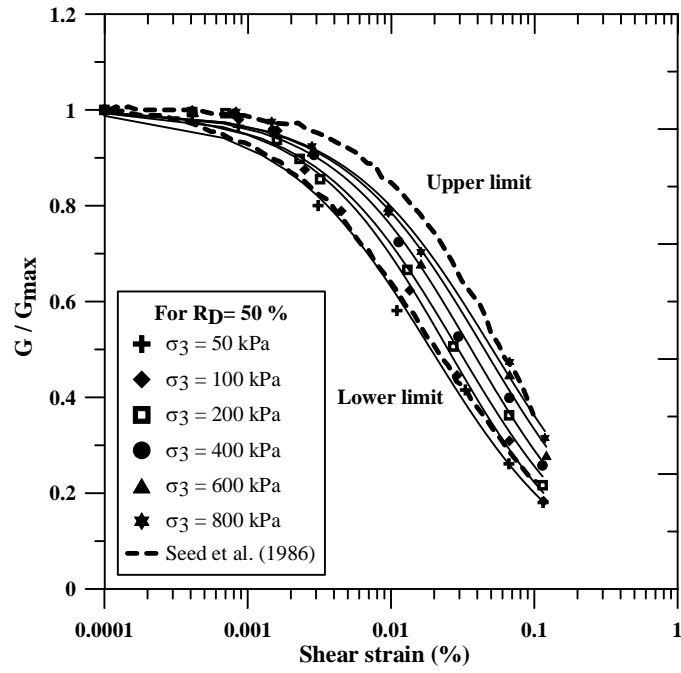
Figure 5.11: Variation of modulus reduction (G/G_{max}) with shear strain for relative density of 50 %
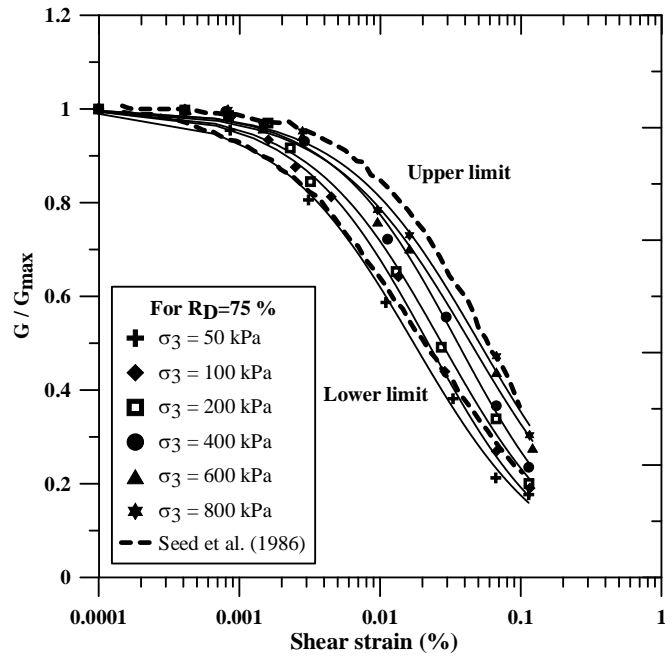

Figure 5.12: Variation of modulus reduction (G/G_{max}) with shear strain for relative density of 75 %

5.3.2   Effect of Confining Pressure on Dynamic Properties

By increasing the confining pressure on the soil specimen prepared at a constant relative density, the shear modulus, damping ratio and Poisson's ratio of the soil sample are determined. The confining pressure is increased from 50 kPa to 800 kPa in this study. Figure 5.13 shows the variation of small strain shear modulus (G_{max}) with confining pressure. It has been observed that the shear modulus increases continuously with increase in the confining pressure. This is because the stiffness of the soil specimen increases with the increase in confining pressure which results in the increase in shear modulus. Since the tests are conducted under undrained conditions, the densification effect due to increase in confining pressure on dynamic soil properties is negligible.
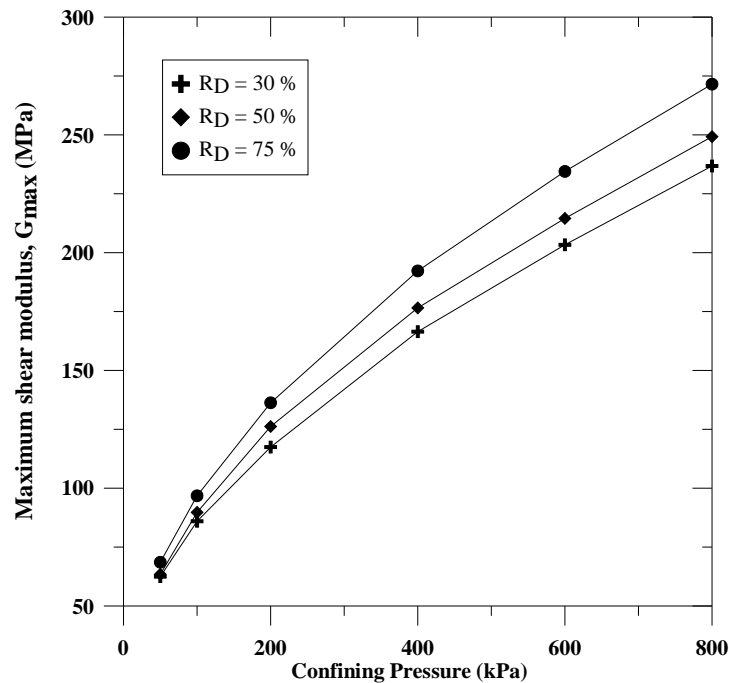
Figure 5.13: Variation of small strain shear modulus with confining pressure

Table 5.3 presents the small strain shear modulus values obtained from present study and various test methods including cyclic triaxial tests, bender/extender element tests etc. available in the literature. To compare the small strain shear modulus (G_{max}) from previous studies with the present, similar test conditions such as confining pressure, void ratio and shear strain are considered. The small strain shear modulus (G_{max}) obtained from the present study is comparable with the values obtained from various test methods at same

shear strain. It can be noticed that the reported by Hardin and Drnevich (1972) is slightly higher than the rest of the values due to lower void ratio (higher relative density) results in stiffer specimen.

Table 5.3: Comparison of small strain shear modulus (G_{max}) of sandy soils obtained from various test methods

Reference	Test Method	Confining Pressure (kPa)	Void ratio	Shear strain (%)	Small strain shear modulus (G_{max}), MPa
Seed and Idriss (1970)	Resonant column	95.76	0.7	10^{-4}	98.05
Hardin and Drnevich (1972)	Resonant column	88.27	0.57	10^{-4}	121.65
Kokusho (1980)	Cyclic triaxial	98.06	0.696	2×10^{-4}	111.68
Iwasaki et al. (1978)	Resonant column	98.06	0.7	10^{-4}	87.25
Kumar and Madhusudhan (2010)	Bender and extender element	100	0.71	10^{-4}	95
Present Study	Resonant column	100	0.72	10^{-4}	96.78

The small strain shear modulus (G_{max}) can also be calculated from well-established empirical correlations given by Hardin and Richart (1963) and Hardin and Drnevich (1972). Figures 5.14, 5.15 and 5.16 present the comparison of small strain shear modulus obtained in the present study with those obtained from the empirical equations. It was observed that the small strain shear modulus obtained in the present study agrees well with those calculated using the empirical correlations. The average difference in small strain shear modulus obtained using Hardin and Richart (1963) and Hardin and Drnevich (1972) are found to be 2.3 % and 1.2 % respectively.
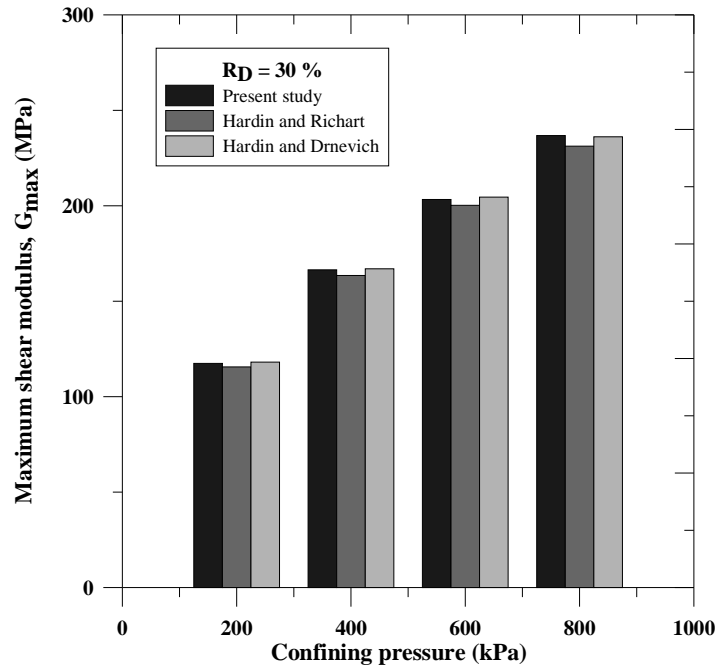
Figure 5.14: Comparison of small strain shear modulus for relative density of 30 %
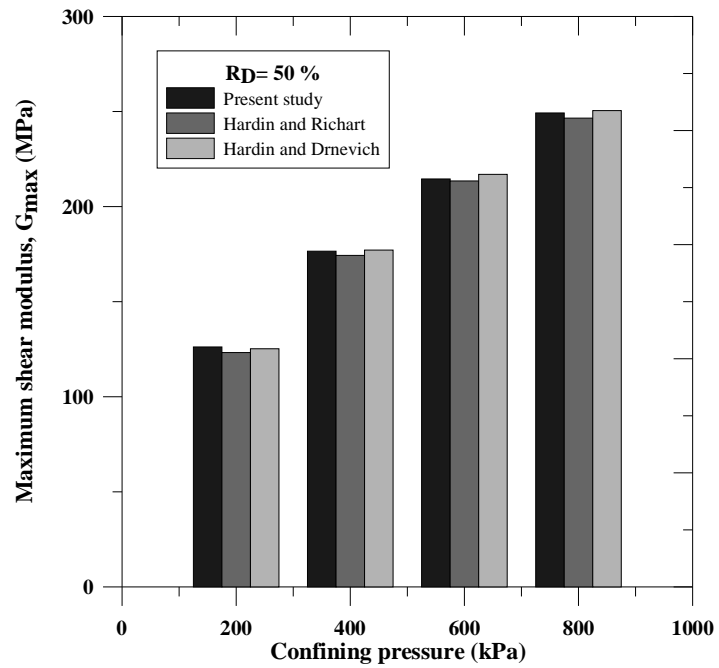

Figure 5.15: Comparison of small strain shear modulus for relative density of 50 %
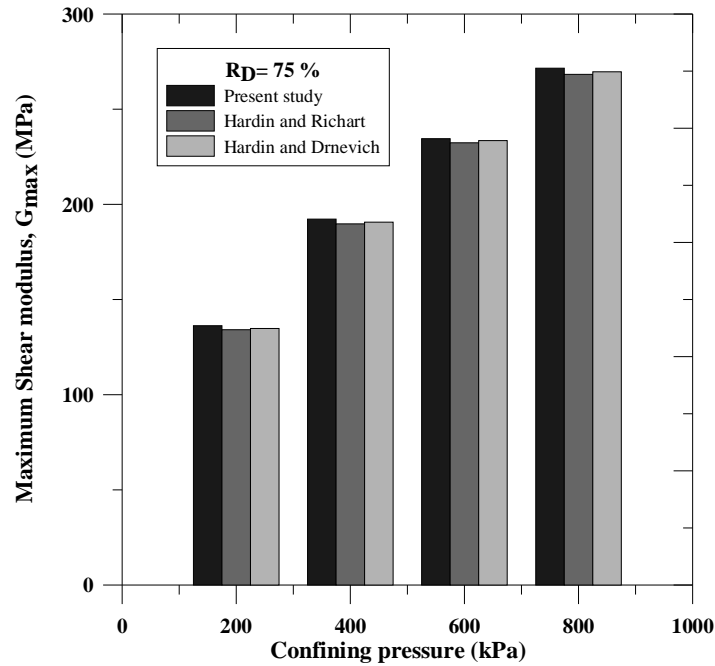
Figure 5.16: Comparison of small strain shear modulus for relative density of 75 %

Figure 5.17 presents the variation of small strain damping ratio of the soil with increase in confining pressure. It is seen that the damping ratio decreases with increase in the confining pressure. This can be explained on the basis of the relationship between damping ratio and stiffness of the soil which is given by equation (5.1).

$$D = \frac{c}{c_c} = \frac{c}{2\sqrt{km}}$$ (5.1)

where, D = damping ratio of the material; c = damping coefficient; c_c = critical damping

coefficient; k = stiffness of the sample; m = mass of the sample.

It is seen that there exists an inverse relationship between damping ratio and stiffness of the

soil. Hence, with the increase in confining pressure, the stiffness of the soil increases and

which results in the reduction in the damping ratio of soil. It is observed that the rate of

decrease of damping ratio is high for the confining pressure up to 400 kPa. But with further

increase in the confining pressure, the rate of decrease is found to be less.

Figure 5.17: Variation of small strain damping ratio with confining pressure

Figure 5.18 shows the variation of small strain Poisson's ratio (v_{min}) with increase in confining pressure. It is observed that the small strain Poisson's ratio (v_{min}) Poisson's ratio value decreases with increase in the confining pressure. This is because of the reduction in shear strain with increase in confining pressure. The observation made in this study regarding the variation of Poisson's ratio is similar to that of the observations made by Kokusho (1980), Bates (1989), Nakagawa et al. (1996), Kumar and Madhusudhan (2010).

5.3.3 Effect of relative density on dynamic properties

Figures 5.19, 5.20 and 5.21 show the variation of small strain shear modulus (G_{max}), damping ratio (D_{min}) and Poisson's ratio (v_{min}) respectively with relative density. With the increase in relative density it is seen that the shear modulus increases and the damping ratio decreases. This is because with the increase in relative density there is a reduction in void ratio which signifies denser packing of the soil grains and increased the stiffness of the soil. It can be seen that the variation of shear modulus and damping ratio with relative density is almost linear. It is also observed that the small strain Poisson's ratio (v_{min}) decreases with increase in relative density (decrease in void ratio) of sand.

71

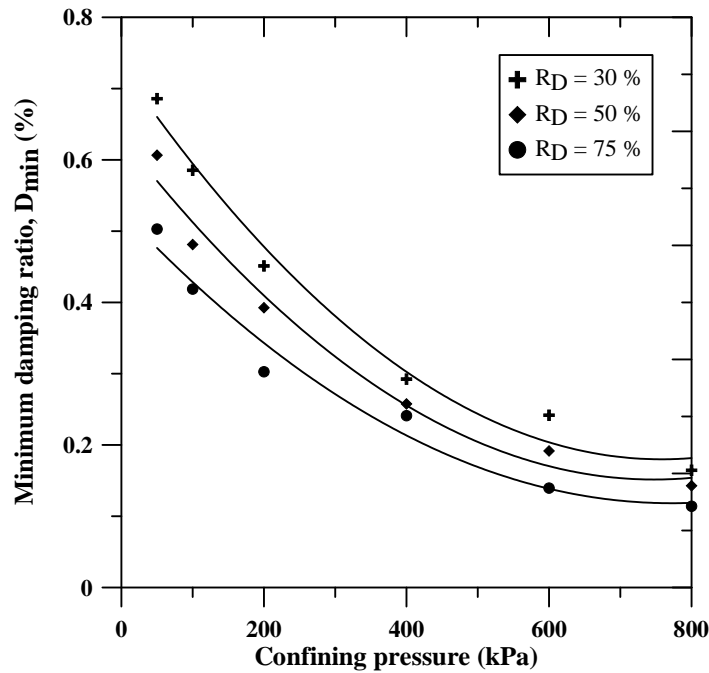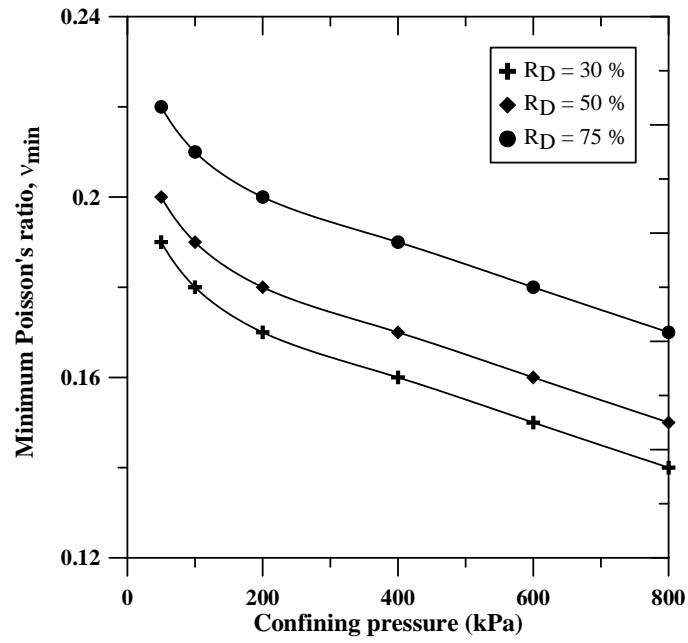**Figure 5.18: Variation of Poisson's ratio with confining pressure**
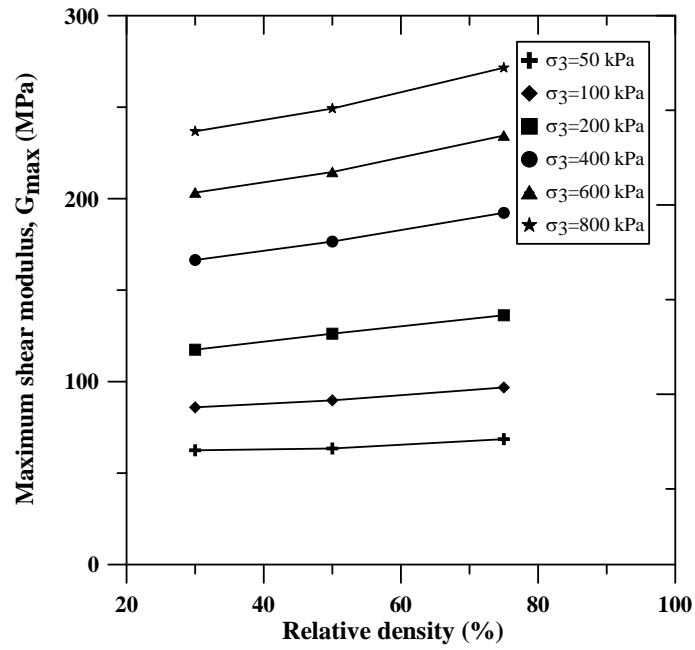
Figure 5.19: Variation of small strain shear modulus with relative density
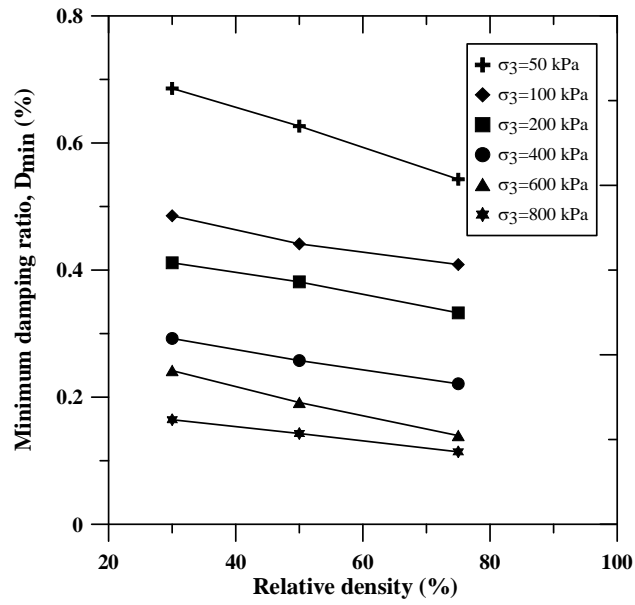
Figure 5.20: Variation of small strain damping ratio with relative density
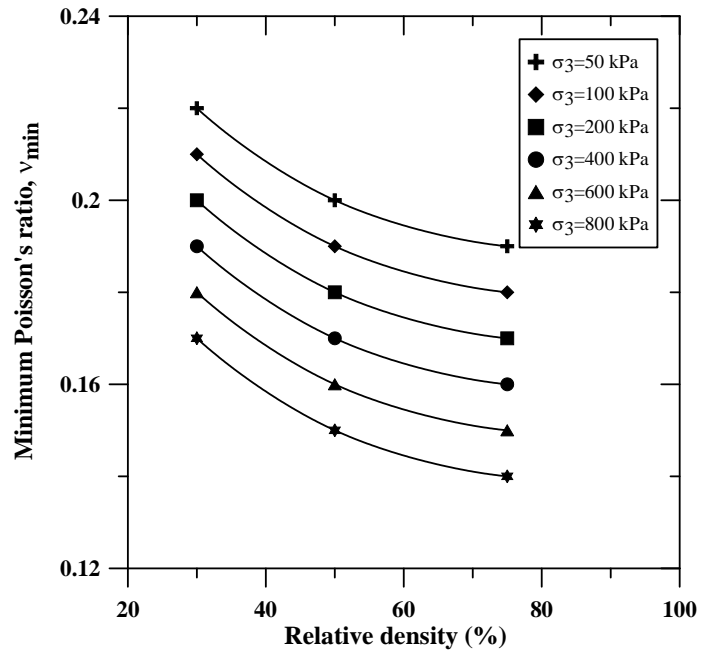
Figure 5.21: Variation of Poisson's ratio with relative density

5.3.4   Variation of shear modulus with Poisson's ratio

Figures 5.22, 5.23 and 5.24 show the variation of shear modulus (G) with Poisson's ratio. It is observed that the shear modulus (G) decreases with increase in Poisson's ratio (v) of the soil. This is because a higher value of Poisson's ratio (v) signifies a higher rate of shear strain, which leads to a reduction in the shear modulus of the soil. Similar observations were made by Ohsaki and Iwasaki 1973, Kumar and Madhusudhan 2010, Gu et al. 2013. From Figures 5.22, 5.23, and 5.24, it is interesting to note that the variation of shear modulus (G) is linear only at low confining pressures (50 to 100 kPa) and is found to be very non-linear at high confining pressures (200-800 kPa) with an increase in shear strain. This non-linearity decreases with increase in the relative density of the soil specimen.

Figure 5.22 Variation of shear modulus with Poisson's ratio for relative density of 30 %

74

Figure 5.23 Variation of shear modulus with Poisson's ratio for relative density of 50 %
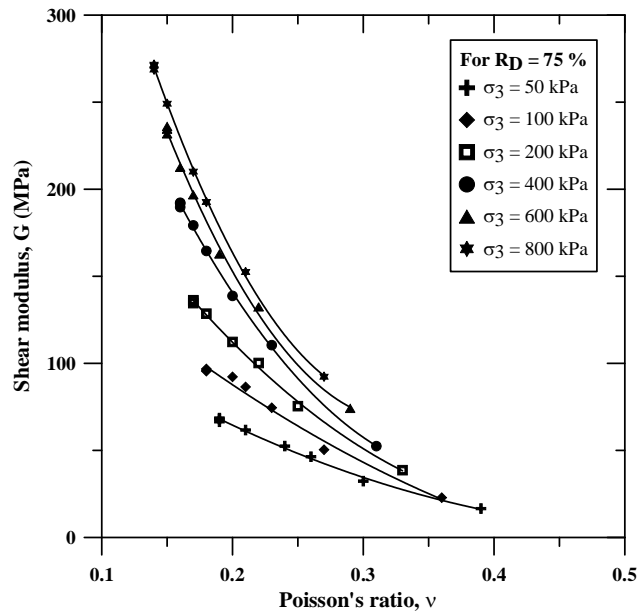
Figure 5.24 Variation of shear modulus with Poisson's ratio for relative density of 75 %

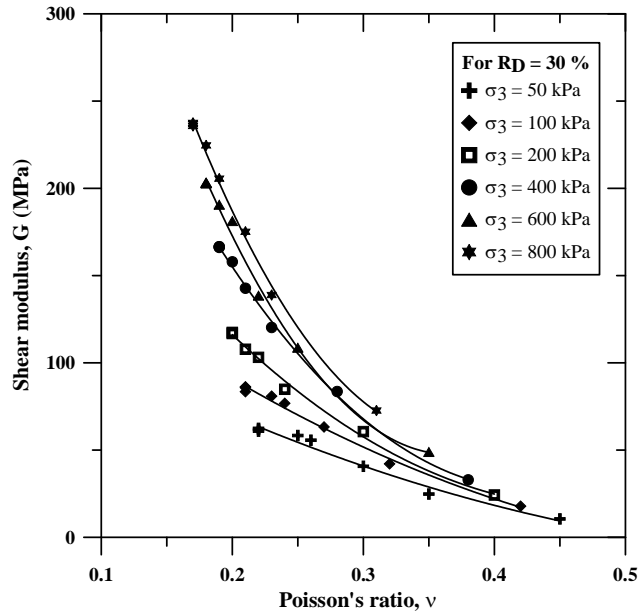Figure 5.25 shows the combined variation of shear modulus (G) with Poisson's ratio (v) for three different relative densities. These variations are shown for only three different confining pressures i.e. 50 kPa, 200 kPa and 800 kPa and plotted for a range of shear strain values from 10^{-4} % to 10^{-1} %. Kumar and Madhusudhan (2010) presented similar data on small strain shear modulus with Poisson's ratio and found that the variation is linear. However in this study, the variation of shear modulus (G) is found to be non-linear at very small values of shear strain but becomes linear at higher values of shear strain. It can be seen that the variation of shear modulus (G) with Poisson's ratio is nonlinear at strains 0.0001% and 0.0014%, but with increase in strain it was found to be linear. The deviation observed may be because Kumar and Madhusudhan (2010) performed experiments on fine grained, medium grained and coarse grained sands separately using bender and extender elements test. But the present study has been performed on poorly graded sand with major portion of representing the medium grained sand and the Poisson's ratio is determined using resonant colum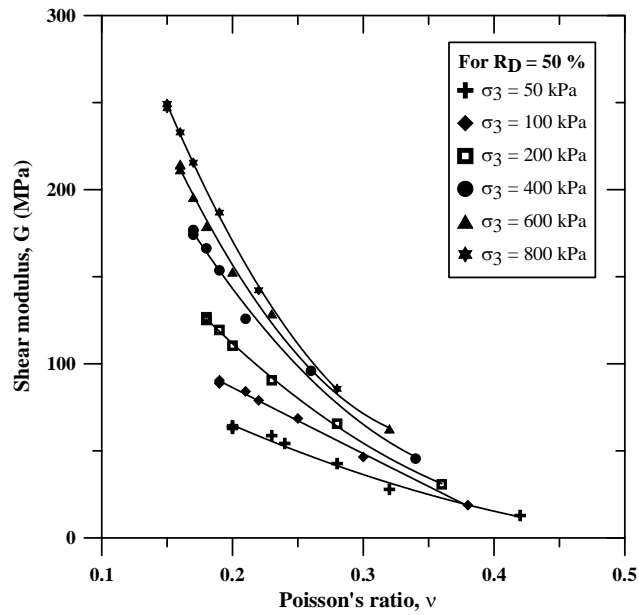n test. Further study is required to validate the variation of shear modulus (G) with Poisson's ratio for different relative densities.

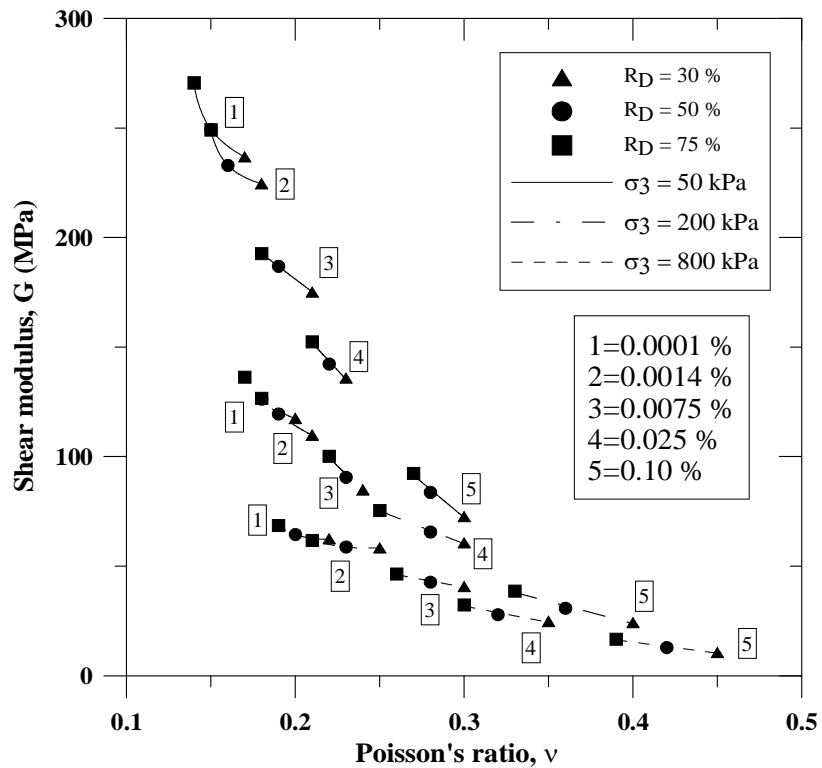**Figure 5.25 Variation of shear modulus with Poisson's ratio for different confining pressures, relative densities and shear strains**

76

5.3.5 Effect of saturation on dynamic properties

To study the influence of saturation on the dynamic properties of sand, resonant column tests were further performed on fully saturated sand. Figures 5.26, 5.27 and 5.28 give the influence of saturation on shear modulus of clean sand for relative density (R_D) of 30 %, 50 % and 75 % respectively. It was observed that shear modulus (G) reduces marginally for all the relative densities of soil. The shear modulus (G) of fully dry sand and fully saturated sand (S_r=100 %) is equal. With the increase in degree of saturation from 0 % to certain optimum value, the shear modulus (G) increases but with further increase in degree of saturation the shear modulus (G) of the soil reduces till it reaches the same value of shear modulus of soil as 0 % degree of saturation (Wu 1983, Wu et al. 1984, Qian et al. 1993, Kumar and Madhusudhan 2012). The optimum degree of saturation values as obtained by Wu et al. (1984), Qian et al. (1993), Cho and Santamarina (2001) and Kumar and Madhusudhan (2012) are close to 5 %, 3.6-18 %, 0.64 % and 0.69-0.92 %. The determination of optimum degree of saturation is beyond the scope of this study. The observed reduction in shear modulus (G) of fully saturated sand as compared to dry sand in the present study may be due to the reason that sand used is air dried sand and has a degree of saturation (S_r) of 0.39 %- 0.44 % and not completely dry sand (S_r= 0 %). Figures 5.29, 5.30 and 5.31 give the influence of saturation on damping ratio (D) of clean sand for relative density (R_D) of 30 %, 50 % and 75 % respectively. The percentage difference in damping ratio (D) of saturated sand as compared to dry sand is very less around 0.4-0.6 %. By performing resonant column tests on sand, Madhusudhan and Kumar (2013) observed a damping ratio (D) variation of 0.5-1 % with saturation and stated that damping ratio variation with saturation can be neglected if dynamic behaviour of sand is to be modelled. Figures 5.32, 5.33 and 5.34 give the influence of saturation on Poisson's ratio (v) of clean sand for relative density (R_D) of 30 %, 50 % and 75 % respectively. It is observed that Poisson's ratio (v) of clean sand is close to 0.5 for fully saturated sand and does not with increase in confining pressure as well as relative density of sand. This is because under undrained condition, saturated soil behaves as an incompressible material, so volume change is essentially zero and the Poisson's ratio (v) approaches limiting value of 0.5. Similar observation was made by Kumar and Madhusudhan (2012) by performing bender and extender element tests on sand.
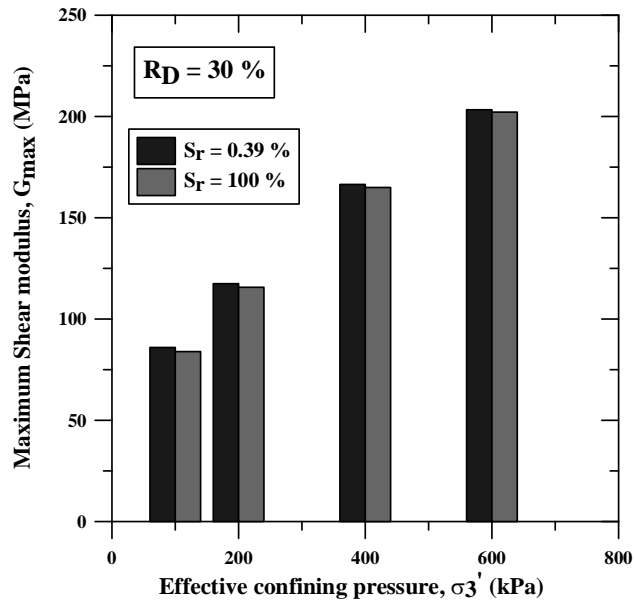
Figure 5.26: Effect of saturation on small strain shear modulus for relative density of 30 %
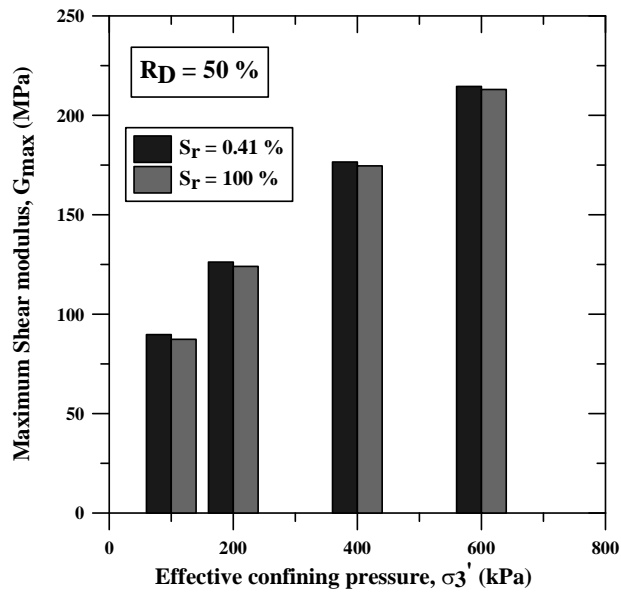
Figure 5.27: Effect of saturation on small strain shear modulus for relative density of 50 %
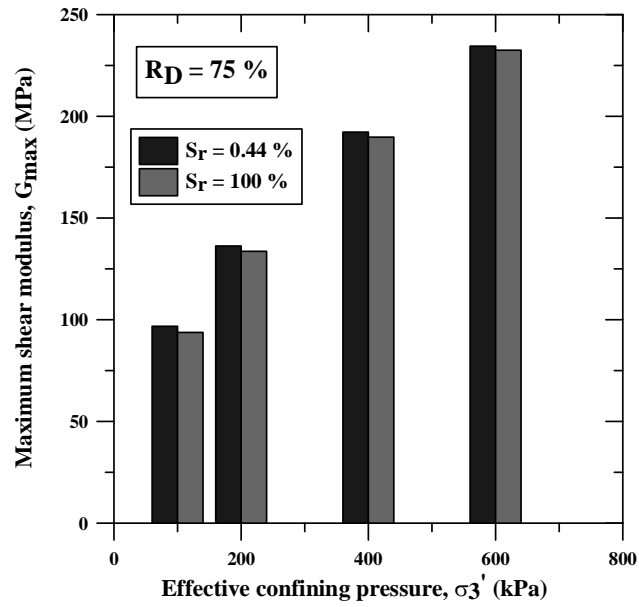
Figure 5.28: Effect of saturation on small strain shear modulus for relative density of 75 %
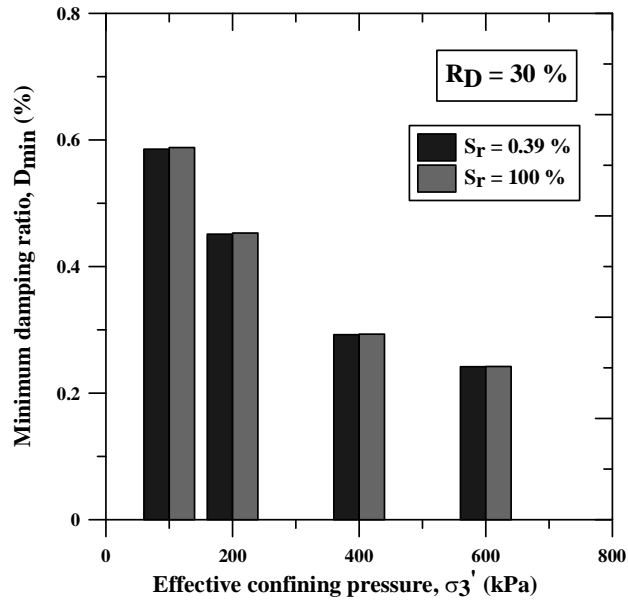
Figure 5.29: Effect of saturation on small strain damping ratio for relative density of 30 %

79
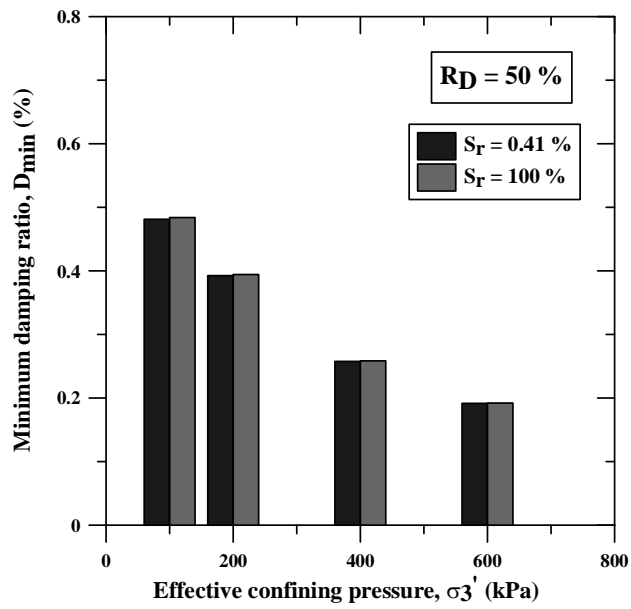
Figure 5.30: Effect of saturation on small strain damping ratio for relative density of 50 %
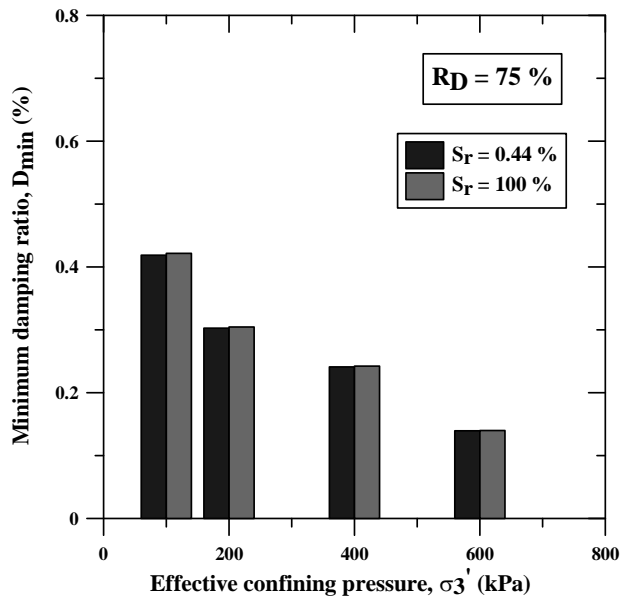
Figure 5.31: Effect of saturation on small strain damping ratio for relative density of 75 %
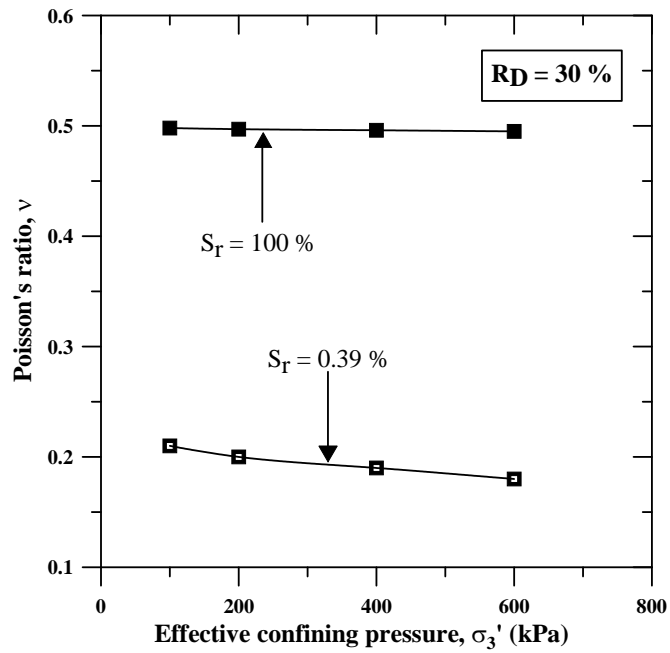
Figure 5.32: Effect of saturation on Poisson's ratio for relative density of 30 %
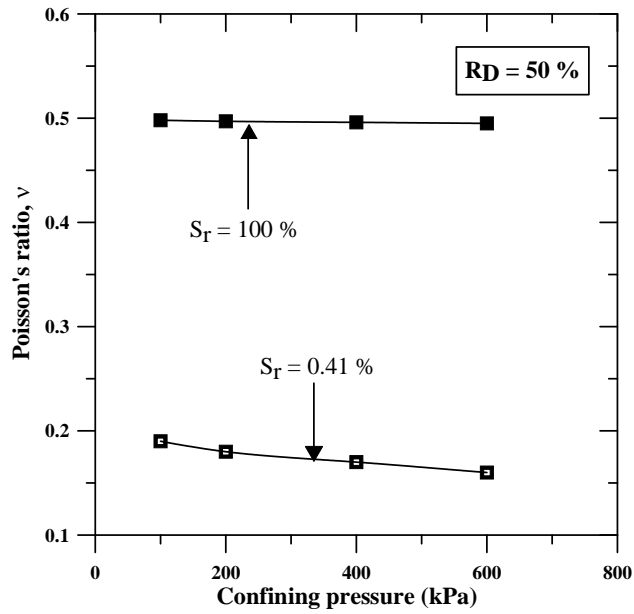
Figure 5.33: Effect of saturation on Poisson's ratio for relative density of 50 %
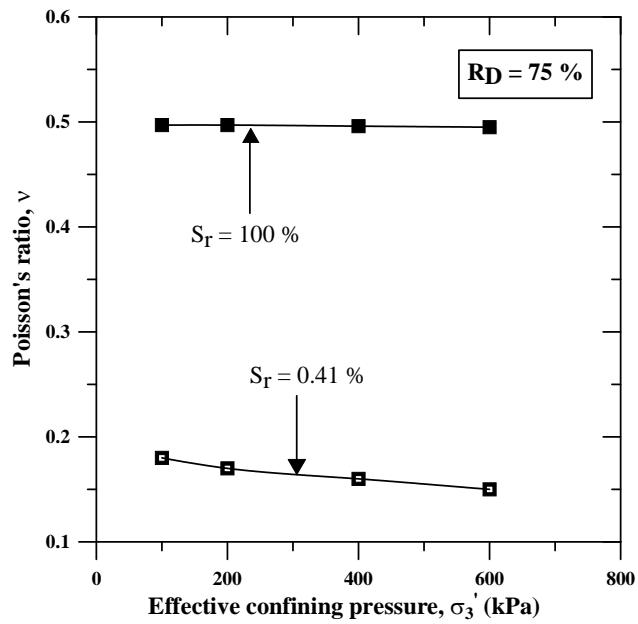
Figure 5.34: Effect of saturation on Poisson's ratio for relative density of 75 %

5.4 Summary

In this chapter, the dynamic properties of clean sand were elaborately discussed. The dynamic properties studied are shear modulus (G), damping ratio (D) and Poisson's ratio (ν). The effect of different parameters viz. confining pressure, shear strain and relative density on the dynamic properties are also presented in this chapter. The obtained results are compared with the available literatures on clean sand. Finally, the effect of saturation on the dynamic properties of sand is discussed.

Chapter 6

Dynamic Properties of Expansive Clay

6.1   Introduction

In this chapter, the dynamic properties of expansive soil are discussed. The dynamic properties studied are shear modulus (G), damping ratio (D) and Poisson's ratio (v). The influence of confining pressure, shear strain and degree of saturation on the dynamic properties are stated. An empirical correlation is also proposed for the determination of Poisson's ratio (v) from shear modulus (G) of expansive soil. The confining pressure variation was made from 25 kPa to 200 kPa. The shear strain was increased from 10^{-4} % to 10^{-1} %.

6.2   Test sequence

In this study two series of tests were performed on expansive soil. In the first series, resonant column tests were performed on expansive soil prepared at optimum moisture content and compacted to maximum dry density. The degree of saturation of samples prepared at optimum moisture content is 92 %. In the second series of tests, the soil specimen was allowed to saturate and the specimens were consolidated at an isotropic effective confining pressure. The full saturation is ensured by performing the B check. A *B-value* close to 0.99 signifies that the specimen is close to 100 percent saturation. While performing the resonant column tests, the drainage valve was closed to conduct the tests under undrained condition to determine the shear modulus (G), damping ratio (D) and Poisson's ratio (v) of the soil. Finally, filter paper tests were performed to estimate the suction present in partially saturated soil specimen.

6.3   Measurement of suction using filter paper test

The suction of the soil specimen prepared at optimum moisture content is measured by means of filter paper technique (ASTM D5298-10). Filter paper test is the simplest and cheapest of all the available methods for soil suction measurement. Filter paper test can be used to measure soil suction from 10 kPa to 100,000 kPa. In this test the filter paper is allowed to absorb the moisture from the soil, and when the equilibrium is reached, the suction value of the filter paper is equal to the suction of the soil (Ridley and Wray, 1995). The filter paper comes to equilibrium with the soil either through vapor (total suction measurement) or liquid (matric suction measurement) flow. After equilibrium is established between the filter paper and the soil, the water content of the filter paper is measured. The water content of filter paper is converted to suction using calibration curves. In this study, Whatman No. 42 filter papers were used, so the calibration curve proposed by Whatman was used. Figure 6.1 shows the test setup used for performing the filter paper test. In this test, sample prepared at optimum moisture content were kept in desiccators to prevent loss of moisture. A filter paper of diameter 5.5 cm is kept at a specified height on top of the soil sample so that the filter paper does not touch the soil specimen. It is done by placing a stack of O rings as the O rings will not absorb the moisture from the specimen. The sample was then kept for seven days inside the desiccators so that suction of the filter paper and the specimen should be allowed to equilibrate. After seven days, the weight of the filter paper is noted and from which filter paper water content is determined. From the water content of the filter paper, the suction of the soil can determined by using Whatman's equations which are given below:

$$\log s = 5.327 - 0.0779 w_f \quad \text{for } 0 < w_f < 45 \tag{6.1}$$

$$\log s = 2.412 - 0.0135 w_f \quad \text{for } 45 < w_f < 90 \tag{6.2}$$

where, S=suction in kPa, w_f= filter paper water content in percent.

Figure 6.1: Test setup for performing suction test

6.4   Results and discussions

6.4.1   Effect of Shear Strain on Dynamic Properties

The dynamic properties of soil are significantly influenced by the shear strain. Figure 6.2 gives variation of shear modulus (G) with the increase in shear strain. It is seen that shear modulus (G) decreases with the increase in shear strain and increases with the increase in confining pressure. The explanation is similar to that already discussed for the shear modulus of clean sand in Chapter 5. It is observed that shear modulus (G) reduction is very less up to shear strain of 10^{-3} % but with further increase in shear strain, shear modulus (G) reduces drastically. However it is also observed that shear modulus (G) increase with confining pressure is very less at shear strain of 10^{-1} %. The threshold values of shear strain for different confining pressure are reported in Table 6.1. It has been observed that the threshold value of strain increases with increase in confining pressure.
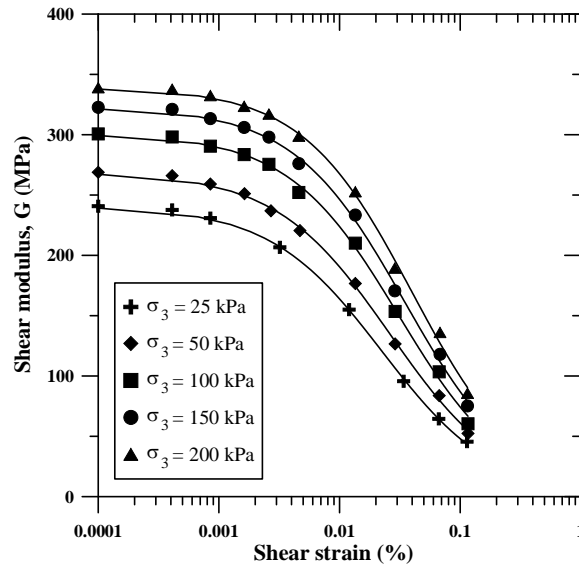
Figure 6.2: Variation of shear modulus (G) with shear strain for expansive soil

Table 6.1: Values of threshold shear strain of expansive soil

Confining Pressure (kPa)	Threshold Shear Strain 10^{-4} (%)
25	3.43
50	3.97
100	4.67
150	7.06
200	9.61

Figure 6.3 give the variation of modulus degradation (G/G_{max}) with the increase in shear strain for different confining pressures. It is observed that the (G/G_{max}) ratio increases with increase in confining pressure. The modulus degradation curves have been compared with design modulus degradation (G/G_{max}) curves of clays proposed by other researchers. It is seen that the obtained modulus reduction curves matches well with those proposed by Zhang et al. (2005) and Xenaki et al. (2008). Though the modulus degradation (G/G_{max}) curve is quite comparable to that proposed by Hardin and Drnevich (1972) at small to medium shear strain (shear strain up to 10^{-2} %) but for shear strain greater than 10^{-2} %,

Hardin and Drnevich (1972) modulus degradation (G/G$_{max}$) values are higher than those obtained in this study.

Figures 6.4 give the variation of damping ratio (D) with shear strain of expansive soil. It is observed that damping ratio increases with increase in shear strain (%) and decreases with the increase in confining pressure. The explanation is similar to that already discussed for the damping ratio of clean sand in Chapter 5. It is observed that increase in damping ratio with shear strain is very less up to a shear strain of 10^{-2} % after that it increases significantly. Moreover, it is also observed that reduction in damping ratio with confining pressure is marginal when the shear strain is less than 10^{-2} % but with further increase in shear strain considerable reduction in damping ratio is observed. At a shear strain of 10^{-1} %, a high value of damping ratio close to 9 is observed for samples subjected to 25 kPa confining pressure.
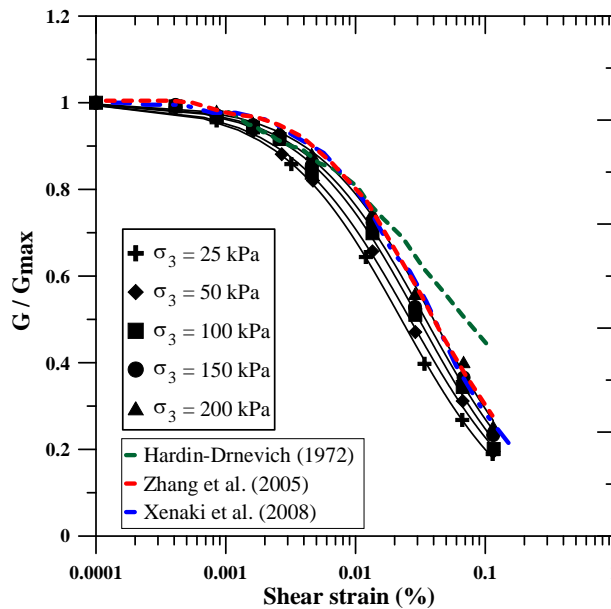
Figure 6.3: Variation of modulus reduction (G/G_{max}) with shear strain for expansive soil
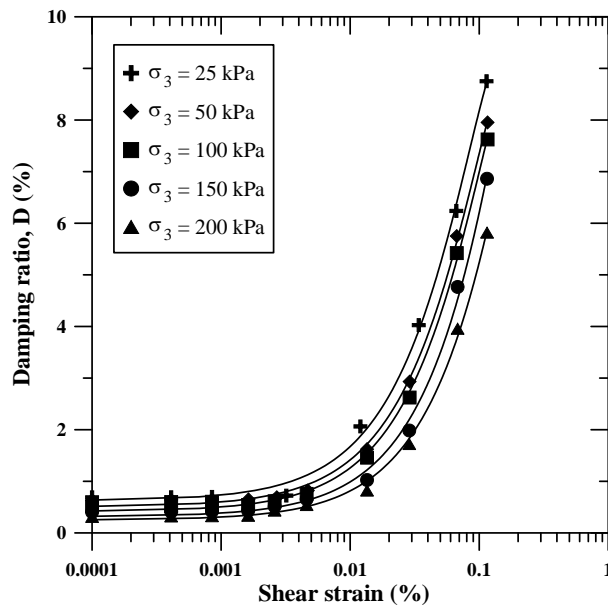
Figure 6.4: Variation of damping ratio with shear strain of expansive soil

Figure 6.5 give the variation of Poisson's ratio (v) with shear strain of expansive soil. It is seen that Poisson's ratio increases with the increase in shear strain. The increase in Poisson's ratio (v) is very less upto shear strain of 8×10^{-4} % but after that it increases drastically. However with the increase in confining pressure, Poisson's ratio (v) decreases. This is because increase in confining pressure increases the stiffness of the specimen which gives higher resistance to specimen deformation. A Poisson's ratio (v) value close to 0.5 is obtained for shear strain of 0.1 % and confing pressure of 25 kPa.
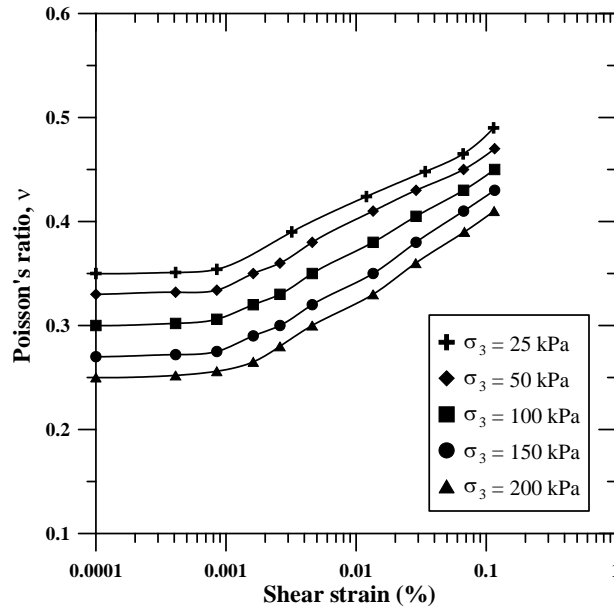
Figure 6.5: Variation of Poisson's ratio with shear strain of expansive soil

6.4.2   Effect of Confining Pressure on Dynamic Properties

Figure 6.6 gives the variation of small strain shear shear modulus (G_{max}) with confining pressure. Small strain shear modulus (G_{max}) is determined at a shear strain of 0.0001%. It is seen that small strain shear modulus increases monotonically with the increase in confining pressure. The increase in confining pressure results in increased number of particle-particle bonds which provides resistance to the specimen to deformation (Mitchell 1976). This means that there is an increased stiffness of the soil specimen with increase in the confining pressure. Besides, it is possible to fit power regression functions of the form $G_{max} = A\left(\sigma_{o}^{'}\right)^{B}$ to represent the variation of maximum shear modulus with confining pressure where A is the value of G_{max} (MPa) at effective confining pressure of 1 kPa and B is the slope of best fit curve (Mancuso et al, 1993; Hoyos et al., 2004). The values of A and B for the expansive soil are 141 and 0.6 respectively. Table 6.2 give the comparison of small strain shear modulus obtained in this study to those obtained by Hoyos et al. (2004) by performing resonant column tests on sulfate rich expansive clay of Texas. It is observed that small strain shear modulus values obtained by Hoyos et al. (2004) are greater than those obtained in this study for 25 kPa and 50 kPa but with further increase in confining pressure the values obtained in this study are higher than those obtained by Hoyos et al. (2004). The observed difference in small strain shear modulus of the two expansive soils may be due to difference in plasticity indices and clay percentages of the two expansive soils. Expansive

89

soil used in this study is having a plasticity index and clay fraction of 38 % and 40 % respectively and that of Texas clay are 45 % and 25 % respectively.

Figure 6.7 and 6.8 gives the variation of small strain damping ratio (D_{min}) and small strain Poisson's ratio (v_{min}) with confining pressure for expansve soil. It is observed that there is decrease in small strain damping ratio (D_{min}) as well as small strain Poisson's ratio (v_{min}) of the soil with the increase in confining pressure. This is because increase in confining pressure increases the rigidity of the soil specimen and reduces the strains induced in the soil resulting in lower value of damping ratio and Poisson's ratio of the soil.

$$G_{max}=141\,(\sigma_o')^{0.16}$$
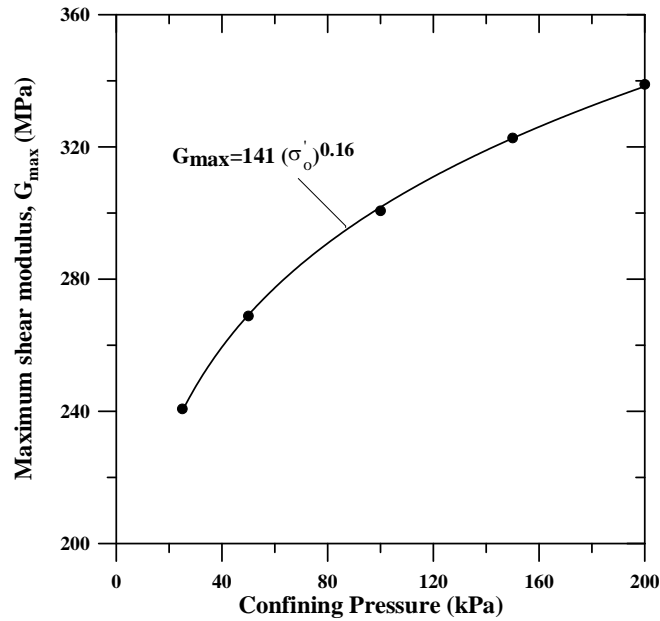
Figure 6.6: Variation of small strain shear modulus (G_{max}) with confining pressure for expansive soil

Table 6.2: Comparison of small strain shear modulus (G_{max}) of expansive soil

Confining pressure (kPa)	G_{max} (MPa)	
	Present Study	**Hoyos et al. (2004)**
25	240.75	268.98
50	268.86	278.47
100	300.68	288.29
150	322.71	294.20
200	338.94	298.46
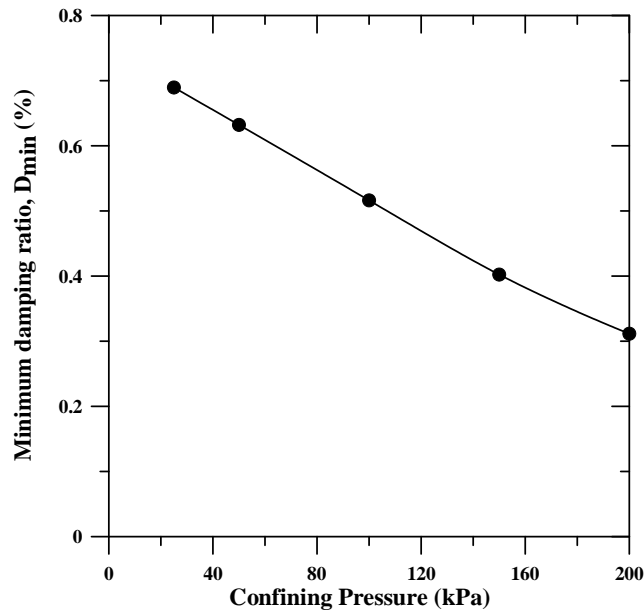
Figure 6.7: Variation of small strain damping ratio (D_{min}) with confining pressure for expansive soil
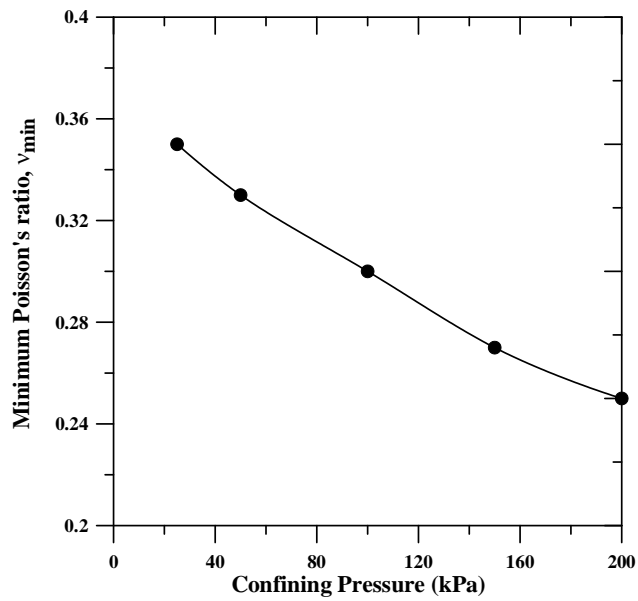
Figure 6.8: Variation of small strain Poisson's ratio (D_{min}) with confining pressure for expansive soil

91

6.4.3 Relation of Poisson's ratio with shear modulus

Figure 6.9 give the variation of Poisson's ratio with shear modulus (G) for the expansive soil. It is observed that Poisson's ratio (v) of soil shows a decreasing trend with the increase in shear modulus (G). Though there is some degree of scatter present in the data, regression analysis has been performed to develop an empirical correlation for the determination of Poisson's ratio from shear modulus (G) of expansive soil. The correlation to estimate the value of Poisson's ratio from the shear modulus of the expansive soil is given below:

$$\upsilon = 0.471 - 2.066 \times 10^{-4} \times G - 1.253 \times 10^{-6} \times G^2 \tag{6.3}$$

where, v = Poisson's ratio of expansive soil, G= shear modulus of the soil (MPa).

This correlation can be used to make a reasonable estimate of the Poisson's ratio of the expansive soil from the shear modulus (G).
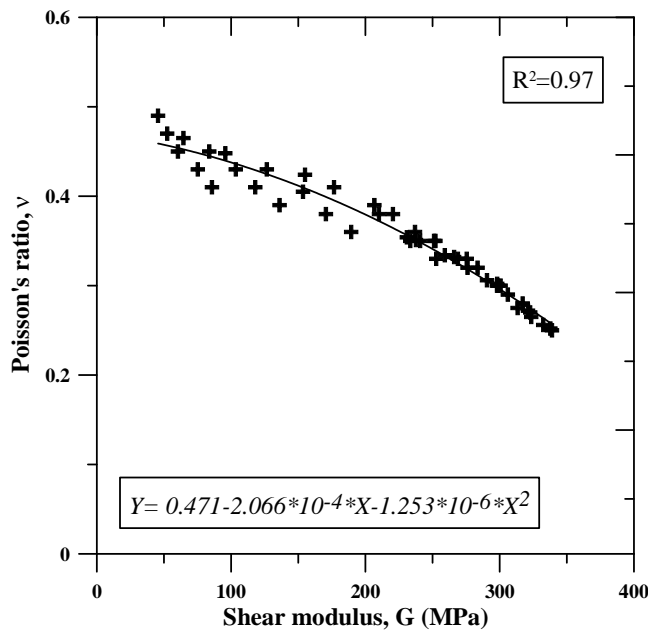
Figure 6.9: Variation of Poisson's ratio with shear modulus

6.4.4 Effect of saturation on dynamic properties

To study the influence of saturation on the dynamic properties of expansive clay, resonant column tests were further performed on fully saturated expansive clay. Figure 6.10 gives the variation of shear modulus (G) with shear strain for partially saturated and fully saturated condition. The soil sample prepared at optimum moisture content is having a degree of saturation of 92 %. It is seen that the shear modulus (G) for a partially saturated soil is greater than fully saturated soil. This is due to the presence of suction in the partially saturated soil which is responsible for higher stiffness of the specimen. This effect is more prominent at lower effective confining pressures and reduces considerably with increase in effective confining pressure. It is also seen that the increase in shear modulus (G) for partially saturated soil as compared to fully saturated soil for small to medium strain range but the difference reduces considerably at higher shear strain. The shear modulus of partially saturated samples are found to be 9.88 %, 4.92 % and 1.83 % higher than fully saturated samples at respectively 25 kPa, 100 kPa and 200 kPa confining pressures at 10^{-4}% shear strain. From Figure 6.10, it can be seen that for effective confining pressure of 25 kPa, the difference between the shear modulus (G) for partially saturated and fully saturated soil reduces considerably for shear strain of 10^{-2} % and above. Similarly for effective confining pressures of 100 kPa and 200 kPa, the difference between the shear modulus (G) for partially saturated and fully saturated soil is noticeable for shear strains up to 10^{-2} % and thereafter the difference is practically negligible. Similar results were obtained for 50 kPa and 150 kPa confining pressures. This means that suction effect is seen to be prominent at low to medium strain range but at high shear strain its influence is found to be negligible. By performing resonant column tests and cyclic triaxial tests on sandy-silty clay, Xenaki and Athanasopoulos (2008) observed similar variations of shear modulus (G) with shear strain. It was observed that the effect of water content on shear modulus (G) value is more pronounced at low values of shear strain and the effect becomes less prominent at strain value greater than 10^{-2} %.

Figure 6.11 presents the variation of normalized shear modulus (G/G_{max}) with shear strain (modulus reduction curves) for effective confining pressures of 25 kPa, 100 kPa and 200 kPa. It is seen that degree of saturation has a little influence on the modulus reduction (G/G_{max}) vs. shear strain curve. Similar observations were made by Mancuso et al. (1993) and Xenaki et al. (2008). However it was also observed that normalized shear modulus (G/G_{max}) value for fully saturated soil is slightly higher than partially saturated soil.

Figure 6.12 gives the variation of damping ratio (D) with increase in shear strain for effective confining pressures of 25 kPa, 100 kPa and 200 kPa. It is observed that the degree of saturation has a negligible effect on the damping ratio (D) with shear strain. Similar observations were also made by Mancuso et al. (1993) and Xenaki and Athanasopoulos (2008) on silty clayey soils. From Figure 6.12, it is seen that for the effective confining pressure of 25 kPa, the damping ratio for a fully saturated soil is 10.5 % to 6.88 % higher than the partially saturated soil when the shear strain is in the range of 10^{-4} % to 10^{-2} % and thereafter the difference is found to be negligible. At higher effective confining pressures, there is a negligible effect of saturation on the damping ratio (D).
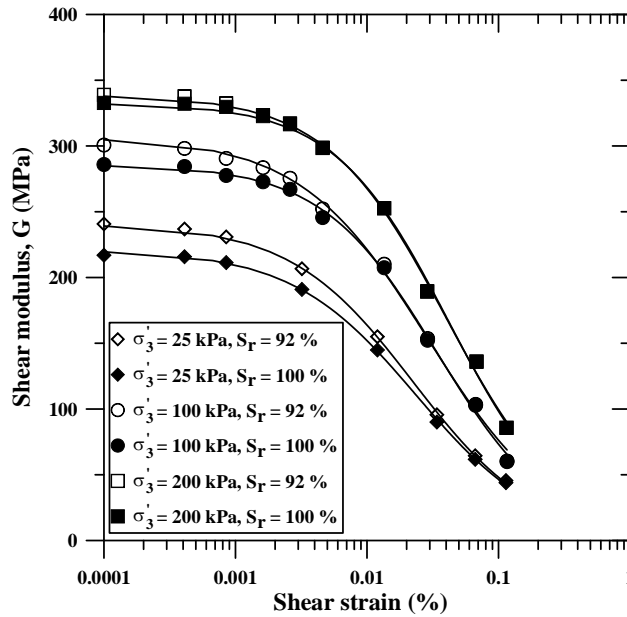

Figure 6.10: Variation of shear modulus (G) with shear strain for partially and fully saturated conditions
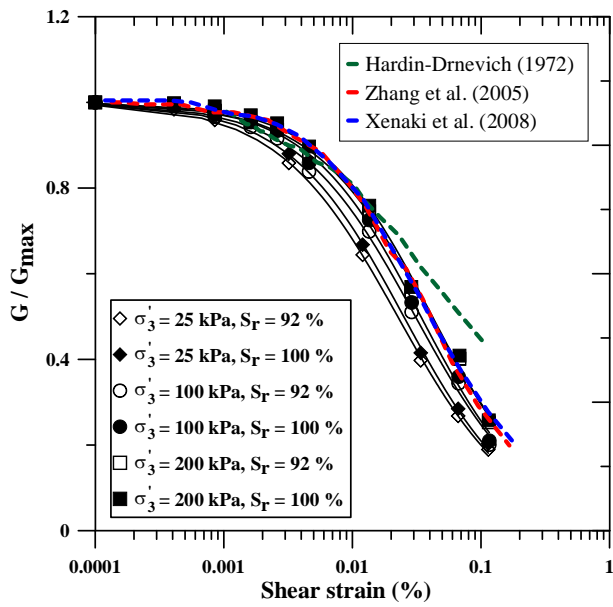
Figure 6.11: Variation of modulus reduction (G / G_{max}) with shear strain for partially and fully saturated conditions

Figure 6.12: Variation of damping ratio (*D*) with shear strain for partially and fully saturated conditions

Figure 6.13 gives the variation of Poisson's ratio (v) with increase in shear strain for effective confining pressures of 25 kPa, 100 kPa and 200 kPa. For the partially saturated soil, there is increase in Poisson's ratio (v) with the increase in shear strain for all the three confining pressures and has been already discussed before in this chapter. However for fully saturated soils, Poisson's ratio (v) is close to 0.5 for all confining pressures. The Poisson's ratio (v) of the soil is independent of any changes in shear strain. Poisson's ratio (v) value for a fully saturated soil under undrained condition is 0.5 because the soil behaves as a perfectly incompressible material with zero volume change. Yokota and Konno (1980) by performing axially vibrating dynamic triaxial apparatus observed that for a fully saturated soil under undrained condition the Poisson's ratio (v) is close to 0.5 and it becomes independent of any increase in shear strain amplitude. In this study it is observed that for partially saturated soil the Poisson's ratio (v) increases with increase in shear strain but for a fully saturated soil under undrained condition it remains constant at 0.5.
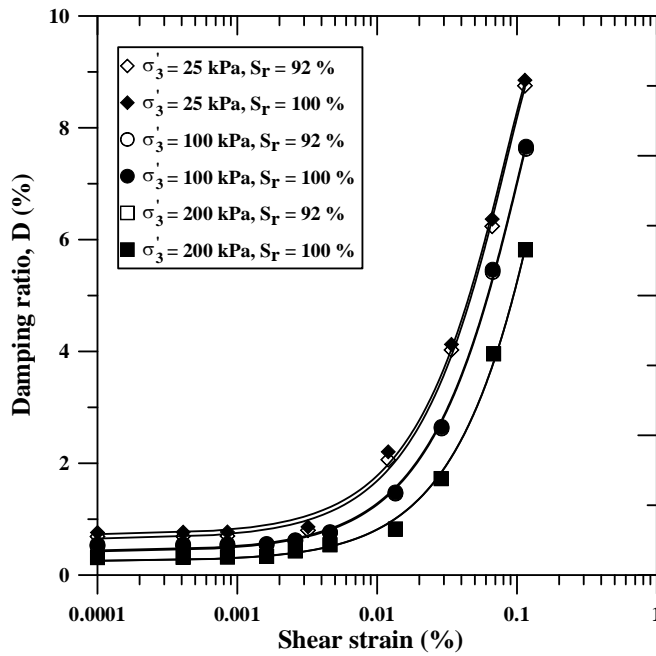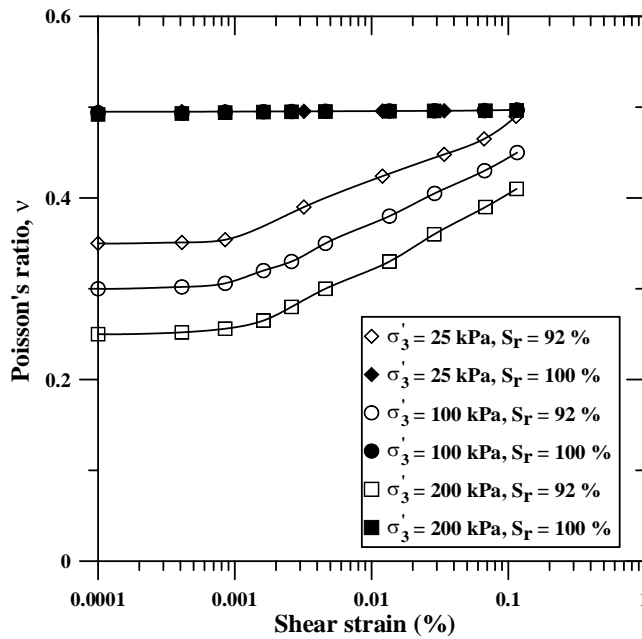

Figure 6.13: Variation of Poisson's ratio with shear strain for partially and fully saturated conditions

96

Figure 6.14 illustrates the variation of small strain shear modulus (G_{max}), which is calculated at a very low shear strain of 10^{-4} %, with effective confining pressure. It is also seen that small strain shear modulus (G_{max}) is higher for the partially saturated soil as compared to the fully saturated soil. However, this reduction in G_{max} with saturation is highly noticed at low effective confining pressure. The percentage difference in the maximum shear modulus for the partially saturated and fully saturated case is found to vary from 9.88 % at effective confining pressure of 25 kPa to 2 % at effective confining pressure of 200 kPa. This can be explained on the basis of capillary induced suction that is present in partially saturated soil. The presence of capillary suction results in higher value of effective confining pressure which results in the higher value of maximum shear modulus of the soil. For the samples prepared at optimum moisture content, a suction value of 3973 kPa is obtained from filter paper test. However for a soil in dry as well as completely saturated condition the effect of capillary suction is absent. In the field, an effective confining pressure of 25 kPa is equivalent to 1.4 m of overburden pressure whereas 200 kPa is equivalent to 11 m of overburden pressure for the density used in this study. It is well understood that the capillary suction effect is present in soil at shallow depths and it decreases as the depth increases. This results in noticeable difference in maximum shear modulus for saturated and partially saturated soils at shallow overburden depth. Therefore if the data which is collected for partially saturated case is considered the same for saturated condition or dry condition it may result in inaccurate design and can be unsafe in certain cases.
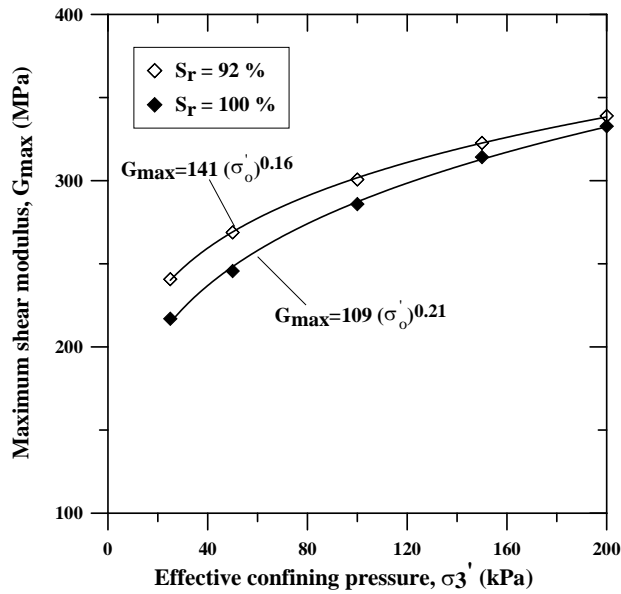
Figure 6.14: Variation of small strain shear modulus (G_{max}) with confining pressure for partially and fully saturated conditions

Figure 6.15 gives the variation of small strain damping ratio (D_{min}) with increase in confining pressure. It is observed that there is an increase in the small strain damping ratio (D_{min}) of the soil for fully saturated case as compared to partially saturated case. Similar to shear modulus, the difference between small strain damping ratio (D_{min}) for fully saturated and partially saturated cases are found to be high when effective confining pressure is less but it reduces as the effective confining pressure increases. The percentages difference in the minimum damping ratio for the partially saturated and fully saturated cases are found to vary from 10.5 % at effective confining pressure of 25 kPa to 1.12 % at effective confining pressure of 200 kPa. This difference can also be explained on the basis of capillary induced suction which increases the effective confining pressure of the soil specimen.

Figure 6.16 gives the variation of small strain Poisson's ratio (v_{min}) with effective confining pressure for both partially saturated as well as fully saturated soils. For partially saturated soil, it is observed that there is a continuous reduction in small strain Poisson's ratio (v_{min}) of the soil with the increase in effective confining pressure. However it is observed that small strain Poisson's ratio (v_{min}) of the fully saturated soil in undrained condition is close to 0.5 and there is no influence of confining pressure on the small strain Poisson's ratio (v_{min}). As already discussed, under undrained condition, saturated soil behave as an incompressible material, so volume change is essentially zero and the Poisson's ratio

approaches limiting value of 0.5. Yokota and Konno (1980) observed that irrespective of sand and clay when tested in undrained condition gives a Poisson's ratio of 0.5. Similar observation was also made by Kokusho (1980) by performing cyclic triaxial tests on Toyoura sand. By performing bender and extender element tests on sand, Kumar and Madhusudhan (2012) observed that small strain Poisson's ratio (v_{min}) of sand increases with increase in the degree of saturation and its value reaches close to 0.5 at 100% degree of saturation and does not depend upon either on confining pressure or relative density for fully saturated sample.
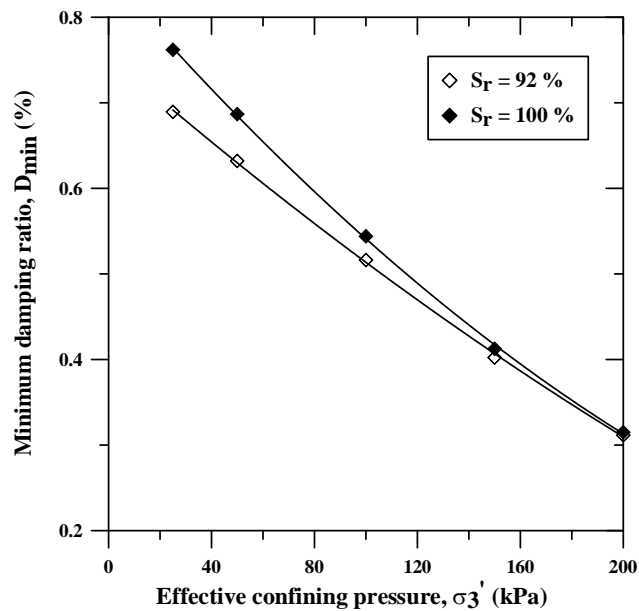
Figure 6.15: Variation of small strain damping ratio (D_{min}) with confining pressure for partially and fully saturated conditions
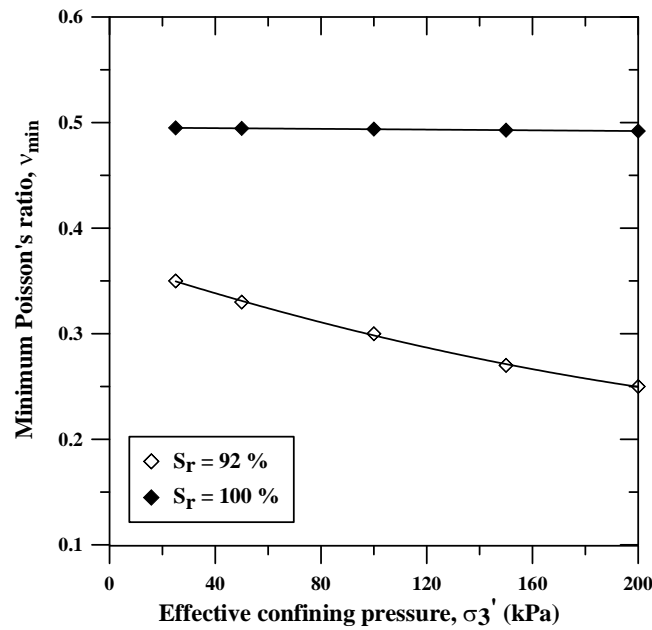
Figure 6.16: Variation of small strain Poisson's ratio (v_{min}) with confining pressure for partially and fully saturated conditions

6.5   Summary

In this chapter, the dynamic properties of expansive clay are discussed. The dynamic properties studied were shear modulus (G), damping ratio (D) and Poisson's ratio (v). The influence of shear strain, confining pressure and saturation on the dynamic properties are also presented. Moreover, an empirical correlation has been proposed in this chapter for the determination of Poisson's ratio of expansive clay from the shear modulus.

100

Chapter 7

Dynamic Properties of Stabilized Expansive Clay

7.1 Introduction

Expansive soil contains minerals like montmorillonite which causes excessive swelling of the soil when it comes in contact with water and can damage light weight structures resting on it. Lime, cement and fly ash are considered as traditional stabilizers to treat expansive soil. Unlike lime and cement which are manufactured products, fly ash is an industrial by product which is obtained from flue gas of the furnace of thermal power plants. Fly ash can be classified as non self cementing (class F) and self cementing (class C) based on ASTM C 618-12a. Bituminous coal has small concentration of calcium compounds and class F fly ash produced from combustion of this type of coal has no self cementing characteristics. Activators like lime should be added to class F fly ash for using it in various stabilization applications. Class C fly ash obtained from sub bituminous fly ash has higher concentration of Calcium Oxide (CaO) and can be effectively used for stabilization purposes. The use of fly ash as a stabilizing agent is an attractive alternative to lime and cement as fly ash is an industrial by-product and is inexpensive (Federal Highway Administration 2003). By using fly ash for stabilization purposes which otherwise would be dumped in landfill, promotes sustainable construction and reduces energy use and reduction in green house gases (Tastan et al. 2011). In the present study, Class C fly ash obtained from Neyveli thermal power plant had been used to treat a moderately expansive soil having a free swell index of 50 %. The percentage of fly ash was increased from 5 % to 20 % at 5 % increments.

7.2 Mechanism of chemical stabilization

When fly ash is blended with soil, calcium oxide (CaO) present in the fly ash reacts with Silica (SiO_2) present in the soil to form hydrated products. The two principal products of hydration are calcium hydroxide (CH) which is crystalline in nature and an amorphous calcium silicate hydrate (C–S–H) gel. The reactions involved in the process of fly ash stabilization are given below:

$$CaO + H_2O \rightarrow Ca(OH)_2 \tag{7.1}$$

$$Ca(OH)_2 \rightarrow Ca^{2+} + 2[OH]^- \tag{7.2}$$

$$Ca^{2+} + 2[OH]^- + SiO_2 \rightarrow \text{C–S–H gel} \tag{7.3}$$
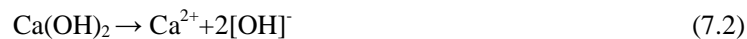
These reactions are called as pozzolanic reactions and leads to the formation of cementitious gels. These cementitious products are responsible for the long term strength of the treated soil. Since, the CaO content present in a fly ash is limited compared to the conventional stabilizers such as lime or cement, the production of hydrated products are also limited which can be seen from the XRD results.

7.3 Test sequence

In this study, various tests were performed to understand the influence of fly ash stabilization on expansive soil. Consistency index tests, free swell index tests and Eades and Grim pH tests were performed to understand the influence of fly ash on the Atterberg limits, free swell and pH respectively of the expansive soil. Resonant column tests were performed to study the influence of fly ash stabilization on the dynamic properties of soil. The samples for RC tests were prepared at optimum moisture content and compacted to its maximum dry density. All RC tests were performed on unsaturated samples. No attempt has been made to saturate the treated samples. This is because with stabilization there is significant increase in the strength of the soil and to fully saturate treated samples is not only difficult but also require significant duration of time. As the samples were tested under partially saturated conditions, suction tests were performed to understand the influence of fly ash stabilization on the suction of treated soils. Unconfined compressive strength tests were done to study the influence of stabilization on the strength characteristics of treated soils. X-ray diffraction (XRD) tests were performed to qualitatively identify the compounds present in untreated

and treated soils. Moreover, a design problem is discussed to show the application of the data obtained in the present study.

7.4 Test procedure

7.4.1 Atterberg limit test

The liquid limit and plastic limit of both untreated and treated expansive soil was determined as per the ASTM D4318-10e1. Liquid limit is the moisture content corresponding to 25 numbers of blows in a standard Casagrande's apparatus for the closure of a groove of specified length and width. Plastic limit is the moisture content, at which soil rolled into a thread of 3 mm diameter starts to crumble. Both liquid limit and plastic limits are expressed in percentage.

7.4.2 Free swell index test

Free swell index test is performed to determine the expansion potential of expansive soil in water. It is used to determine the expansion of soil caused by diffuse double layer repulsion and changes in soil fabric (Holtz and Gibbs, 1954). In this test, ten grams of oven dried soil passing $425\ \mu m$ were poured into graduated cylinders of 100 ml capacity. One of the cylinders is filled with distilled water and other with kerosene to the 100 ml mark. It is stirred by means of a glass rod to remove entrapped air and allowed to settle for 24 hours. After 24 hours final volumes of the soils are read out.

$$\text{Free swell index }(\%) = \frac{\left(V_d - V_k\right)}{V_k} \times 100 \tag{7.4}$$

where, V_d = volume of the soil specimen recorded from the graduated cylinder containing distilled water; V_k = volume of the soil specimen recorded from the graduated cylinder containing kerosene.

7.4.3 pH test

Eades and Grim (1963) described a quick test to obtain the optimum lime content required to fulfill initial reactions and provide adequate lime for long term strength gain. This test requires sufficient lime to be added to the soil to satisfy all immediate reactions and still provide sufficient residual lime to maintain pozzolanic reactions. The addition of lime creates a high pH environment to dissolve the silica and alumina. It also provides sufficient

free calcium for long term strength gain by pozzolanic reactions. A pH value of 12.4 is ideal value for stabilization purposes and the mix which gives that value can be taken as the optimum dosage of stabilizer. The same test is performed to determine the optimum fly ash content for the stabilization.

A 20 gm soil passing through 425 μ size sieve was taken in a 150 ml bottle with a screw lid at the top. The stabilizer was added in different percentages to 100 ml distilled water and the mix was added to the soil to make soil-stabilizer mixture. The bottles were shaken about 30 seconds after every 10 minutes for an hour. The slurry was transferred into a beaker after one hour and the pH concentration of the slurry was measured with the electronic pH meter.

7.4.4 Unconfined Compressive Strength (UCS) tests

Specimens of size 50 mm diameter and 100 mm height were prepared in triplicate for all the mixes at their corresponding OMC and MDD. The casted specimens were then cured in a stability chamber under controlled moisture (70% humidity) and temperature (25^0C) conditions for a period of 1, 7 and 28 days. Samples were then tested according to ASTM D1633-07 standard test method at the end of each curing period.

7.4.5 X-Ray powder diffraction (XRPD) studies

X-ray powder diffraction study has been performed on Class C fly ash, expansive soil and treated expansive soil to identify qualitatively the minerals present. In XRPD test, a powdered specimen is subjected to an intense X-ray beam and detecting the diffracted beam with the help of a detector. The detector then converts the analog signals into digital data which can be plotted to obtain peaks. In the present study, XRPD data were collected using PANalytical X'Pert Pro MPD diffractometer in a θ-θ configuration employing C_uK_α radiation (λ = 1.54 A°) with a fixed divergence slit size 0.5° and a rotating sample stage. The ground powders were manually frontloaded into a standard sample holder. The samples were scanned between 5° and 100° by using an X'Celerator detector. The peaks were then analyzed according to the intensities using PCPDFWIN software to confirm the presence of certain minerals.

7.5   Results and discussions

7.5.1   Effect of fly ash on Atterberg limits

Figure 7.1 gives the variation of Atterberg limits with the increase in fly ash content. It is seen that the liquid limit and plastic limit of the soil increase whereas plasticity index of the soil decreases with the increase in fly ash content. The increase in liquid limit and plastic limit is due to flocculation and conglomeration of the clay particles which increases the water holding capacity and which in turn increases the liquid limit and plastic limit of the soil (Mateos 1964, George et al. 1992). However, the increase in plastic limit is greater than the liquid limit causing a corresponding decrease in the plasticity index of the soil and which confirms the fact that the decrease in plasticity index is not due to reduction of liquid limit but due to increase in plastic limit of the soil (George et al. 1992). Furthermore, based on the PI of the soil, the degree of expansion of the fly ash treated soil can now be considered as *low* (Chen, 1975, Holtz and Gibbs, 1956).
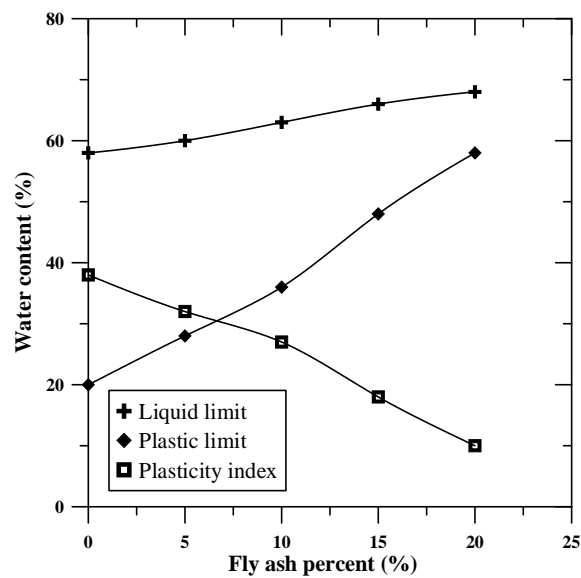

Figure 7.1: Variation of Atterberg's limits and plasticity index with fly ash content

105

7.5.2 Effect of fly ash on free swell index

Table 7.1 gives the variation of free swell index of the soil with the increase in percentage of fly ash. It is observed that there is a considerable reduction in the free swell index of the soil, with the increase in percentage of fly ash. This is because Class C fly ash can provide a slew of multivalent cations (Ca^{2+}, Al^{3+}, Fe^{3+} etc.) which causes flocculation of clay particles by cation exchange. Due to flocculation, the specific area and water affinity is greatly reduced which cause reduction in free swell index of treated soils. The degree of expansiveness of the treated soils can be considered as *low* according to ASTM D2487-11 and IS 1498-1970.

Table 7.1: Swell index of untreated and treated soils

Percentage of fly ash	Free swell index (%)
0	50
5	45
10	30
15	20
20	10

7.5.3 Effect of fly ash on pH

Table 7.2 shows variation of the pH of the soil with the increase in fly ash percentage. It is observed that with the increase in fly ash content, the pH of the soil increases. Optimum pH value of 12.5 is obtained at fly dosage of 20 %.

Table 7.2: pH values for untreated and treated soils

Percentage of fly ash	pH
0	8.6
5	9.8
10	11
15	12.1
20	12.5

7.5.4 Effect of Fly Ash on Dynamic Properties of Soil

Figures 7.2, 7.3, 7.4 give the variation of shear modulus with increase in shear strain for 25 kPa, 100 kPa and 200 kPa confining pressures respectively for different percentages of fly ash and 28 days curing period. It is observed that with the increase in shear strain, there is reduction in shear modulus (G) of both untreated and treated soil. This is due to reduction in the stiffness of the soil with increase in shear strain. With the increase in fly ash percentage, there is increase in shear modulus (G) of the soil. This is because of the cementation effect of fly ash on the soil caused by cation exchange and pozzolanic reactions and which provides a confinement effect at the clay to clay interfaces. This causes higher rigidity of the treated specimen resulting in higher values of shear modulus (G). The percentages increase in shear modulus for soil treated with 20 % fly ash as compared to untreated soil at 200 kPa confining pressure are 200 % and 52 % for shear strain of 10^{-4} % and 10^{-1} % respectively. This shows that increase in shear modulus is significant at lower values of shear strain and the improvement reduces considerably with the increase in shear strain. This is due to the breakage of cementation bonds between the soil particles at higher value of shear strain. Similar observations were made by D'Onofrio and Penna (2003) by performing resonant column tests on lime treated silty sands. Table 7.3 gives the threshold value of shear strain for different dosage of fly ash. It is observed that with the increase in fly ash percent there is reduction in threshold shear strain.
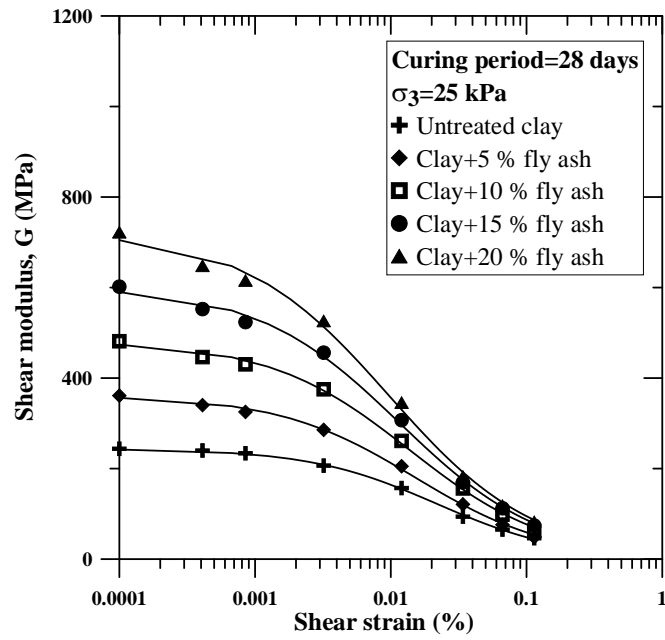
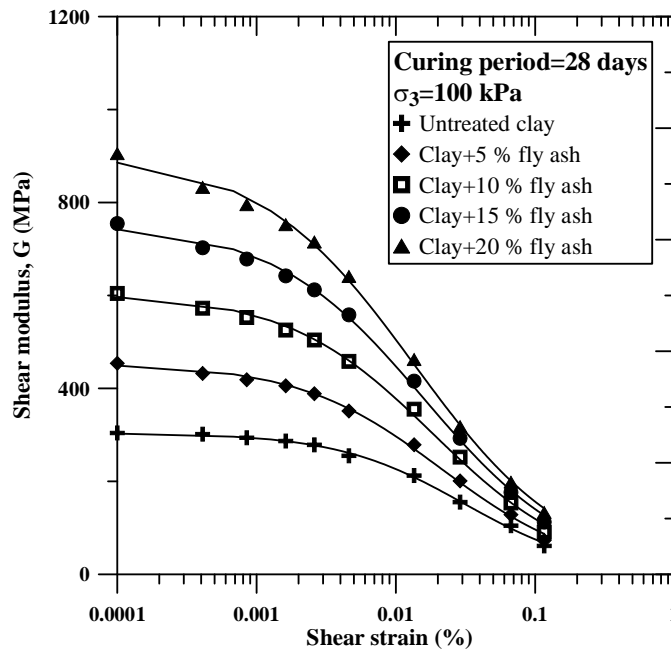**Figure 7.2: Variation of shear modulus (G) with shear strain for 25 kPa confining pressure and 28 days curing period**

Figure 7.3: Variation of shear modulus (G) with shear strain for 100 kPa confining pressure and 28 days curing period
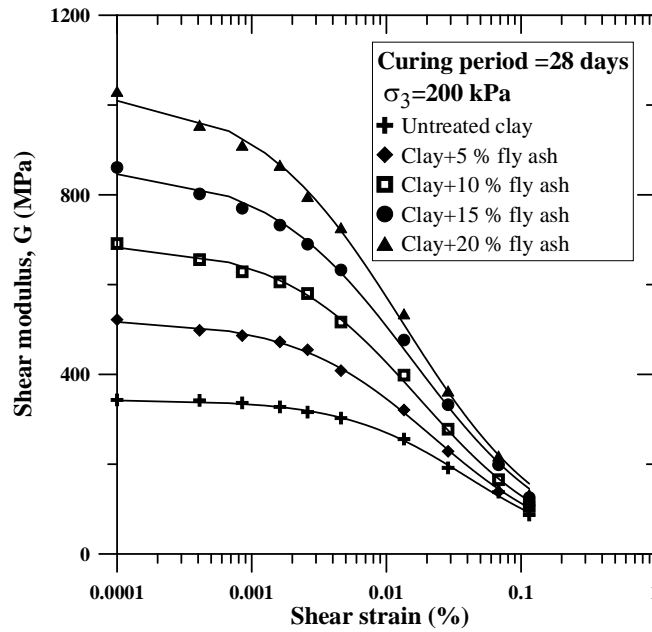
Figure 7.4: Variation of shear modulus (G) with shear strain for 200 kPa confining pressure and 28 days curing period

Table 7.3: Values of threshold shear strain for different dosage of fly ash

Curing period (days)	Confining pressure (kPa)	Fly ash (%)	Threshold Shear Strain 10^{-4} (%)
28	25	0	2.91
28	25	5	1.53
28	25	10	1.42
28	25	15	1.37
28	25	20	1.30
28	100	0	4.67
28	100	5	1.64
28	100	10	1.58
28	100	15	1.45
28	100	20	1.38
28	200	0	9.61
28	200	5	1.68
28	200	10	1.59
28	200	15	1.46
28	200	20	1.42

Figures 7.5, 7.6, 7.7 give the variation of shear modulus with increase in shear strain for 25 kPa, 100 kPa and 200 kPa confining pressures respectively for different curing periods for 20 % fly ash percentage. It is observed that with the increase in curing period, there is increase in shear modulus of the treated soil. The increase in shear modulus due to curing is because of time dependent cementitious and pozzolanic properties of fly ash which results in the further increase of the rigidity of the soil with curing. This increase in shear modulus is also notable from small strain to medium shear strain but with further increase in the shear strain there is a less improvement of shear modulus with curing. At shear strain of 0.1 %, there is small improvement (about 6 %) in the shear modulus of the treated soil with the curing. Similar observations were made at other dosages of fly ash as well and were not provided to avoid repetition. Table 7.4 gives the variation of threshold shear strain with the in curing period. It is observed that with the increase in curing period, threshold value of shear strain reduces.
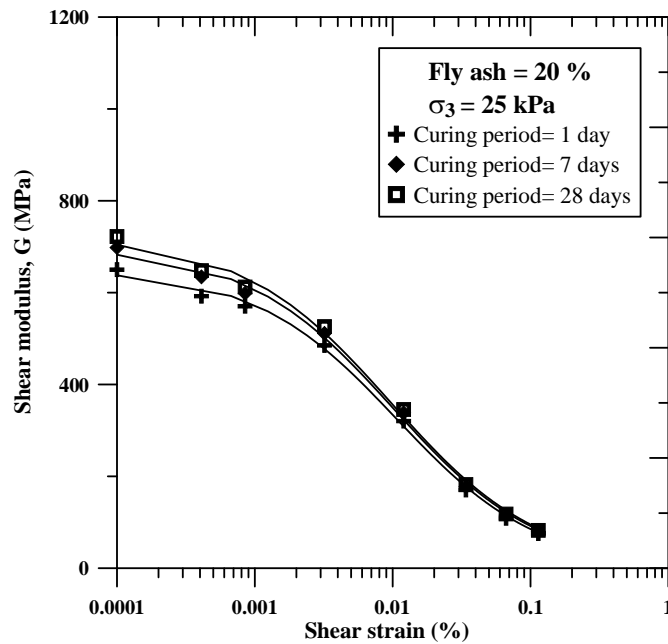

Figure 7.5: Variation of shear modulus (G) with shear strain for 25 kPa confining pressure and 20 % fly ash content
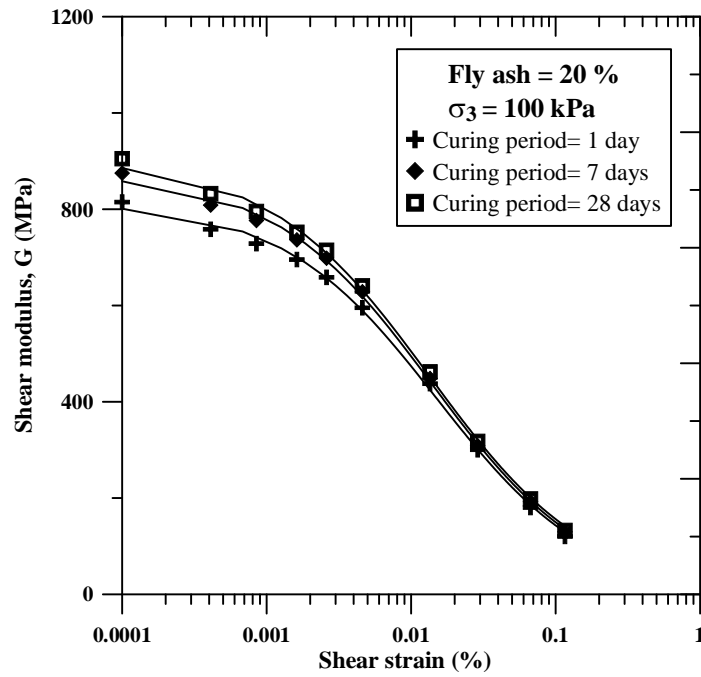
Figure 7.6: Variation of shear modulus (G) with shear strain for 100 kPa confining pressure and 20 % fly ash content
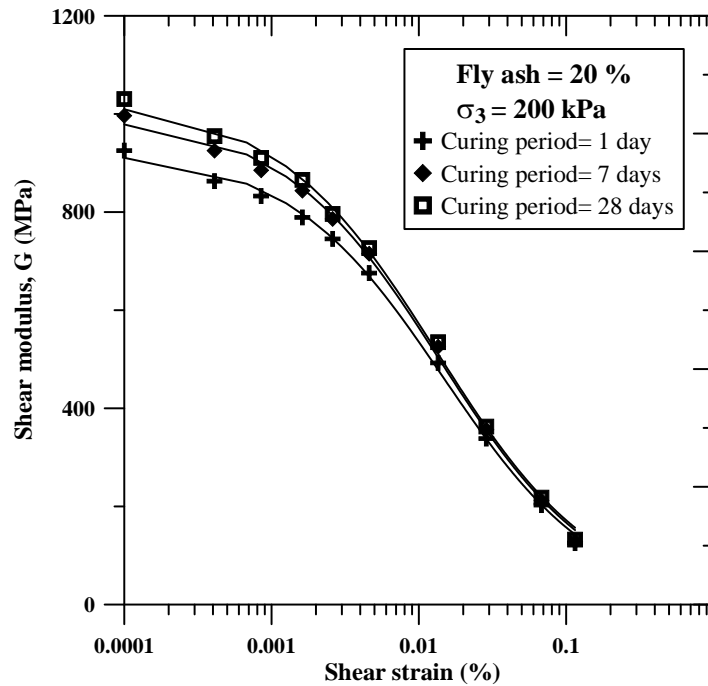

Figure 7.7: Variation of shear modulus (G) with shear strain for 200 kPa confining pressure and 20 % fly ash content

111

Table 7.4: Values of threshold shear strain for different dosage of fly ash

Fly ash (%)	Confining pressure (kPa)	Curing period (days)	Threshold Shear Strain 10^{-4} (%)
20	25	1	1.39
20	25	7	1.33
20	25	28	1.30
20	100	1	1.44
20	100	7	1.40
20	100	28	1.38
20	200	1	1.46
20	200	7	1.43
20	200	28	1.42

Figures 7.8, 7.9, 7.10 give the variation of modulus reduction (G/G_{max}) with increase in shear strain for 25 kPa, 100 kPa and 200 kPa confining pressures respectively for 28 days curing period. It is observed that (G/G_{max}) value decreases with the increase in shear strain. This is due to the degradation of shear modulus with the increase in shear strain. It is further observed that with the increase in fly ash content, the (G/G_{max}) ratio decreases. This means that degradation of stabilized soils take place at a faster rate than untreated soil. This is due to the high initial shear stiffness of the treated specimens than the untreated specimen. Similar observations were made by D'Onofrio and Penna (2003) and Delfosse-Ribay et al. (2004).

Figures 7.11, 7.12, 7.13 give the variation of modulus reduction (G/G_{max}) with increase in shear strain for 25 kPa, 100 kPa and 200 kPa confining pressures respectively for different curing periods for 20 % fly ash percentage. It is seen that there is negligible influence of curing period on modulus reduction (G/G_{max}) of treated soils. However, there is a marginal reduction in modulus degradation (G/G_{max}) value with increase in curing period for all the three confining pressures. Similar observations were made at other dosages of fly ash as well.

Figure 7.8: Variation of modulus reduction (G / G_{max}) with shear strain for 25 kPa confining pressure and 28 days curing period

Figure 7.9: Variation of modulus reduction (G / G_{max}) with shear strain for 100 kPa confining pressure and 28 days curing period
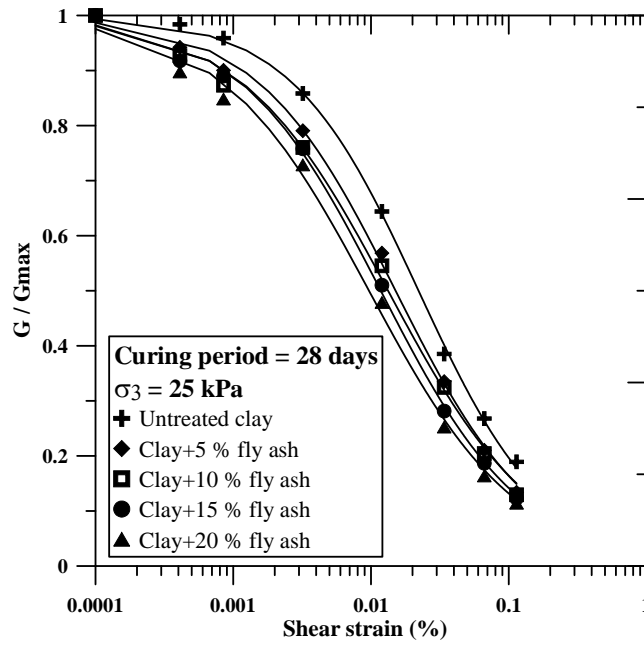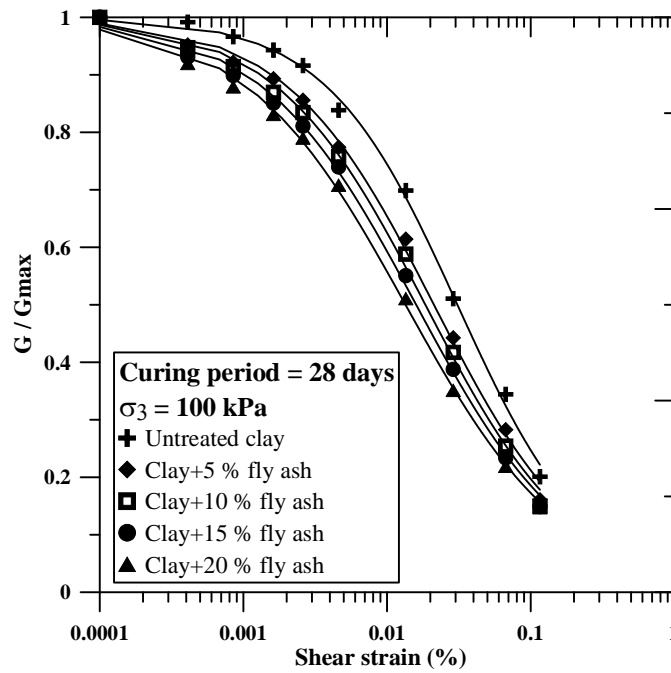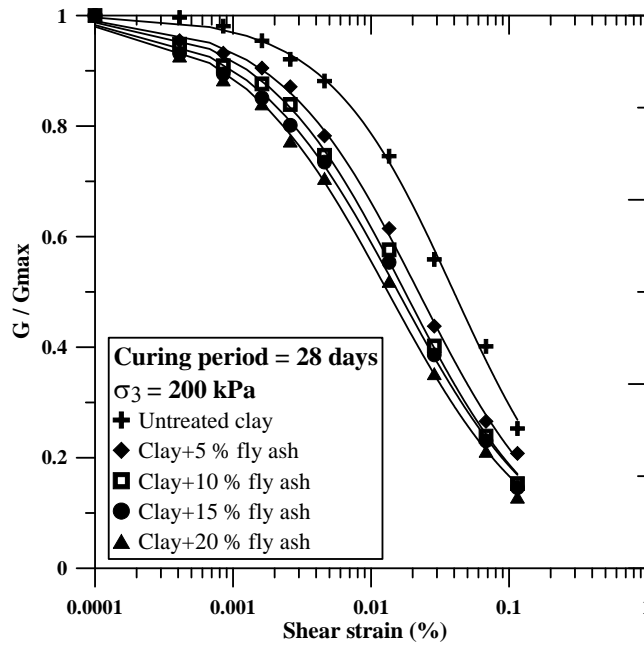
Figure 7.10: Variation of modulus reduction (G/G_{max}) with shear strain for 200 kPa confining pressure and 28 days curing period

Figure 7.11: Variation of modulus reduction (G/G_{max}) with shear strain for 25 kPa confining pressure and 20 % fly ash content
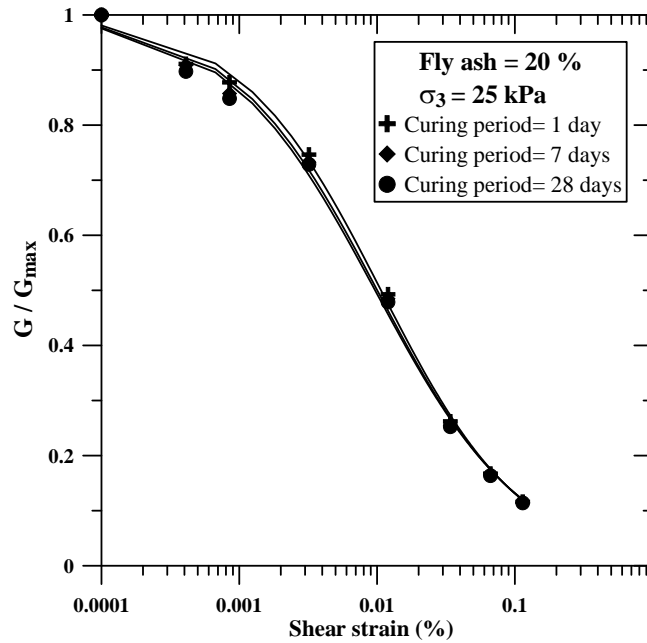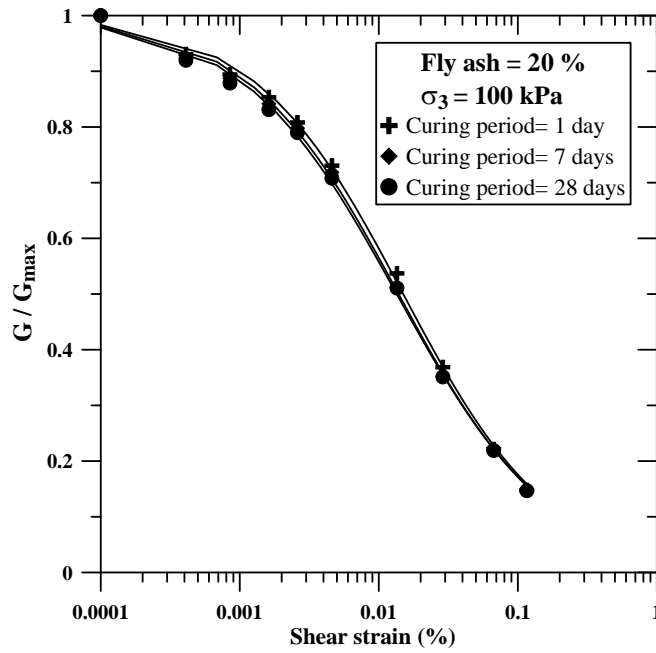
Figure 7.12: Variation of modulus reduction ($G / G_{\max}$) with shear strain for 100 kPa confining pressure and 20 % fly ash content
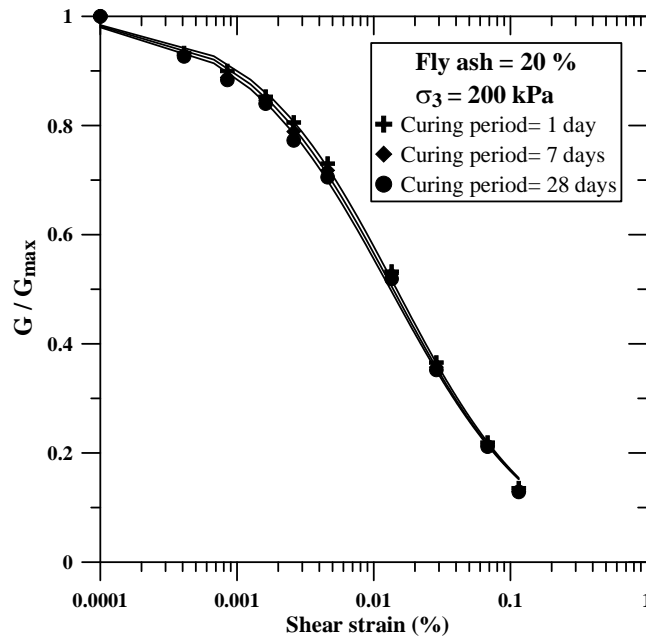

Figure 7.13: Variation of modulus reduction ($G / G_{\max}$) with shear strain for 200 kPa confining pressure and 20 % fly ash content

115

The present study generated extensive modulus degradation data on fly ash treated moderate expansive clays at different fly ash dosages, curing periods and isotropic confining pressures. This data is collectively used to obtain the range of G/G_{max} values at different shear strain values to develop lower and upper bounds modulus degradation curves for the treated expansive soils. The upper bound represents the modulus degradation of untreated and low fly ash stabilized clays subjected to low confining pressures. The lower bound represents the modulus degradation values of clays stabilized with high fly ash content and subjected to high confining pressures. Figure 7.14 presents the range of modulus degradation (G/G_{max}) with shear strain for all the fly ash treated clay specimens. To validate the proposed upper and lower bounds of modulus degradation curves, very limited data available in the literature is considered. Hoyos et al. (2004) have performed low strain RC tests on fly ash, cement and lime with fibres treated surface rich expansive soils. The expansive clay was treated with 20 % class F fly ash, 5-10% type V sulfate resistant cement and 8% lime with 0.3% fibers. The specimens were cured for 7 days and resonant column tests were performed between low to medium shear strain intervals and 17.25 kPa (2.5 psi) to 138 kPa (20 psi) confining pressures. The G/G_{max} values were calculated from this study and presented in the Figure 8. It can be seen that the G/G_{max} values of class F fly ash and lime with fibres treated specimens plot towards the upper bound curve. This may be due to the low CaO content (1.1%) present in the class F fly ash used in the study, which might have produced marginal pozzolanic reactions in sulfate rich expansive soil specimens. The normalized stiffness modulus of 10% cement treated specimens plot towards the lower bound curve. High modulus degradation is expected in these specimens as the cement content is high. In another study, Chepkoit and Aggour (2000) have performed resonant column studies to determine the dynamic properties of lime stabilized (8%) high plastic clays. The samples were compacted to the respective OMCs and cured in a humidity chamber and then kept in an oven maintained at 105 ^{o}C for 65 hrs before tested at 1 kPa to 210 kPa isotropic confining pressures. It can be seen that the modulus degradation data of lime treated clay specimens plot along the upper bound curve (Figure 7.14). The initial low strain shear modulus (G_{max}) is expected to be low in these specimens due to aggressive curing conditions. This might be the reason for lime treated specimens plot towards the upper bound curve.

As can be clearly seen that the modulus degradation data, obtained from high PI clays, sulfate rich expansive clays and moderate expansive clays stabilized with lime with and without fibers, cement and class C/F fly ash, falls within the proposed upper and lower bound curves. Hence, the proposed curves may be generalized and can be used to estimate the modulus degradation (G/G_{max}) data of any type of stabilized clays.
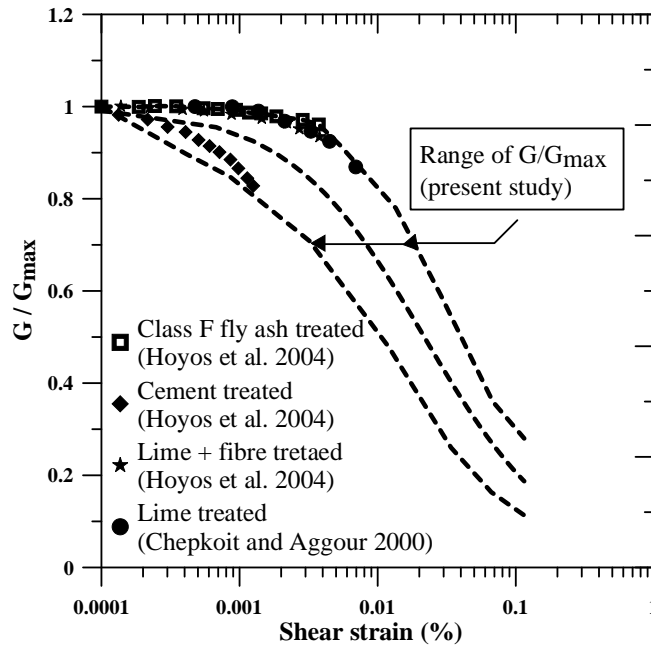

Fig. 7.14: Comparison of modulus degradation (G/G_{max}) with shear strain for treated clays obtained from present study with Hoyos et al. (2004) and Chepkoit and Aggour (2000)

Figures 7.15, 7.16, 7.17 give the variation of damping ratio (D) with increase in shear strain for 25 kPa, 100 kPa and 200 kPa confining pressures respectively for 28 days curing period. It is seen that there is increase in damping ratio with the increase in shear strain. The damping ratio is a measure of the dissipation of energy during cyclic loading. Higher the degree of particle slippage and particle rearrangement, higher is the damping ratio of the soil (Fahoum et al. 1996). With the increase in strain level, there are greater chances of particle slippage and rearrangement which results in higher value of damping ratio. It is also observed that there is reduction in damping ratio (D) value with increase in fly ash dosage. Addition of fly ash increases the rigidity of the soil which causes reduced particle slippage and particle rearrangement resulting in lower value of damping ratio. Similar observations were made by Acar et al. (1987), Dobry and Vucetic (1987) and Fahoum et al. (1996). Figures 7.17, 7.19, 7.20 give the variation of damping ratio (D) with increase in shear strain

117

for 25 kPa, 100 kPa and 200 kPa confining pressures respectively for different curing periods for 20 % fly ash percentage. It is observed that there is a marginal decrease in damping ratio with curing and can be neglected for any design purpose. Similar observations were made at other dosages of fly ash as well.

Figure 7.15: Variation of damping ratio (D) with shear strain for 25 kPa confining pressure and for 28 days curing period

118

Figure 7.16: Variation of damping ratio (D) with shear strain for 100 kPa confining pressure and for 28 days curing period
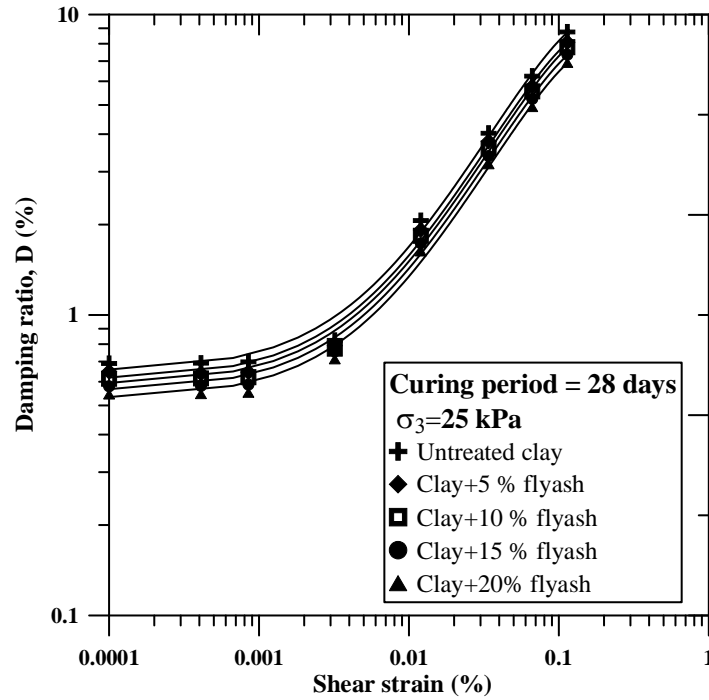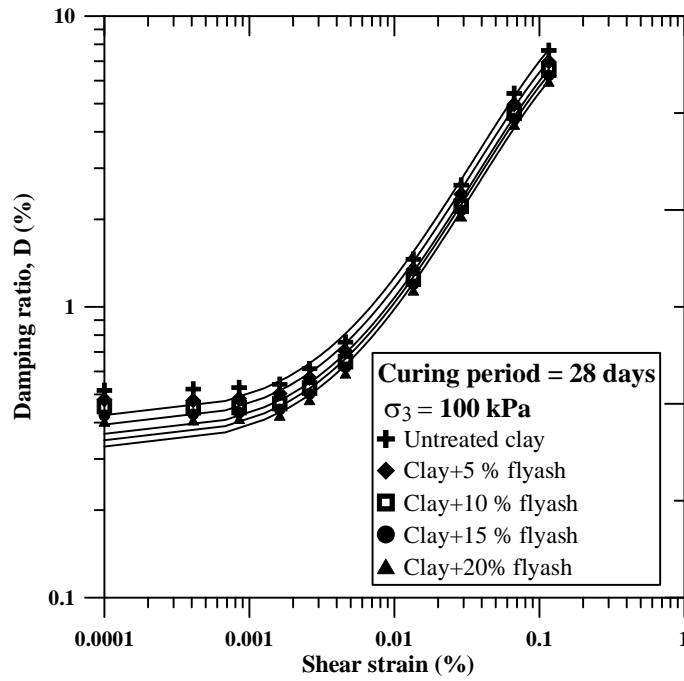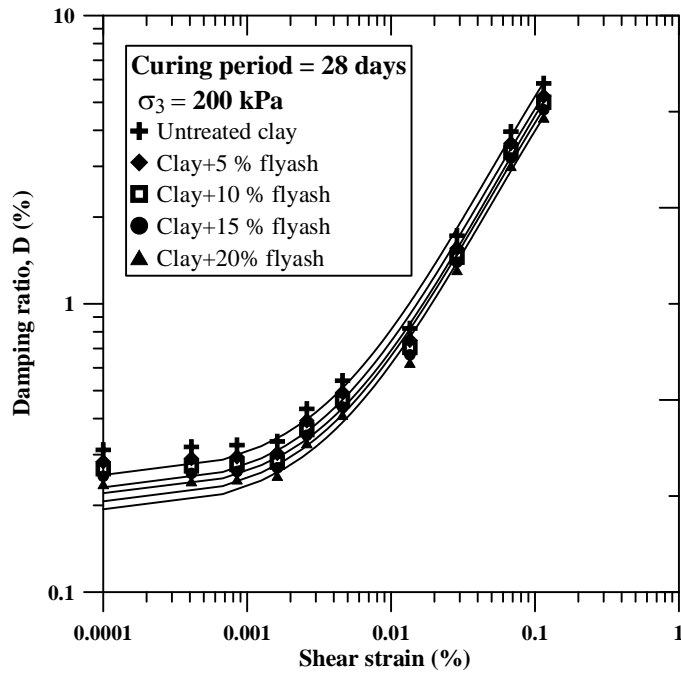

Figure 7.17: Variation of damping ratio (D) with shear strain for 200 kPa confining pressure and for 28 days curing period
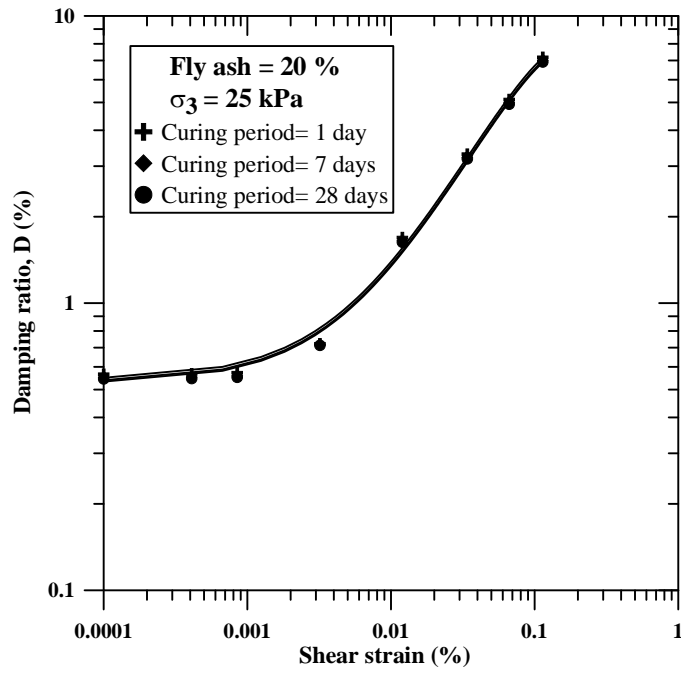
Figure 7.18: Variation of damping ratio (D) with shear strain for 25 kPa confining pressure and 20 % fly ash content
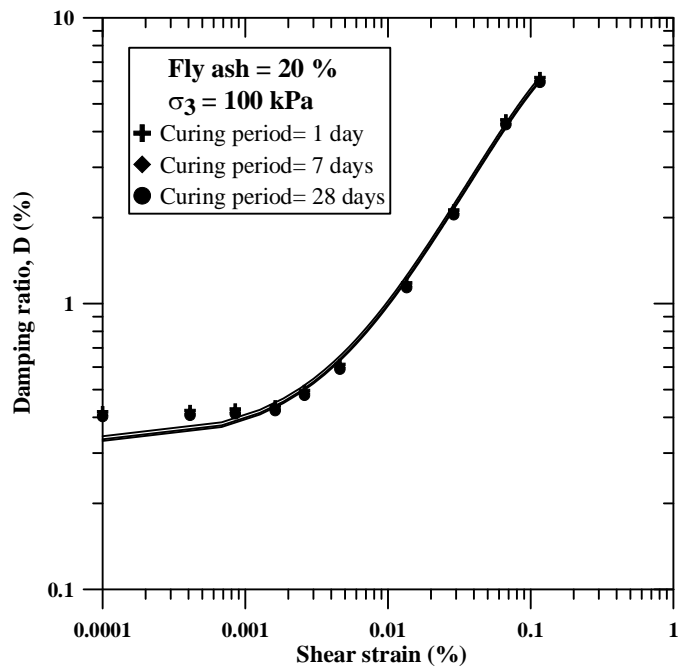

Figure 7.19: Variation of damping ratio (D) with shear strain for 100 kPa confining pressure and 20 % fly ash content
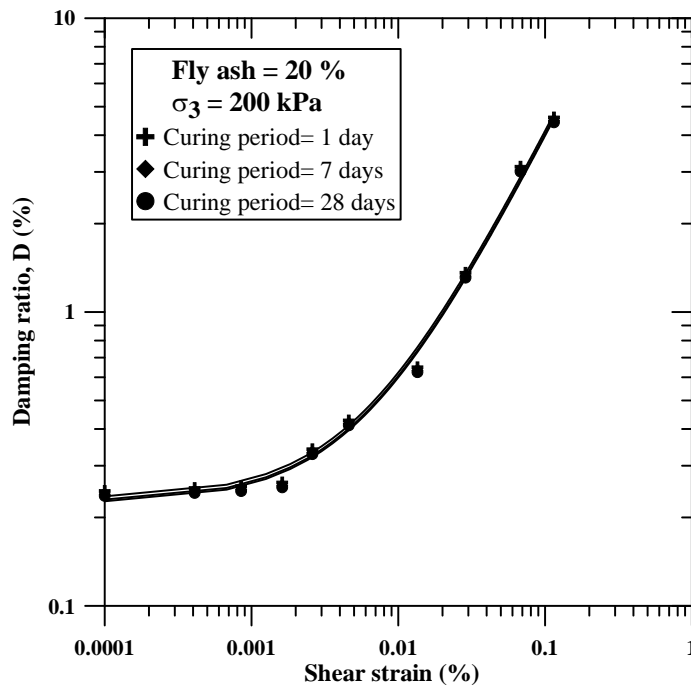
120

Figure 7.20: Variation of damping ratio (D) with shear strain for 200 kPa confining pressure and 20 % fly ash content

Figures 7.21, 7.22, 7.23 give the variation of Poisson's ratio (ν) with increase in shear strain for 25 kPa, 100 kPa and 200 kPa confining pressures respectively for 28 days curing period. It is seen that with the increase in shear strain, Poisson's ratio (ν) of the untreated and treated soil increases. The increase is less up to a shear strain of 9×10^{-4} % but after that there is gradual increase in Poisson's ratio (ν) of soils. It is also observed that Poisson's ratio (ν) decreases with increase in fly ash dosages. This is because with the increase in fly ash content, the stiffness of the soil increases which gives higher resistance to specimen deformation. Figures 7.24, 7.25, 7.26 give the variation of Poisson's ratio (ν) with increase in shear strain for 25 kPa, 100 kPa and 200 kPa confining pressures respectively for different curing periods for 20 % fly ash percentage. There is a slight reduction in Poisson's ratio with the increase in the curing period unlike on the shear modulus and damping ratios, where the influence of curing interval is negligible. Similar observations were made at other dosages of fly ash. Omine et al. (1999) by performing falling weight deformation modulus test, a kind of non-destructive test on cement stabilized soils reported a reduction in Poisson's ratio (ν) with the increase in curing period.

Figure 7.21: Variation of Poisson's ratio (ν) with shear strain for 25 kPa confining pressure and 28 days curing period

Figure 7.22: Variation of Poisson's ratio (ν) with shear strain for 100 kPa confining pressure and 28 days curing period

Figure 7.23: Variation of Poisson's ratio (ν) with shear strain for 200 kPa confining pressure and 28 days curing period

Figure 7.24: Variation of Poisson's ratio (ν) with shear strain for 25 kPa confining pressure and 20 % fly ash content
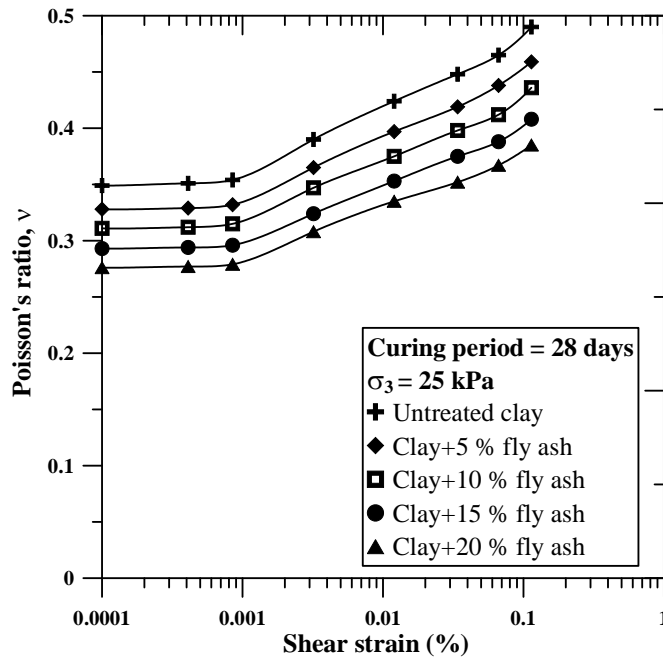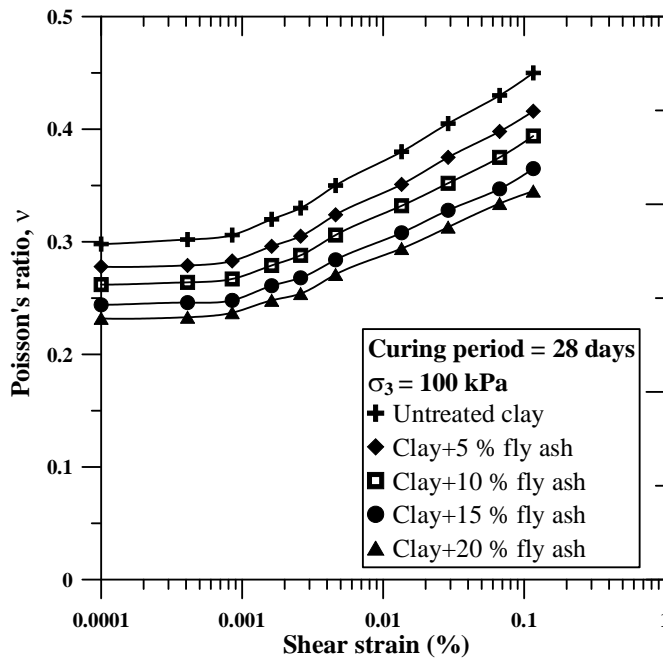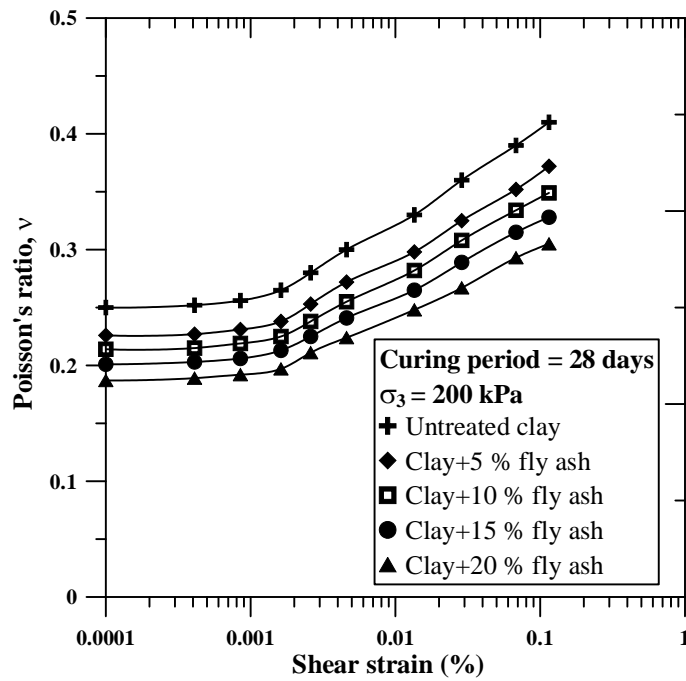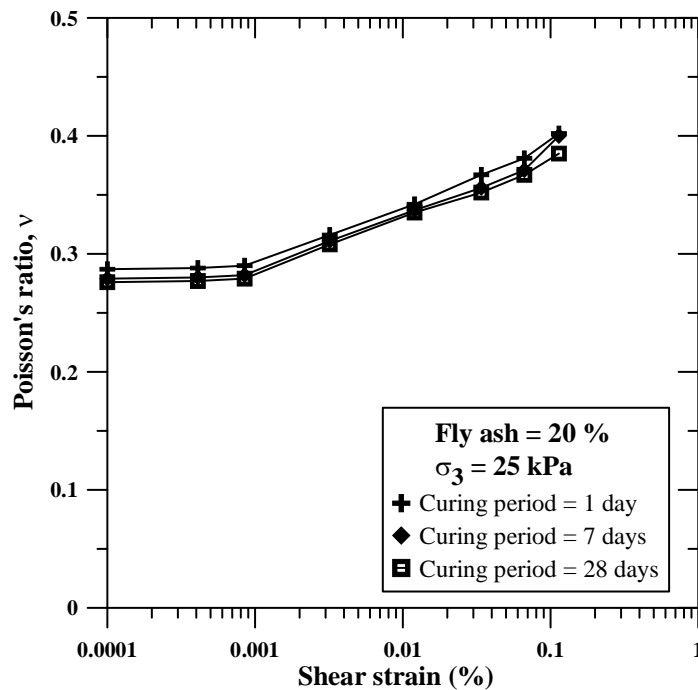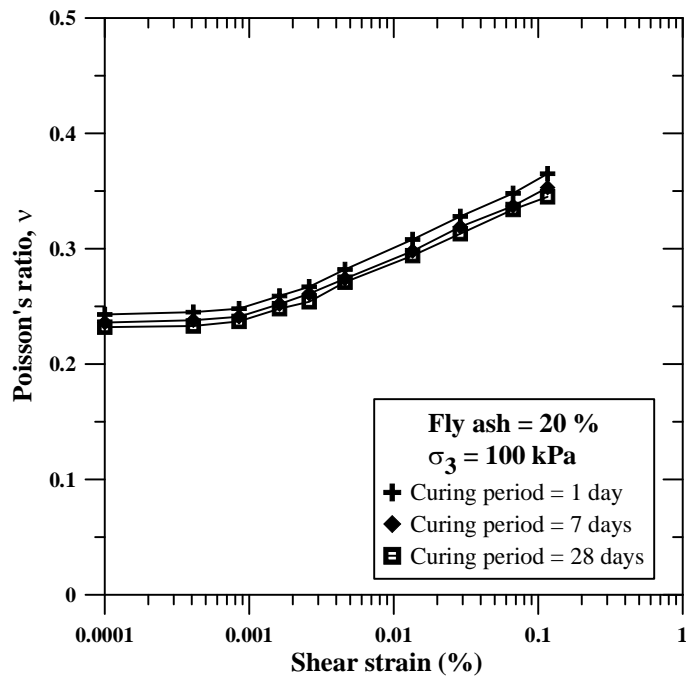
123

Figure 7.25: Variation of Poisson's ratio (ν) with shear strain for 100 kPa confining pressure and 20 % fly ash content
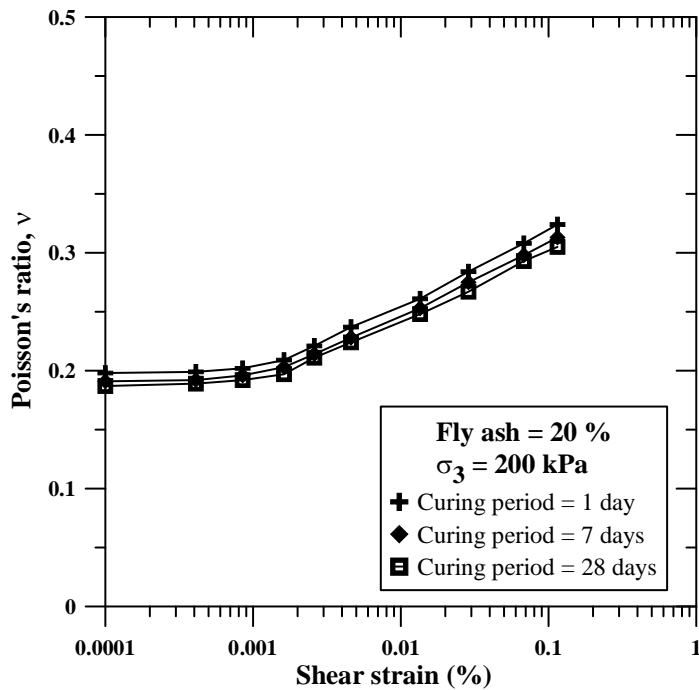

Figure 7.26: Variation of Poisson's ratio (ν) with shear strain for 200 kPa confining pressure and 20 % fly ash content

124

Figure 7.27 presents the variation of small strain shear modulus (G_{max}) with the increase in confining pressure for different dosages of fly ash for 28 days curing period. The small strain shear modulus (G_{max}) is determined at shear strain of 10^{-4} %. It is observed that small strain shear modulus (G_{max}) increases with the increase in confining pressure as well as increase in fly ash percent. Figure 7.28 gives the variation of small strain damping ratio (D_{min}) with the increase in confining pressure for different dosages of fly ash for 28 days curing period. The small strain damping ratio (D_{min}) is determined at shear strain of 10^{-4} %. It is observed that damping ratio decreases with the increase in confining pressure as well as fly content. However, it is observed that at higher confining pressure (at 200 kPa), the reduction in damping ratio is minimal. Figure 7.29 gives the variation of small strain Poisson's ratio (v_{min}) with the increase in confining pressure for different dosages of fly ash for 28 days curing period. The small strain Poisson's ratio (v_{min}) is determined at shear strain of 10^{-4} %. There is reduction in small strain Poisson's ratio (v_{min}) with the increase in confining pressure as well as fly content of the treated soil. As already discussed in Chapter 5 for dynamic properties of sand, the increase in small strain shear modulus (G_{max}) and reduction of small strain damping ratio (D_{min}) and small strain Poisson's ratio (v_{min}) with the increase in confining pressure is because with increase in confining pressure, there is increased number of particle-particle bonds which provides higher resistance to the specimen to deformation (Mitchell 1976).
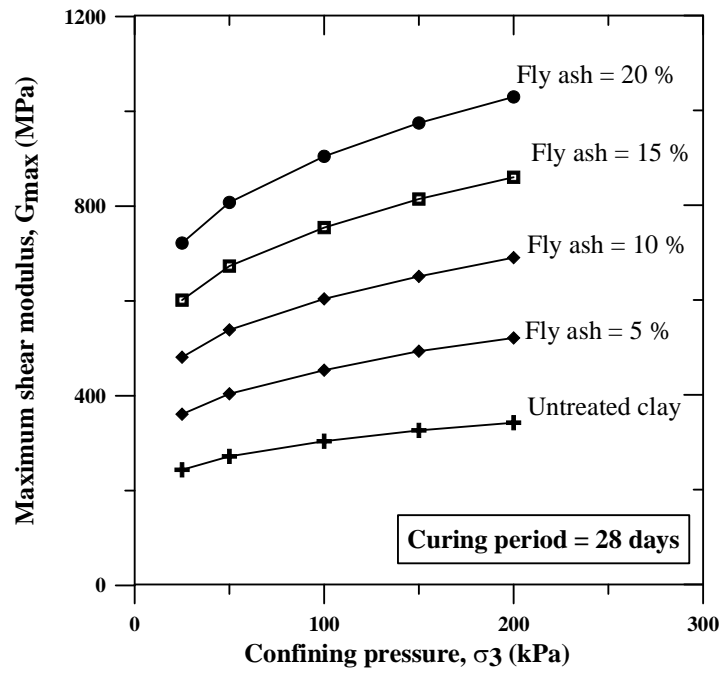
Figure 7.27: Variation of small strain shear modulus (G_{max}) with confining pressure for different dosage of fly ash
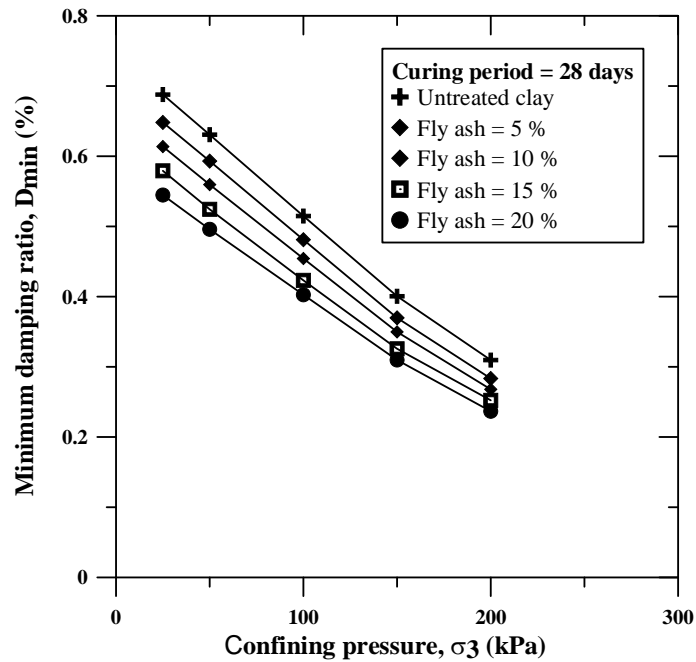
Figure 7.28: Variation of small strain damping ratio (D_{min}) with confining pressure for different dosage of fly ash
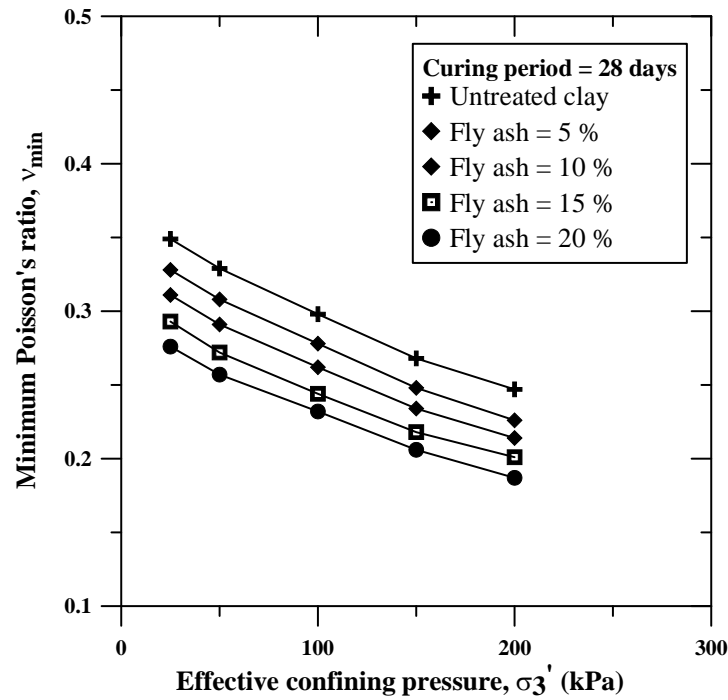
Figure 7.29: Variation of Poisson's ratio with confining pressure for different dosage of fly ash

Figures 7.30, 7.31 and 7.32 give the variation of small strain shear modulus (G_{max}) with fly ash content for 25 kPa. 100 kPa and 200 kPa confining pressure respectively. It is observed that with the increase in curing period, the small strain shear modulus (G_{max}) of the treated soil increases. Figures 7.33, 7.34 and 7.35 give the variation of small strain damping ratio (D_{min}) with fly ash content for 25 kPa. 100 kPa and 200 kPa confining pressure respectively. It is observed that with the increase in curing period, the small strain damping ratio (D_{min}) of the treated soil decreases. Figures 7.36, 7.37 and 7.38 give the variation of small strain Poisson's ratio (v_{min}) with fly ash content for different curing periods. It is seen that small strain Poisson's ratio (v_{min}) decreases with the increase in curing period. The increase in shear modulus and decrease in damping ratio and Poisson's ratio due to curing is because of time dependent cementitious and pozzolanic properties of fly ash which results in the further increase of the rigidity of the soil with curing.
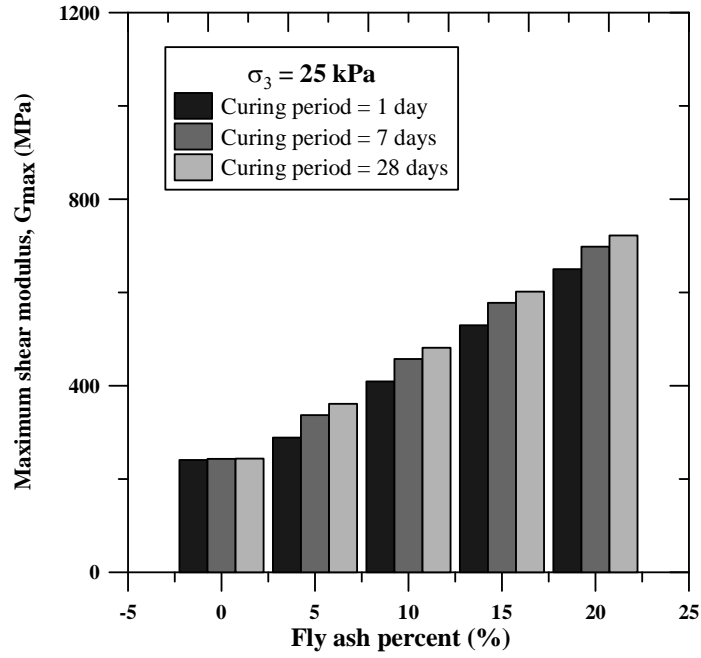
Figure 7.30: Variation of maximum shear modulus (G_{max}) with fly ash content for 25 kPa confining pressure
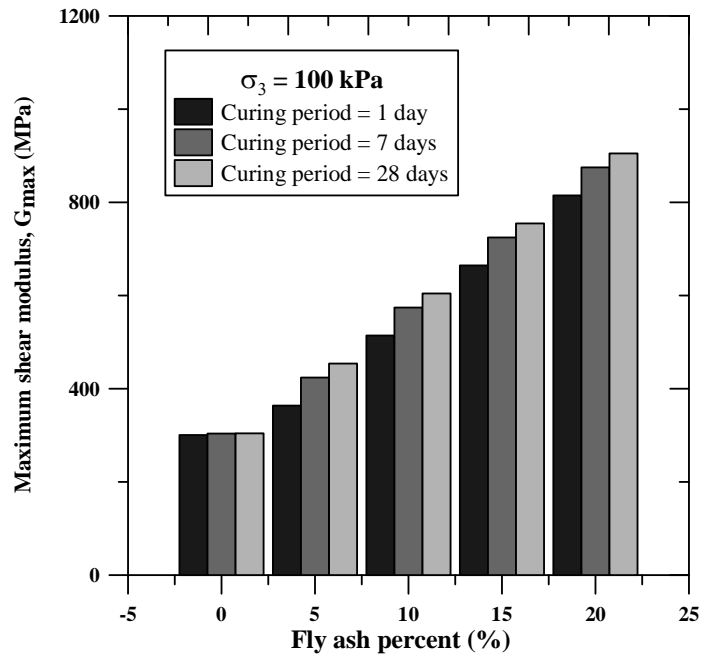
Figure 7.31: Variation of maximum shear modulus (G_{max}) with fly ash content for 100 kPa confining pressure

128
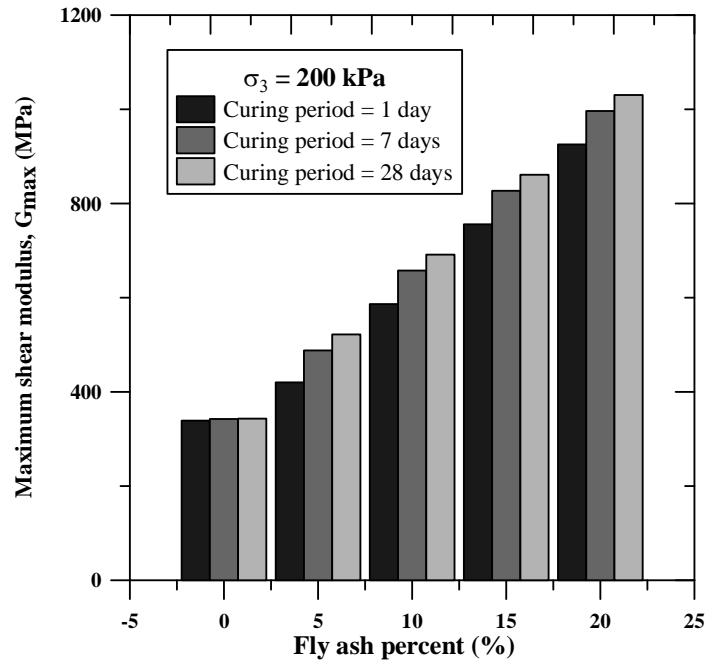
Figure 7.32: Variation of maximum shear modulus (G_{max}) with fly ash content for 200 kPa confining pressure
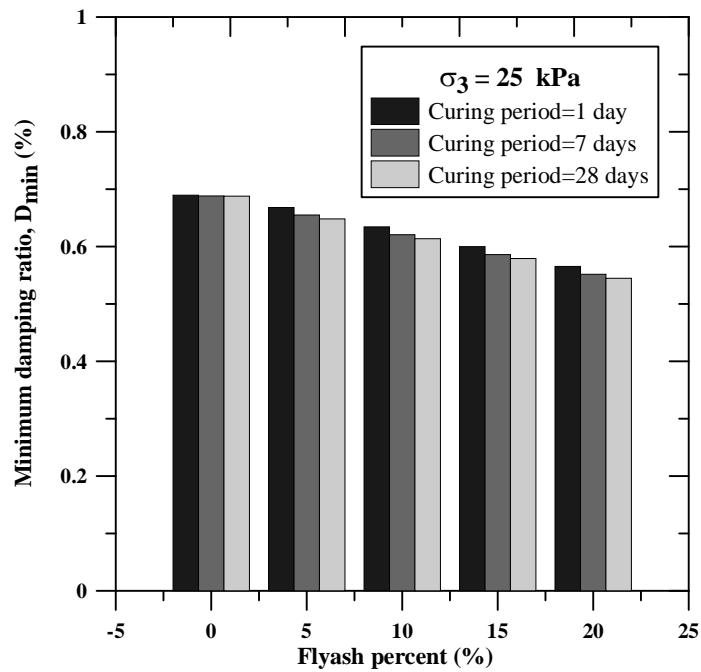
Figure 7.33: Variation of minimum damping ratio (D_{min}) with fly ash content for 25 kPa confining pressure

129
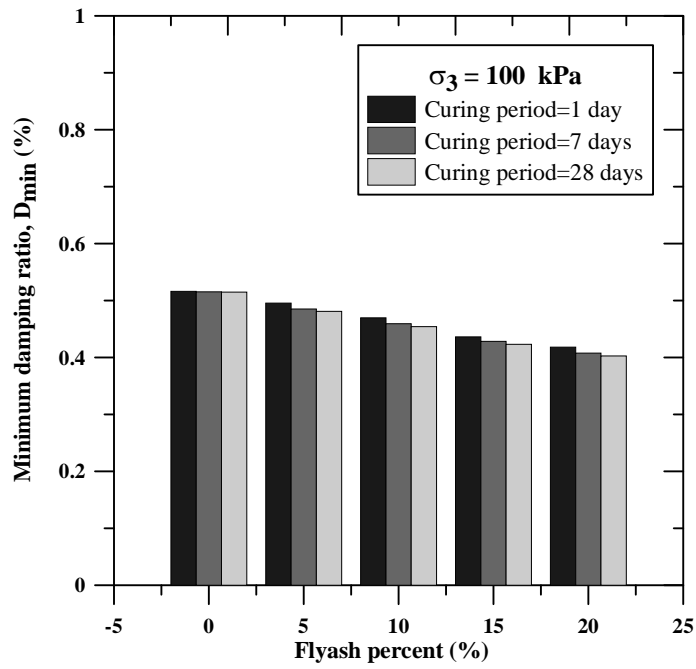
Figure 7.34: Variation of minimum damping ratio (D_{min}) with fly ash content for 100 kPa confining pressure
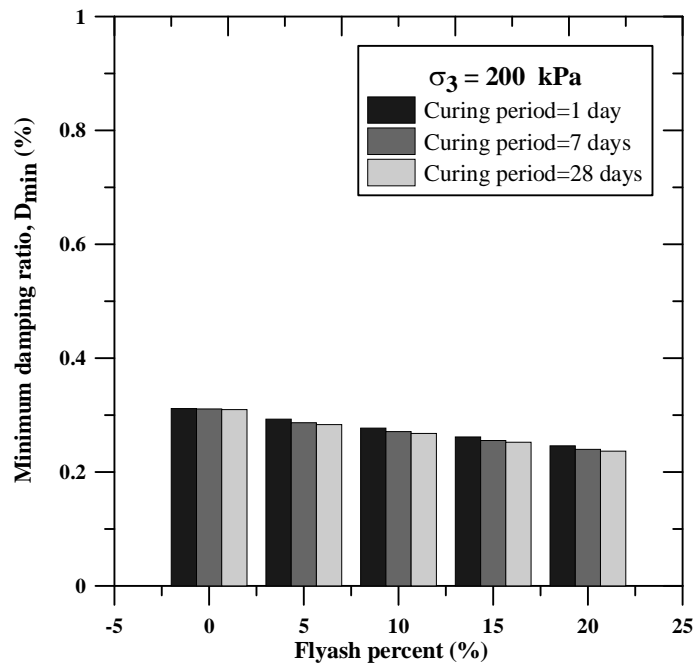
Figure 7.35: Variation of minimum damping ratio (D_{min}) with fly ash content for 200 kPa confining pressure
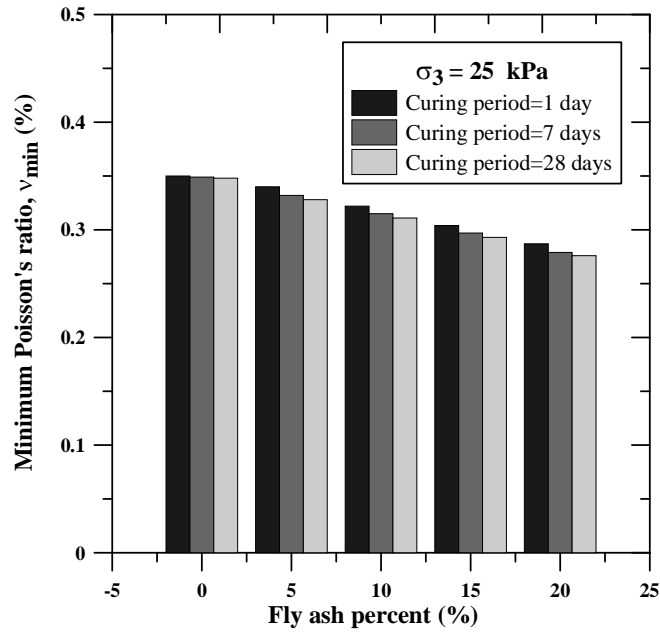
Figure 7.36: Variation of minimum Poisson's ratio (ν_{min}) with fly ash content for 25 kPa confining pressure
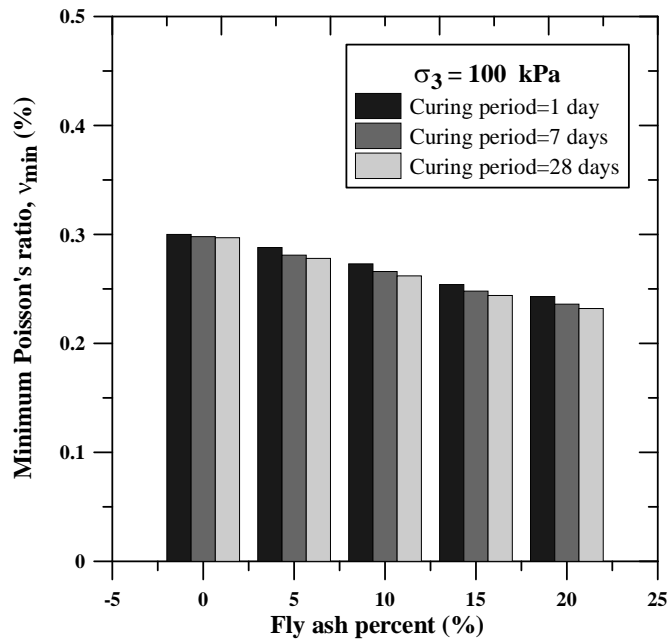
Figure 7.37: Variation of minimum Poisson's ratio (ν_{min}) with fly ash content for 100 kPa confining pressure

131
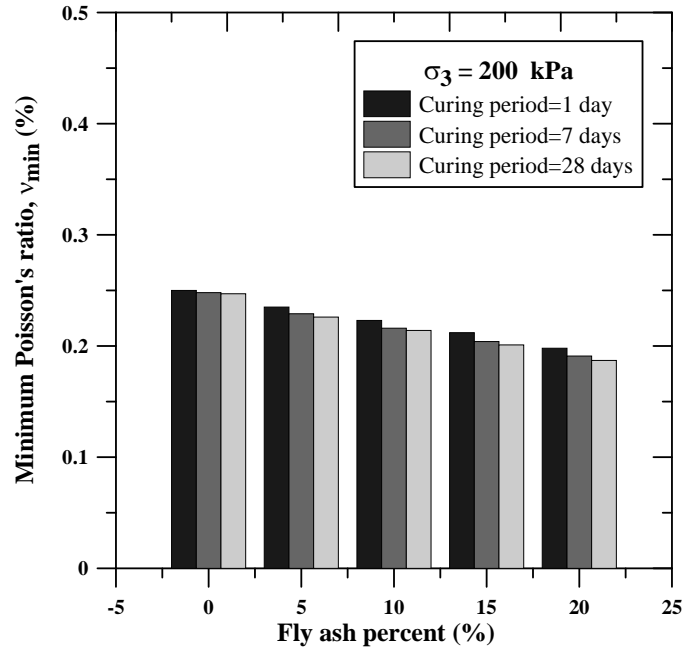
Figure 7.38: Variation of minimum Poisson's ratio (v_{min}) with fly ash content for 100 kPa confining pressure

7.5.5 Effect of fly ash on unconfined compressive strength

Unconfined compressive strength tests were performed to determine the compressive strength of both untreated and treated expansive soils. Unconfined compressive strength tests were performed in accordance with ASTM D2166-85. Figures 7.39, 7.40 and 7.41 give the axial stress vs. axial strain response of untreated and treated soil specimens for 1 day, 7 days and 28 days curing period respectively. It is observed that there is increase in axial stress and reduction in failure strain of the specimen with increase in fly ash dosages. The reduction in failure strain is because ductile nature of the expansive soil becomes brittle with fly ash stabilization. Figure 7.42 gives the variation of unconfined compressive strength of expansive soil subjected to different dosages of fly ash for different curing periods. It is observed that unconfined compressive strength increases with the increase in fly ash content and curing period. It is also noted that the increase is rapid up to a fly ash dosage of 5% and gradual thereafter. For 20% fly ash treated specimens, there is a 2.7 fold increase in UC strength between 1 and 28 days curing periods. The increase in unconfined

compressive strength is due to cation exchange reactions of divalent or trivalent ions present in fly ash which causes flocculation of the particles and on curing results in the formation of CSH and CAH gel compounds which give additional strength due to curing. The formation of pozzolanic compounds due to fly ash treatment can be further witnessed through the mineralogical studies such as X-ray powder diffraction (XRPD) studies.
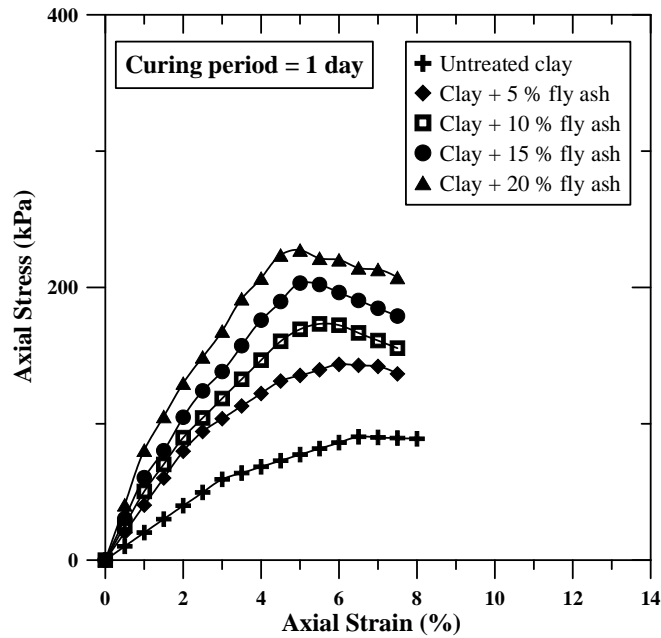
Figure 7.39: Stress strain response of samples treated for 1 day curing period
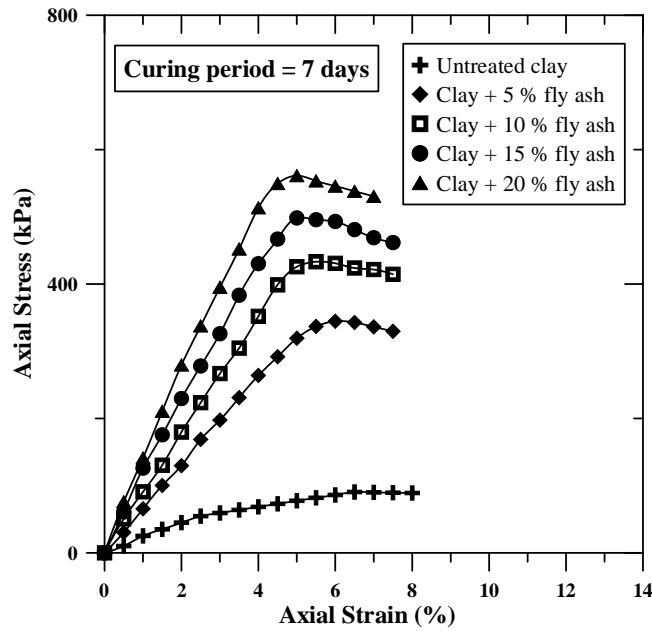
Figure 7.40: Stress strain response of samples treated for 7 days curing period
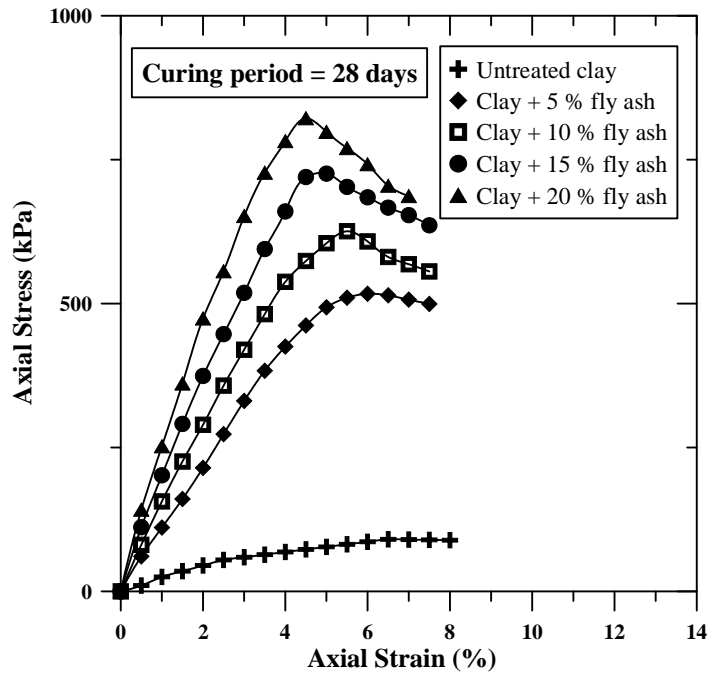
Figure 7.41: Stress strain response of samples treated for 28 days curing period

134
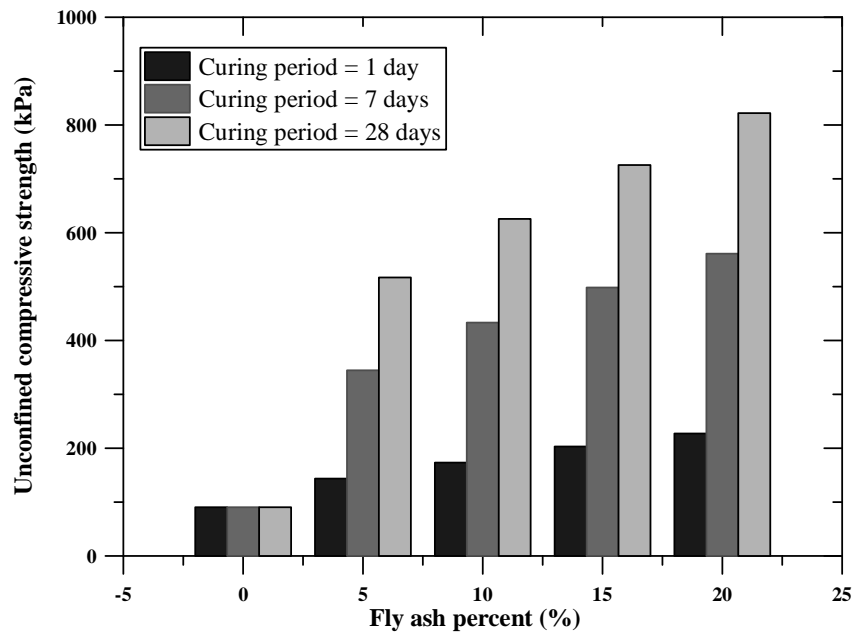
Figure 7.42: Variation of unconfined compressive strength with fly ash content for different curing periods

7.5.6 Effect of fly ash on suction

Filter paper tests as described in Chapter 6 were performed on expansive soil treated with fly ash. As the resonant column tests and unconfined compressive strength tests of treated soil were performed on partially saturated soil specimens, an accurate estimation of the suction is essential. Figure 7.43 gives the variation of suction with fly ash content for different curing period. It can be observed that suction increases with the increase in fly ash dosage as well as curing periods. The increase in suction with increase in fly ash content can be attributed to the fact that with the increase in fly ash content the calcium ion concentration in the soil increases which results in increase in the osmotic suction of the total suction (Rao and Shivanada 2005 and Stoltz et al. 2012). With the increase in curing period, there is reduction in the water content of the treated soil as the water will be used up in the formation of cementitious compounds by pozzolanic reactions (Stoltz et al. 2012). This results in further increase in suction of the treated soil with curing period. It can be inferred from the results that improvement in strength and stiffness of the fly ash treated soil is brought about not only by the formation of cementitious products but also by increase in suction.

135
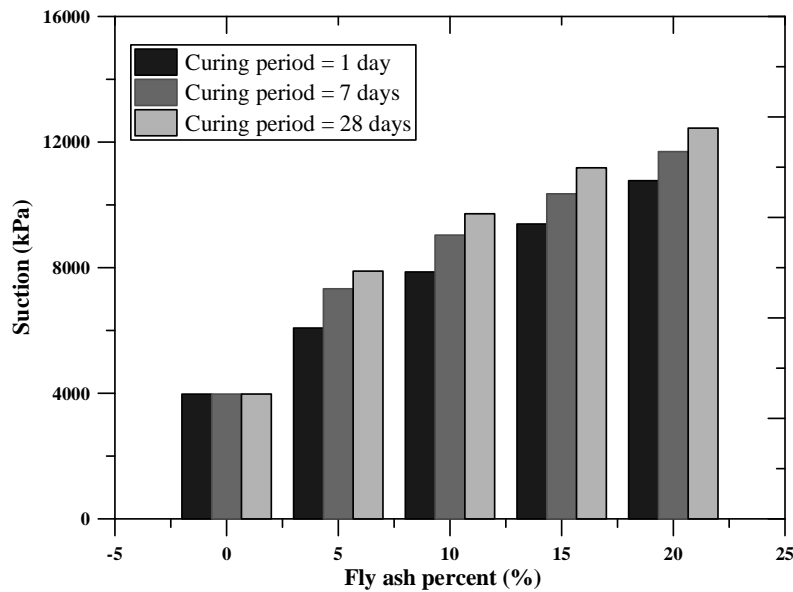
Figure 7.43: Variation of suction with fly ash content for different curing periods

7.5.7   X-Ray powder diffraction (XRPD) analysis

Figure 7.44 gives the XRD results of the fly ash used in the study. The important compounds present in the fly ash are silica (SiO_2), calcium oxide (CaO), mullite ($3Al_2O_3SiO_2$), and hematite (Fe_2O_3). Calcium oxide (CaO) present in the fly ash reacts with silica (SiO_2) present in the soil to form hydrated products.

Figure 7.45 gives the XRD results of untreated and treated samples (fly ash content of 10 % and 20 %) for 28 days curing period. The presence of montmorillonite minerals confirms the expansive nature of the soil. It is observed that not much effect is observed in the peaks of montmorillonite minerals with treatment. However, there are formations of other hydration compounds as result of treatment. When the specimen is treated with 10 % fly ash, sufficient number of calcium hydroxide ($Ca(OH)_2$) peaks were observed. $Ca(OH)_2$ is a hydration product which is formed due to reaction of calcium oxide (CaO) of fly ash with water (H_2O). Calcium hydroxide ($Ca(OH)_2$) further reacts with the silica present in the soil to form cementitious products which is a time dependent process and provides long term strength of the treated soil. Peaks of CSH compounds are also observed but the number of peaks obtained is less for samples treated with 10 % fly ash. When the specimens were treated with 20 % fly ash, sufficient numbers of CSH peaks are observed. This is because with the increase in fly ash dosage, the pH of the specimen increases which helps in the formation of CSH compounds. Un-reacted Calcium Hydroxide ($Ca(OH)_2$) compounds for

136

soils treated with lower dosages of fly ash can be effectively utilized by addition of alkali like (NaOH) in the mixture.

Figure 7.46 gives the XRD results of samples treated with 20 % fly ash for different curing periods. It is observed that no CSH compounds are formed for samples cured for 1 day but for higher curing period peaks of CSH compounds are observed. This proves that formation of pozzolanic compounds (CSH) is time dependent and it gives long term strength of the specimen. Similar observations were made at other dosage of fly ash as well.
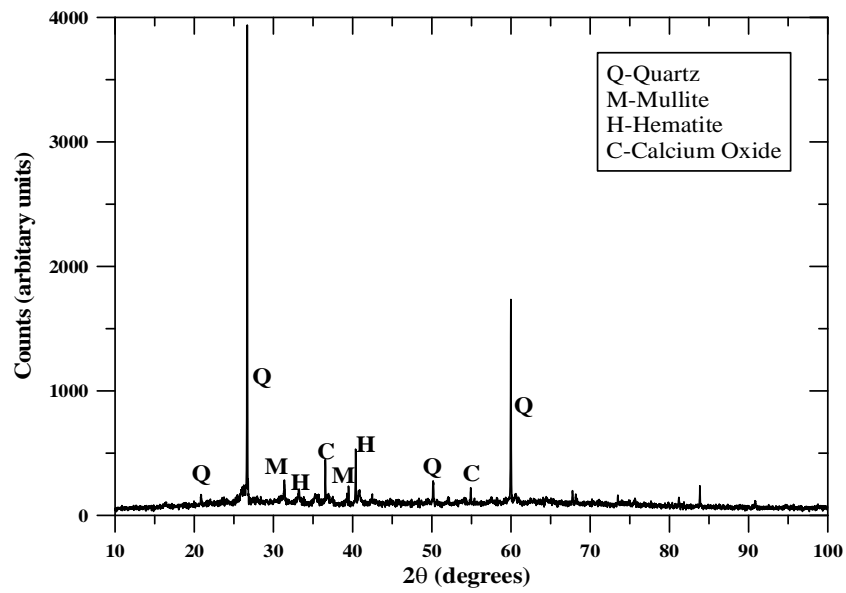
Figure 7.44: XRD results in fly ash
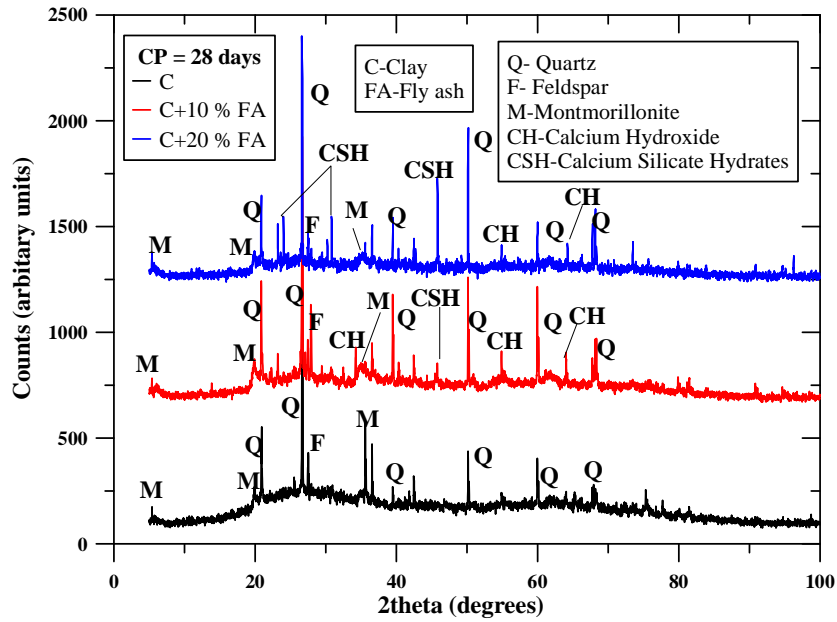
Figure 7.45: XRD results of samples for 28 days curing period
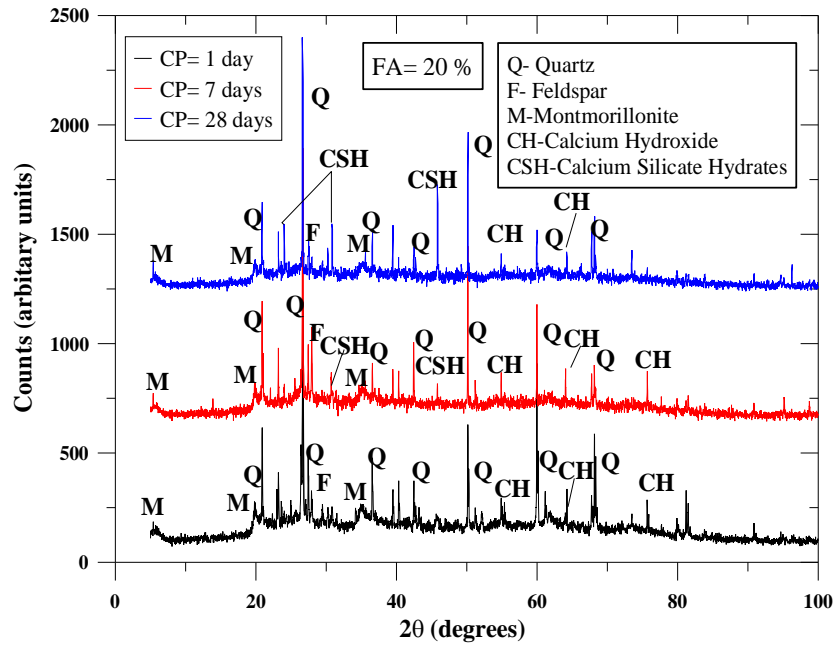
Figure 7.46: XRD results of samples treated with 20 % fly ash for different curing periods

138

7.5.8 Design application

Lysmer and Richart (1966) elastic half space method has been adopted to design a typical machine foundation subjected to vertical vibration. The main assumptions of this method are that the soil is homogeneous, isotropic and elastic with shear modulus (G) and Poisson's ratio (v). Although the equation was earlier developed for circular footing, by calculating equivalent radius for any other shape (i.e. for square or rectangular) of footing gives reasonable estimation of the resonant frequency of the foundation-soil system [100]. It should be noted that damping automatically enters into the solution of elastic half space method. In this method following steps are adopted for the design of a foundation:

1) Calculation of equivalent radius from the length and width of the foundation by using the equation (7.5):

$$r_o = \sqrt{\frac{BL}{\pi}} \tag{7.5}$$

where, r_o= equivalent radius, L= length of the foundation, B = width of the foundation.

2) Calculation of mass ratio from the weight of the machinery and foundation block, density and Poisson's ratio of the soil by using equation (7.6):

$$B_Z = \left(\frac{1-v}{4}\right)\left(\frac{W}{\gamma r_o^3}\right) \tag{7.6}$$

Where, B_z = mass ratio, W= weight of the machine and the foundation, v= Poisson's ratio of the soil, γ = unit weight of the soil, r_o= equivalent radius.

(3) Calculation of resonant frequency of the foundation-soil system from the shear modulus of the soil, density of the soil, equivalent radius, mass ratio by using equation (7.7):

$$f_{mr} = \left[\left(\frac{1}{2\pi}\right)\sqrt{\left(\frac{4Gr_o}{1-v}\right)\frac{\gamma}{W}}\right]\sqrt{1-2\left(\frac{0.425}{\sqrt{B_Z}}\right)^2} \tag{7.7}$$

(4) For no resonance condition to happen, the following check should be made:

$$\text{Factor of safety} = f_{mr}/f_o > 2 \text{ (Das and Ramana 2011)}$$

where, f_o is the operating frequency of the machine.

If the condition is not satisfied, two alternatives can be adopted

   a) Increase the size of the footing.
   b) Improve the strength of the soil by means of stabilization.

The following design problem is done to show the application of the data obtained from the present study. The weight coming from the foundation and the machine is assumed as 800 kN. Operating frequency of the machine is assumed as 1500 cpm. A rectangular footing of size 4m×3m is considered. The strains coming to the soil from a machine foundation are usually in the range of 10^{-4} % to 10^{-3} % (Chowdhury and Dasgupta 2008). Hence for conservative design a strain value of 8×10^{-3} % is considered and shear modulus and Poisson's ratio of the soil are taken at this strain level. The values of shear modulus and Poisson's ratio were taken for 25 kPa confining pressure as it signifies a foundation depth of 1.5 m. Moreover the values of shear modulus and Poisson's ratio were taken for 28 days curing period for treated soils. Table 7.5 gives the factor of safety obtained for different dosage of fly ash. It is observed that the factor of safety of the foundation system has increased gradually with fly ash content to reach a limiting value of factor of safety of 2 at a fly ash percentage of 15 %. It shows that for improving the factor of safety of machine foundations, appropriate soil stabilization method can be adopted. Further, an economical and sustainable design alternative can be obtained with fly ash stabilization.

Table 7.5: Factor of safety of the machine foundation

	Untreated Soil	5 % fly ash	10 % fly ash	15 % fly ash	20 % fly ash
Shear modulus (MPa)	233.85	325.15	420.48	535.65	612.48
Poisson's ratio	0.354	0.332	0.315	0.296	0.279
Equivalent radius (m)	1.95	1.95	1.95	1.95	1.95
Mass ratio	1.03	1.08	1.13	1.17	1.22
Resonant frequency of foundation-soil system (cpm)	2114.02	2442.32	2735.98	3038.56	3192.67
Factor of safety	1.41	1.62	1.82	*2.02*	*2.13*

7.6   Summary

In this chapter, the dynamic properties of stabilized expansive soil are discussed. The dynamic properties presented are shear modulus (G), damping ratio (D) and Poisson's ratio (ν). The influences of increasing fly ash content and curing period on the dynamic properties are elaborately presented. Unconfined compressive strengths of the untreated and treated expansive clay are also mentioned in the chapter. X-ray powder diffraction analysis (XRPD) has been performed on both untreated and treated expansive clay to qualitatively identify the compounds formed after treatment with fly ash. Finally, design of a machine foundation, resting on expansive soil, subjected to vertical vibrations is demonstrated to control the resonance of the stabilized soil-foundation system.

Chapter 8

Conclusion

A series of resonant column tests have been performed on clean sand and expansive soil to determine the dynamic properties. Class C fly ash has been used to stabilize the expansive soil and resonant column tests were further performed on fly treated expansive soil to understand the influence of fly stabilization on dynamic properties. The following conclusions can be drawn from this research.

1. The increase in shear strain decreases the shear modulus but increases the damping ratio and Poisson's ratio of soil.

2. The shear modulus increases, whereas damping ratio and Poisson's ratio of soil decreases with increase in the confining pressure.

3. With the increase of relative density of sand, the shear modulus increases whereas damping ratio and Poisson's ratio of soil decreases.

4. A threshold value of shear strain at which G/G $_{max}$ is greater than or equal to 0.99 is calculated. This threshold shear strain is found to increase with increase in confining pressure and relative density.

5. The shear modulus values when plotted against Poisson's ratios of soil show a decreasing trend. This is because the higher value of Poisson's ratio signifies a higher rate of shear strain and which results in reduction of shear modulus of soil.

6. The small strain shear modulus (G_{max}) is higher for partially saturated soils compared to fully saturated soils. This is due to the presence of capillary induced suction in partially saturated soils. As high as 4000 kPa of total suction was

measured in the partially saturated soils at its optimum moisture content (92% saturation level).

7. The difference between small strain shear modulus of partially saturated soil and small strain shear modulus of fully saturated soil is higher at low effective confining pressure and it reduces considerably at higher effective confining pressures. This suggests that capillary induced suction is more predominant at less overburden depth and it reduces as the depth increases.

8. The small strain damping ratio is lesser for partially saturated soils as compared to the fully saturated soil. The difference between small strain damping ratio of partially saturated soil and small strain damping ratio modulus of fully saturated soil is 10.5% greater at low effective confining pressure and it reduces significantly at higher effective confining pressure.

9. The Poisson's ratio of the fully saturated soil in undrained condition is close to 0.5 and there is no influence of confining pressure on the Poisson's ratio of the soil for a fully saturated case.

10. The degree of saturation has a little influence on the modulus reduction (G/G_{max}) with increase in shear strain. However it was also observed that normalized shear modulus (G/G_{max}) value for fully saturated soil is slightly higher than partially saturated soil.

11. The degree of saturation has no influence on variation of damping ratio (D) with increase in shear strain.

12. With increase in dosage of fly ash, the maximum dry density increases and optimum moisture content decreases.

13. The liquid limit and plastic limit of the expansive soil increase whereas the plasticity index of the soil decreases with increase in the fly ash content.

14. A considerable reduction in the free swell index of the expansive soil is observed with increase in the percentage of fly ash.

15. With increase in fly ash percentage, there is an increase in the shear modulus (G) of the soil. This increase in shear modulus is more prominent up to a shear strain of 10^{-2} % and thereafter a very less increase of shear modulus (G) with increase in fly ash content is observed.

16. With increase in curing period, there is an increase in shear modulus (G) of the treated soil. This is because of time dependent cementitious and pozzolanic properties of fly ash with curing. This increase in shear modulus is also observed from the small shear strain to medium shear strain range and thereafter is a negligible improvement of shear modulus (G) with curing.

17. With increase in fly ash content the modulus reduction (G/G_{max}) ratio decreases. A generalized upper and lower bound modulus degradation curves have been proposed to estimate the G/G_{max} of any treated clay samples. Curing period has practically has no influence on the G/G_{max} values of treated specimens.

18. Damping ratio (D) decreases with the increase in the fly content. As the degree of cementation of the soil increases, the soil becomes more rigid and particle slippage and particle rearrangement become considerably reduced resulting in decrease of damping ratio of the soil.

19. There is reduction in Poisson's ratio (v) with increase in the confining pressure as well as fly content of the treated soils. With increase in confining pressure and fly ash content, the stiffness of the specimen increases which gives higher resistance to the specimen deformation.

20. Unconfined compressive strength increases with increase in the fly ash content and curing period. The increase in unconfined compressive strength is due to cation exchange reactions of divalent or trivalent ions present in fly ash which causes

flocculation of the particles and on curing results in the formation of C-S-H and C-A-H gel compounds which give additional strength due to curing.

References

[1] B. O. Hardin and F. E. Richart Jr. Elastic wave velocities in granular soils. Journal of the Soil Mechanics and Foundations Division ASCE 89 (1), (1963) 33-65.

[2] B. O. Hardin, V. P. Drnevich. Shear modulus and damping in soils: design equation and curves. Journal of Soil Mechanics and Foundations Division ASCE 98 (7), (1972a) 667–691.

[3] B. O. Hardin and V. P. Drnevich. Shear modulus and damping in soils: Measurement and parameter effects. Journal of the Soil Mechanics and Foundations Division ASCE 98 (6), (1972b) 603-624.

[4] H. B. Seed, R. T. Wong, I. M. Idris and K. Tokimatsu. Moduli and damping factors for dynamic analysis of cohesionless soils. Journal of Geotechnical Engineering ASCE 112 (11), (1986) 1016–1032.

[5] V. P. Drnevich, B. O. Hardin and D. J. Shippy. Modulus and damping of soils by the resonant column method. Dynamic Geotechnical Testing 654, (1978) 91- 125.

[6] ASTM D 4015-07. Standard test methods for modulus and damping of soils by resonant column method. Annual Book of ASTM Standards, ASTM International, West Conshohocken, PA, 2007.

[7] F. E. Richart Jr., J. R. Hall Jr. and R. D. Woods. Vibrations of soils and foundations. Prentice-Hall, Englewood Cliffs, NJ, 1970.

[8] H. B. Seed and I. M. Idriss. Soil moduli and damping factors for dynamic response analysis. Rep. No. EERC 70-10, Earthquake Engineering Research Center, Berkeley, California, 1970.

[9] T. Iwasaki, F. Tatsuoka and Y. Takagi. Shear moduli of sands under cyclic torsional shear loading. Soils and Foundations 18 (1), (1978) 39–56.

[10] T. Kokusho, Y. Yoshida and Y. Esashi. Dynamic properties of soft clay for wide strain range. Soils and Foundations 22 (4), (1982) 1–18.

[11] M. Vucetic and R. Dobry. Effect of soil plasticity on cyclic response. Journal of Geotechnical Engineering ASCE 117 (1), (1991) 89–107.

[12] I. Ishibashi and X. J. Zhang. Unified dynamic shear moduli and damping sand and clay. Soils and Foundations 33 (1), (1993) 182–191.

[13] K. M. Rollins, M. D. Evans, N. B. Diehl, W. D. Daily III. Shear modulus and damping relationships for gravels. Journal of Geotechnical and Geoenviromental Engineering ASCE 124 (5), (1998) 396–405.

[14] M. Vucetic. Cyclic threshold shear strain in soils. Journal of Geotechnical Engineering ASCE 120 (12), (1994) 2208-2228.

[15] K. H. Stokoe II, M. B. Darendeli, R. D. Andrus and L. T. Brown. Dynamic soil properties: laboratory, field and correlation studies. Proc., 2nd International Conference on Earthquake Geotechnical Engineering, Vol. 3, Lisbon, Portugal, (1999) 811–845.

[16] K. H. Stokoe II, M. B. Darendeli, R. B. Gilbert, F. Y. Menq and W. K. Choi. Development of a new family of normalized modulus reduction and material damping curves. Proc., NSF/PEER Int. Workshop on Uncertainties in Nonlinear Soil Properties and their Impact on Modeling Dynamic Soil Response, University of California at Berkeley, 2004.

[17] T. Kokusho. Cyclic triaxial test of dynamic soil properties for wide strain rate. Soils and Foundations 20 (2), (1980) 45-60.

[18] C. R. Bates. Dynamic soil property measurements during triaxial testing. Géotechnique 39 (4), (1989) 721–726.

[19] K. Nakagawa, K. Soga and J. K. Mitchell. Observation of biot compressional wave of the second kind in granular soils. Géotechnique 47 (1), (1997) 133–147.

[20] J. Kumar and B. N. Madhusudhan. Effect of relative density and confining pressure on Poisson's ratio from bender and extender elements tests. Géotechnique 60 (7), (2010) 561-567.

[21] Y. S. Chae and Y. C. Chiang. Dynamic properties of lime and LFA treated soils. Proceedings of Earthquake Engineering and Soil Dynamics ASCE Specialty Conference, Vol. 1, Pasadena, California, (1978) 308-324.

[22] W. C. Au and Y. S. Chae. Dynamic shear modulus of treated expansive soil. Journal of Geotechnical Engineering Division ASCE 106 (3), (1980) 255-273.

[23] K. Fahoum, M. S. Aggour and F. Amini. Dynamic properties of cohesive soils treated with lime. Journal of Geotechnical Engineering ASCE 122 (5), (1996) 382-389.

[24] L.R. Hoyos, A. J. Puppala, and P. Chainuwat. Dynamic properties of chemically stabilized sulfate rich clay. Journal of Geotechnical and Geoenvironmental Engineering ASCE 130(2), (2004) 153-162.

[25] M. Ishimoto and K. Iida. Determination of elastic constants of soils by means of vibration methods, Part I, Young's Modulus. Bulletin of Earthquake Research Institute, University of Tokyo 14, (1936) 632-657.

[26] M. Ishimoto and K. Iida. Determination of elastic constants of soils by means of vibration methods, Part II, Modulus of rigidity and Poisson's ratio. Bulletin of Earthquake Research Institute, University of Tokyo 15, (1937) 67-88.

[27] K. Iida. The velocity of elastic waves in sand. Bulletin of Earthquake Research Institute, University of Tokyo 16, (1938) 131-145.

[28] B. O. Hardin. Dynamic versus static shear modulus for dry sand. Materials Research and Standards 5(5), (1965) 232-235.

[29] B. O. Hardin and J. Music. Apparatus for vibration of soil specimens during the triaxial test. Instruments and Apparatus for Soil and Rock Mechanics ASTM STP 392, (1965) 55-74.

[30] F. V. Lawrence Jr. Ultrasonic shear wave velocities in sand and clay. Cambridge, Massachusetts, Department of Civil Engineering, Massachusetts Institute of Technology, 1965.

[31] B. O. Hardin and W. L. Black. Sand stiffness under various triaxial stresses. Journal of the Soil Mechanics and Foundations Division ASCE 92 (2), (1966) 27-42.

[32] W. K. Humphries and H. E. Wahls. Stress history effects on dynamic modulus of clay. Journal of the Soil Mechanics and Foundations Division ASCE 94 (2), (1968) 371-389.

[33] S. S. Afifi and F. E. Richart. Stress-history effects on shear modulus of soils. Soils and Foundations 13 (1), (1973) 77-95.

[34] Y. Ohsaki and R. Iwasaki. On dynamic shear moduli and Poisson's ratio of soil deposits. Soils and Foundations 13 (4), (1973) 61-73.

[35] T. Iwasaki and F. Tatsuoka. Effects of grain size and grading on dynamic shear moduli of sands. Soils and Foundations 17 (3), (1977) 19-35.

[36] T. Iwasaki, F. Tatsuoka and Y. Takagi. Shear moduli of sands under cyclic torsional shear loading. Soils and Foundations 18 (1), (1978) 39-56.

[37] S. Wu, D. H. Gray and F. E. Richart Jr. Capillary effects on dynamic modulus of sands and silts. Journal of Geotechnical Engineering ASCE 110 (9), (1984) 1188-1203.

[38] R. P. Ray and R. D. Woods. Modulus and damping due to uniform and variable cyclic loading. Journal of Geotechnical Engineering ASCE 114 (8), (1988) 861-876.

[39] S. K. Saxena and K. R. Reddy. Dynamic moduli and damping ratios for Monterey No. 0 sand by resonant column tests. Soils and Foundations 29 (2), (1989) 38-51.

[40] R. Dobry and K. Vucetic. State-of-the-art report; Dynamic properties and response of soft clay deposits. Proceedings of International Symposium on Geotechnical Engineering of Soft Soils, 2, (1987) 51-87.

[41] X. Qian, D. H. Gray, R. D. Woods. Voids and granulometry - effects on shear modulus of unsaturated sands. Journal of Geotechnical Engineering ASCE 119(2), (1993) 295-314.

[42] A. Souto, J. Hartikainen and K. Oezuedogru. Measurement of dynamic parameters of road pavement materials by the bender element and resonant column tests. Géotechnique 44(3), (1994) 519-526.

[43] D. C. F. Lo Presti, M. Jamiolkowski, O. Pallara, A. Cavallaro, S. Pedroni. Shear modulus and damping of soils. Géotechnique 47 (3), (1997) 603-617.

[44] G. Cascante, C. Santamarina, and N. Yassir. Flexural excitation in a standard torsional-resonant column device. Canadian Geotechnical Journal 35, (1998) 478-490.

[45] C. McDowell. The relation of laboratory testing to design for pavements and structures on expansive soils. Quarterly of the Colorado School of Mines 54 (4), (1959) 127–153.

[46] D. E. Jones and W. G. Holtz. Expansive Soils – the hidden disaster. Civil Engineering ASCE, 43, (1973) 49-51.

[47] D. E. J. McCaustland. Lime in dirt roads. Proceedings of National Lime Association 7, (1925) 12-18.

[48] National Lime Association. Lime stabilization of roads. Bulletin 323, Washinton D. C., 1954

[49] C. W. Jones. Stabilization of expansive clay with hydrated lime and with Portland cement. Highway Research Bulletin 193, Highway Research Record, National Research Council, Washington D.C., (1958) 40–47.

[50] O. L. Lund and W. J. Ramsey. "Experimental lime stabilization in Nebraska." HRB 231, Highway Research Record, National Research Council, Washington D.C., (1959) 24-59.

[51] J. E. Eades and R. E. Grim. A quick rest to determine lime requirements for lime stabilization. Highway Research Bulletin 139, Highway Research Board, National Research Council, Washington D.C., (1966) 61–72.

[52] J. E. Eades, F. P. Nichols and R. E. Grim. Formation of new minerals with lime stabilization as proven by field experiments in Virginia. Highway Research Bulletin 335, Highway Research Board, National Research Council, Washington D.C., (1963) 31-39.

[53] Thompson, M. R. Lime reactivity of Illinois soils. Journal of Soil Mechanics and Foundation Division 92 (5), (1966) 67-92.

[54] G. Ferguson. Use of self-cementing fly ashes as a soil stabilization agent. Fly ash for soil improvement, Geotechnical Special Publication No. 36, ASCE, New York, (1993) 1–14.

[55] E. Cocka. Use of Class C fly ashes for the stabilization of an expansive soil. Journal of Geotechnical Engineering Division ASCE 127 (7), (2001) 568-573.

[56] A. J. Puppala, E. Wattanasanticharoen and K. Punthutaecha. Experimental evaluations of stabilisation methods for sulphate-rich expansive soils. Ground Improvement 7 (1), (2003) 25–35.

[57] N. Pandian and K. Krishna. The pozzolanic effect of fly ash on the California bearing ratio behavior of black cotton soil. Journal of Testing and Evaluation ASTM 31 (6), (2003) 479–485.

[58] ASTM. Standard specification for coal fly ash and raw or calcined natural pozzolan for use in concrete. ASTM-C618, West Conshohocken PA, (2012).

[59] P. G. Nicholson and V. Kashyap. Fly ash stabilization of tropical Hawaiian soils. Fly Ash for Soil Improvement, Geotechnical Special Publication No. 36, ASCE, New York, (1993) 15–29.

[60] A. Misra. Stabilization characteristics of clays using class C fly ash. Transportation Research Record 1161, Transportation Research Board, Washington, D.C., (1998) 46–54.

[61] T. B. Edil, H. A. Acosta, C. H. Benson. Stabilizing soft fine-grained soils with fly ash. Journal of Materials in Civil Engineering ASCE 18 (2), (2006) 283-294.

[62] Birch, F. and D. Bancroft. The effect of pressure on the rigidity of rocks. I and II. The Journal of Geology 46, (1938) 59-87 & 113-141.

[63] J. R. Hall and F. E. Richart. Dissipation of elastic wave energy in granular soils. Journal of the Soil Mechanics and Foundations Division, ASCE 89(6), (1963) 27-56.

[64] Drnevich, V. P., J. R. Hall, Jr. and F. E. Richart Jr. Effects of amplitude of vibration on the shear modulus of sand. International Symposium on Wave Propagation and Dynamic Properties of Earth Materials, Albuquerque, New Mexico, University of New Mexico Press, 1967.

[65] V. P. Drnevich. Effect of strain history on the dynamic properties of sand, PhD. thesis, University of Michigan, 1967.

[66] D. G. Anderson and K. H. Stokoe II. Shear modulus: a time dependent soil property. Dynamic Geotechnical Testing, ASTM STP 654, West Conshohocken, (1978) 66-90.

[67] D. S. Kim and K. H. Stokoe. Torsional motion monitoring-system for small-strain (10^{-5} to 10^{-3} percent) soil testing. Geotechnical Testing Journal 17(1), (1994) 17-26.

[68] C. Mancuso, R. Vassallo, and A. d'Onofrio, Small strain behavior of a silty sand in controlled-suction resonant column-torsional shear tests. Canadian Geotechnical Journal, 39, (2002) 22-31.

[69] L. R. Hoyos, E. A. Suescún, and A. J. Puppala. Small-strain stiffness of unsaturated soils using a suction-controlled resonant column device with bender elements. Advances in Geotechnical Engineering, GSP 211, Geo-Institute of ASCE, Proceedings of Geo-Frontiers, (2011) 4313-4322.

[70] GDS RCA-Manual. The GDS Resonant Column System Handbook, 2003.

[71] J. F. Zhang, R. D. Andrus, and C. H. Juang. Normalized shear modulus and material damping ratio relationships. Journal of Geotechnical and Geoenvironmental Engineering, ASCE 131 (4), (2005) 453-464.

[72] T. W. Lambe and R. V. Whitman. Soil mechanics. New York: John Wiley, 1979.

[73] X. Gu, J. Yang and M. Huang. Laboratory measurements of small strain properties of dry sands by bender element. Soils and Foundations 53 (5), (2013) 735-745.

[74] S. Wu. Capillary effects on dynamic modulus of fine-grained cohesionless soil. Ph.D. thesis, The University of Michigan, 1983.

[75] J. Kumar, B. N. Madhusudhan. Effect of relative density and confining pressure on Poisson's ratio from bender and extender elements tests. Géotechnique 60 (7), (2010) 561-567.

[76] G. C. Cho and J. C. Santamarina. Unsaturated particulate materials: Particle-level studies. Journal of Geotechnical and Geoenvironmental Engineering ASCE 127 (1), (2001) 84-96.

[77] ASTM. Standard test method for measurement of soil potential (suction) using filter paper. ASTM D5298, West Conshohocken PA, (2010).

[78] V. C. Xenaki and G. A. Athanasopoulos. Dynamic properties and liquefaction resistance of two soil materials in an earth fill dam—laboratory test results. Soil Dynamics and Earthquake Engineering 28, (2008) 605–620.

[79] C. Mancuso, F. Silvestri, F. Vinale. Stress–strain behavior of a dam core material by field and laboratory dynamic tests. Geotechnical engineering of hard soils–soft rock, Rotterdam: Balkema, (1993) 1299–1308.

[80] K. Yokota and M. Konno. Dynamic Poisson's ratio of soil. Proceedings of the 7th World Conference on Earthquake Engineering, Istanbul, Turkey, (1980) 475–478

[81] Federal Highway Administration. Fly ash facts for highway engineers. Technical Report FHWA-IF-03019, 4th Ed., Washington, DC, 2003.

[82] E. O. Tastan, T. B. Edil, C. H. Benson and A. H. Aydilek. Stabilization of organic soils with fly ash. Journal of Geotechnical and Geoenvironmental Engineering ASCE, 137(9), (2011) 819–833.

[83] ASTM. Standard test methods for liquid limit, plastic limit and plasticity index of soils. ASTM D4318-10e1, West Conshohocken PA, (2010).

[84] W. G. Holtz and H. J. Gibbs, Engineering properties of expansive clays. Transactions of the American Society of Civil Engineers 121, (1956) 641-677.

[85] ASTM. Standard test method for compressive strength of molded soil-cement cylinders. ASTM D1633-00 West Conshohocken, PA, 2007.

[86] M. Mateos. Soil lime research at Iowa State University. Journal of Soil Mechanics and Foundations Division, ASCE, 90 (2), (1964) 127-156.

[87] S. Z. George, D. A. Ponniah and J. A. Little. Effect of temperature on lime-soil stabilization. Construction and Building Materials, 6 (4), (1992) 247-252.

[88] Chen, F. H. Foundations on Expansive Soils, Elsevier Science, Amsterdam, 1975

[89] ASTM. Standard practice for classification of soils for engineering purposes (Unified Soil Classification System). ASTM-D2487, West Conshohocken, PA, 2011.

[90] Bureau of Indian Standards. Indian Standard Classification and Identification of Soils for General Engineering Purposes. IS 1498, BIS, New Delhi, 1970.

[91] A. D' Onofrio, and A. Penna. (2003). Small strain behavior of a lime treated silty sand. Proceedings of Third International Symposium on Deformation Characteristics of Geomaterials, Lyon, France.

[92] E. Delfosse-Ribay, Irini Djeran-Maigre, R. Cabrillac and D. Gouvenot. Shear modulus and damping ratio of grouted sand. Soil Dynamics and Earthquake Engineering, 24, (2004) 461-471.

[93] K. K. Chepkoit and M. S. Aggour. Dynamic properties of untreated and treated cohesive soils. Proceedings of 12th World Congress on Earthquake Engineering, Vol. 1, Paper No. 2161, Aukland, New Zealand, (2000) 1-8.

[94] Y. B. Acar and E. A. El-Tahir. Low strain dynamic properties of artificially cemented sand. Journal of Geotechnical Engineering ASCE 112 (11), (1986) 1001-1015.

[95] K. Omine, H. Ochiai, N. Yasufuku, H. Sakka. Prediction of strength deformation properties of cement stabilized soils by non destructive testing. Proceedings of Second International Symposium on Pre-failure Deformation Characteristics of Geo-materials, Torino, Italy, (1999) 323-330.

[96] J. K. Mitchell. Soil Behavior, John Wiley and Sons, New York, N.Y., 1976.

[97] S. M. Rao and P. Shivananda. Role of osmotic suction in swelling of salt-amended clays. Canadian Geotechnical Journal 42 (1), (2005) 307-315.

[98] G. Stoltz, O. Cuisinier and F. Masrouri. Multi-scale analysis of the swlling and shrinkage of lime treated expansive clayey soil. Applied Clay Science 61, (2012) 44-51.

[99] J. Lysmer and F. E. Richart. Dynamic reponse to footings to vertical loading. Journal of Soil Mechanics and Foundations Division ASCE 92 (1), (1966) 65-91.

[100] Y. S. Chae. Vibration of noncircular foundations. Journal of Soil Mechanics and Foundations Division ASCE 95 (6), (1969) 1411-1430.

[101] B. M. Das and G. V. Ramana. Principles of Soil Dynamics, Cengage Learning, Standford, 2011.

[102] I. Chowdhury and S. P. Dasgupta. Dynamics of Structure and Foundation- A Unified Approach, Taylor and Francis, London, UK, 2009.

Papers Published From the Study

[1] Dutta, T. T. and Saride, S. (2014). Dynamic properties of clean sand from resonant column studies. Proceedings of Indian Geotechnical Conference (IGC-2014), Kakinada, Andhra Pradesh. 18-20, December 2014.

[2] Dutta, T.T. and Saride, S. (2015). Dynamic properties of compacted cohesive soil from resonant column studies. Proceedings of International Conference on Geo-Engineering and Climate Change Technologies for Sustainable Environment Management, MNNIT, Allahabad, India. 9-11, October 2015.

[3] Dutta, T. T. and Saride, S. (2015). Effect of confining pressure, relative density and shear strain on the poisson's ratio of clean sand. Proceedings of Indian Geotechnical Conference (IGC-2015), Pune, Maharastra. 17-19, December 2015.

[4] Dutta, T. T. and Saride, S. (2015). Dynamic properties of moderately expansive soil stabilized with class C fly ash. Geo-Chicago 2016 (Preliminary approval received).

154